



National Library
of Canada

Acquisitions and
Bibliographic Services Branch

395 V. Street
Ottawa, Ontario
K1A 0N4

Bibliothèque nationale
du Canada

Direction des acquisitions et
des services bibliographiques

395, rue Wellington
Ottawa (Ontario)
K1A 0N4

Your file *Votre référence*

Our file *Notre référence*

NOTICE

The quality of this microform is heavily dependent upon the quality of the original thesis submitted for microfilming. Every effort has been made to ensure the highest quality of reproduction possible.

If pages are missing, contact the university which granted the degree.

Some pages may have indistinct print especially if the original pages were typed with a poor typewriter ribbon or if the university sent us an inferior photocopy.

Reproduction in full or in part of this microform is governed by the Canadian Copyright Act, R.S.C. 1970, c. C-30, and subsequent amendments.

AVIS

La qualité de cette microforme dépend grandement de la qualité de la thèse soumise au microfilmage. Nous avons tout fait pour assurer une qualité supérieure de reproduction.

S'il manque des pages, veuillez communiquer avec l'université qui a conféré le grade.

La qualité d'impression de certaines pages peut laisser à désirer, surtout si les pages originales ont été dactylographiées à l'aide d'un ruban usé ou si l'université nous a fait parvenir une photocopie de qualité inférieure.


La reproduction, même partielle, de cette microforme est soumise à la Loi canadienne sur le droit d'auteur, SRC 1970, c. C-30, et ses amendements subséquents.

**VECTORIAL EDGE FINITE ELEMENTS
APPLIED TO DETERMINISTIC AND
EIGENVALUE PROBLEMS
FOR THE ANALYSIS OF MICROWAVE
CIRCUITS**

Submitted by
RAJAGOPALAN VENKATACHALAM

A thesis
submitted to the School of Graduate Studies and Research
in partial fulfillment of the requirements for the
Degree of Master of Applied Science
in Electrical Engineering.

Ottawa-Carleton Institute of Electrical Engineering
Department of Electrical Engineering
Faculty of Engineering
University of Ottawa
Ottawa, Ontario
Canada.

 Rajagopalan Venkatachalam, Ottawa, Canada, 1993



National Library
of Canada

Acquisitions and
Bibliographic Services Branch

395 Wellington Street
Ottawa, Ontario
K1A 0N4

Bibliothèque nationale
du Canada

Direction des acquisitions et
des services bibliographiques

355, rue Wellington
Ottawa (Ontario)
K1A 0N4

Your file *Votre référence*

Our file *Notre référence*

The author has granted an irrevocable non-exclusive licence allowing the National Library of Canada to reproduce, loan, distribute or sell copies of his/her thesis by any means and in any form or format, making this thesis available to interested persons.

L'auteur a accordé une licence irrévocable et non exclusive permettant à la Bibliothèque nationale du Canada de reproduire, prêter, distribuer ou vendre des copies de sa thèse de quelque manière et sous quelque forme que ce soit pour mettre des exemplaires de cette thèse à la disposition des personnes intéressées.

The author retains ownership of the copyright in his/her thesis. Neither the thesis nor substantial extracts from it may be printed or otherwise reproduced without his/her permission.

L'auteur conserve la propriété du droit d'auteur qui protège sa thèse. Ni la thèse ni des extraits substantiels de celle-ci ne doivent être imprimés ou autrement reproduits sans son autorisation.

ISBN 0-315-82515-4

Canada



UNIVERSITÉ D'OTTAWA
UNIVERSITY OF OTTAWA

' I hereby declare that I am the sole author of this thesis. I authorize my Research Supervisor and the University of Ottawa to lend this thesis to other institutions or individuals for the purpose of scholarly research only.'

V. RAJAGOPALAN

' I further authorize my Research Supervisor and the University of Ottawa to reproduce this thesis by photocopying or by other legal means, in total or in part, at the request of other institutions or individuals for the purpose of scholarly research only.'

V. RAJAGOPALAN

“ NEW OPINIONS ARE ALWAYS SUSPECTED,
AND USUALLY OPPOSED,
WITHOUT ANY OTHER REASON BUT BECAUSE
THEY ARE NOT ALREADY COMMON.”

- John Locke



“ NOTRE FAIM DE CONNAÎTRE EST UN FEU
TOUJOURS ARDENT.
LE VENT DE NOTRE SAVOIR SOUFFLE ET
L'ATTISE D'AVANTAGE. ”

- Kaydara

AVOWAL

I am indebted to a number of people and I am at a loss of words to express my sincere thanks to:

My Academic Supervisor...

Dr. George I. Costache,
Chairman of the Department of Electrical Engineering,
for his invaluable guidance, constant enthusiastic encouragement
and financial support throughout my research.

My Beloved Parents...

Mrs. V. Kamakshi and Mr. R. Venkatachalam,
for their innate interest in my higher studies, terrific patience,
utmost understanding and timely advice.

Dr. Michel M. Ney and Dr. S. Panchanathan...

for their benevolent help, good recommendations,
helpful insights and for sharing their vast resources.

My Indefatigable Teachers...

for imparting the most precious treasure
of the world - 'education' on me,
for their abundant knowledge and for their tolerance.

The Consultants and Technicians...

especially *Mr. William Keays and Mr. Martin Lee,*
for maintaining and upgrading the computers and other equipments very well,
and for their cheerfulness.

Dr. Kazuhiro Inoue, Dr. Jin-fa Lee and Dr. Jon P. Webb...

who took pains to provide me with time and helpful materials
and useful suggestions and answers for all my questions.

The Families in Ottawa...

The Rajans, The Josephs, The Ramans, The Shans, The Chans and The Edwards,
for their consideration, affection and loving care.

My Colleagues and other researchers...

for their detailed constructive criticisms,
consistent help and timely assistance in improvements during the preparation and
writing of this research work, with particular appreciation to *Mr. Darcy Ladd*
and to *Miss. R. Kamala* for carefully proof-reading this document.

To my smart friends...

for their enlightening inspiration, remarkable competence
and for putting up with me amicably throughout.

... and others who had helped me directly and indirectly for making my research a
possible success. I wish to place on record my deepest sense of gratitude for all of them.

Lapses of memory, no doubt, has made the above list incomplete, and I apologize in
advance to anyone who has been left out.

'RAJA' V. RAJAGOPALAN

CONSPECTUS

New and efficient numerical modelling concepts and procedures based on Tangential Vectorial Finite Element method has been developed for the analysis of generalized microwave and millimeter-wave structures.

A two-dimensional formulation using the Edge finite element method has been developed to determine the electromagnetic field distributions of transmission media of rectangular cross-section and eddy-current problem when the tangential E-field has been known or the tangential H-field has been forced, on the conductive boundaries. The formulation has been developed using the E-field or the H-field and making use of the edge variables in the transversal plane and the node variables in the longitudinal plane, in order to yield a Boundary Value Problem with integral equations. The region of interest has been discretized using six-node triangles, where the end points of the triangles has been used to compute the axial components whereas the midpoints along each sides has been used to find the tangential components, and the field functions has been defined using linear vector shape functions. The frequency domain FEM program has been validated by analyzing simplified geometries and comparing them with analytical or previously published results. The algorithm, which has its own simple mesh generator, has been proved to have a convergent solution and used to analyze microwave structures.

The eigenvalue problems have been solved directly for the propagation constants making use of reliable subroutines from the EISPACK library, and the deterministic problems directly for the field distributions. The structures studied include ordinary shielded microstrip and a dielectric-loaded waveguide. Conclusions has been drawn on the feasibility of using this accurate edge element method for interesting applications in high speed interconnections, using higher order elements and in three dimensions.

CONTENTS

Avowal	i
Conspectus	iii
Contents	iv
List of Figures	vii
List of Symbols	ix
1. Introduction	1
1.1 High Speed Interconnections	1
1.2 Current Trends	2
1.3 Modeling Difficulties and Need for Better Approaches	3
1.4 Literature Review	5
1.5 Objectives	8
1.6 Novel Contributions	9
1.7 Structure of this Thesis	10
2. The Numerical Technique	11
2.1 Prelude	11
2.1.1 Why FEM?	12
2.1.2 Why Edge? - Why not Nodal Vectorial FEM?	13
2.2 Vectorial Finite Element	14
2.3 Mathematical Theory	15
2.3.1 The Affine Transformation	16
2.3.2 Angles between the Vectors	20
2.3.3 The Vectors	22
2.3.4 The Gradient	25
2.3.5 The Divergence	27
2.3.6 The Curl	29

2.3.7 The Laplacean	30
2.4 The Vector Wave Equation	30
2.4.1 Interface Conditions	32
2.4.2 Natural Interface Conditions	34
2.5 Spurious Modes	36
2.6 Advantages and Comparisons	37
3. Application to Transmission Lines	39
3.1 Tangential Finite Element Formulation	39
3.1.1 The Triangular Edge Element	41
3.1.2 Finite Element Discretization	47
3.1.3 Deterministic Problem	51
3.2 Matrix Methods	52
4. Description of the Computer Program	57
5. Results and Discussion	60
5.1 Deterministic Problems:	61
5.1.1 Test Problem : Parallel Plate Waveguide	61
5.1.2 Rectangular Waveguide	63
5.1.3 Eddy Current Problem	66
4.2 Eigenvalue Problem:	71
5.2.1 Test Geometry : Air-filled Rectangular Waveguide	72
5.2.2 Dielectric Waveguide	73
5.2.3 Microstrip Transmission Lines	78
6. Conclusions	87
7. Further Developments	90
Definitions and Notations	96

Appendix A - Chapter 2	99
Appendix B - Chapter 3	104
Appendix C - FORTRAN Source Code	108
Bibliography	134

List of Figures

Fig. 2.1. The Unit tangent and normal vectors on a triangle where side i is opposite vertex i .

Fig. 2.2. The angles between the tangents and normals.

Fig. 3.1. Triangular Edge Element.

Fig. 5.1. Test geometry : Parallel Plate Waveguide.

Fig. 5.2. TM_1 mode for Parallel Plate Waveguide.

Fig. 5.3. Rectangular air-filled Waveguide.

Fig. 5.4. TE_{10} mode - E_y field for Rectangular Waveguide.

Fig. 5.5. Eddy Current Problem.

Fig. 5.6. Comparison between the analytical and simulated results for eddy current problem (a) 50 Hz (b) 500 Hz (c) 5KHz and (d) 50KHz.

Fig. 5.7. Test geometry : Rectangular Cavity.

Fig. 5.8. Modal analysis diagram for simple cavity problem.

Fig. 5.9. Dielectric Waveguide : An Optical structure.

Fig. 5.10. Comparison between the edge-simulated and published results - Dielectric loaded waveguide.

Fig. 5.11. Effective Dielectric constant vs. Frequency for Dielectric Waveguide with permittivity 8.5.

Fig. 5.12. Ordinary shielded microstrip.

Fig. 5.13. Microstrip Problem discretization - two possible ways.

Fig. 5.14. Dispersion Characteristics - Isotropic case.

Fig. 5.15. Dispersion Characteristics - Anisotropic case.

Fig. 5.16. Effective Dielectric constant - Dominant mode.

Fig. 7.1. Valley (or) Groove Microstrip.

Fig. 7.2. Trapezoidal Microstrip : (a) Partial Fill-in, and (b) Full Con-

ductor.

Fig. 7.3. Various possible Optical fiber structures.

Fig. App.A.1. To calculate the dot products between unit tangential and normal vectors.

List of Symbols

Some *abbreviations* used in this thesis are also defined here.

<i>FEM</i>		Finite Element Method
<i>CAD</i>		Computer-Aided Design
<i>CAE</i>		Computer-Aided Engineering
<i>2-D</i>		Two-dimensional
<i>3-D</i>		Three-dimensional
Ω		Domain of interest
H	Magnetic field intensity vector, in A/m	
E	Electric field intensity vector, in V/m	
B	Magnetic flux density vector, in Wb/m ²	
D	Electric flux density vector, in C/m ²	
A	Vector magnetic potential, in Wb/m	
ϕ	Field vector, either E or H	
<i>x, y, z</i>	Axes in Cartesian Coordinate system	
\hat{i}	unit tangential vector	
\hat{n}	unit normal vector	
ω	angular radian frequency, in rad/s	
<i>f</i>	Frequency of operation, in Hz	
\mathcal{F}	Energy functional	
∇	the nabla vector operator	
<i>z</i>	the direction of propagation	
β	the propagation constant, in rad/m	
α	the attenuation constant, in Np/m	
<i>t</i>	time, in s	
ϕ_t	the transversal field vector component	

ϕ_z	the longitudinal field vector component
ϵ_0	Permittivity of free space, 8.8541878E-12 F/m
μ_0	Permeability of free space, 4 π E-07 H/m
σ	Conductivity of the medium, in U/m
$[p]$	the permeability tensor
$[q]$	the permittivity tensor
p_x, p_y, p_z	the permeability tensor components in x, y, z directions
q_x, q_y, q_z	the permittivity tensor components in x, y, z directions
n_x, n_y, n_z	the refractive index components in x, y, z directions
ϵ	the permittivity
μ	the permeability
*	denotes complex conjugate
A_e	the area of the triangular element, in m^2
θ	the angle under concern, in rad
det	denotes determinant of a matrix
Adj	denotes adjoint of a matrix
$tang, tan$	refers to tangential

Chapter 1

Introduction

1.1 High Speed Interconnections

In order to meet the increasing demands for higher speeds in areas of high speed computation, signal processing, data links and related instrumentation, very high speed Integrated Circuits with propagation delay times in the order of a few picoseconds per gate have been developed. However, when one tries to achieve high speeds in LSI/VLSI levels, difficulties like on-chip interconnection delay and crosstalk are anticipated to arise from increased lengths of interconnections. Proper design considerations to minimize them should be made in order to take full advantage of the inherent speed capability of the device.

As digital circuit clock speed increases and rise time decreases, more and more attention has to be paid to the design of the chief limiting factor: *The Interconnections*. Improperly designed interconnections can result in increase in signal rise time because of losses, inadvertent switching because of crosstalk and false switching because of ringing. With subnanoseconds rise times, these phenomena can be observed both with on-chip and chip-to-chip interconnects. Thus being that the ' **High Speed Interconnects** ' are currently of great technological interest, especially in this high-tech world, these present trends have led to increasing demands for proper and precise characterization of

such planar transmission lines. These high speed interconnects, although their lengths are very small, are to be treated as transmission lines because of their high frequencies, as at about 30 GHz their lengths become comparable to the wavelength in question.

As a result of these factors, a significant research has been undertaken in this report by means of investigating a very new method, which is still in the process of evolution, to analyze and understand the high speed interconnections better. As a forerunner to this actual analysis, the method in its entirety has been presented, its scope discussed in great detail and its feasibility has been understood through simpler geometries.

1.2 Current Trends

The fact remains that the 'Mother of Electromagnetics' has been the set of Maxwell Equations and the Finite Element Method (FEM) has been a powerful Computer-Aided Design (CAD) tool to model complicated structures based on them. FEM is a well established technique for propagation analysis of various waveguide components for which closed-form analytical solutions cannot be found. The other basic Numerical algorithms used to analyze microwave devices have been discussed by Jin-Fa Lee [1].

The Finite Element Method offers the following advantages over the other approaches:

- It is flexible in modelling problem geometries. Odd-shaped boundaries can be fitted easier.
- Boundary Conditions can be incorporated into the variational expression.
- The order of polynomial approximation can be increased to obtain more accurate numerical computations.

However, to be useful in modelling microwave devices like cavities, spurious modes that are present in the traditional FEM have to be eliminated. To overcome this, the *penalty function* method has been extensively studied [2,3,4,5] and applied to various

types of dielectric waveguides [6] in which the divergence-free constraint $\nabla \cdot \mathbf{H} = 0$ or $\nabla \cdot \mathbf{D} = 0$ is satisfied in the least square sense and spurious solutions can be suppressed from the guided wave region. However, in this approach, an arbitrary positive constant called the *penalty function* is included, and accuracy of the solution and appearance of the spurious modes in the guided region depends a lot on its magnitude.

The approach detailed in this thesis highlights the tangential vector elements, which attempts to get rid of these non-physical solutions, in order to provide stable numerical solutions for vector wave equations. These versatile elements have been developed only recently and although being in their infancy, they seem to be a strong contender for being a true CAD/CAE tool for microwave devices design.

1.3 Modeling Difficulties and Need for Better Approaches

Increasing speed of electronic devices, added to the decreasing physical size have made the Interconnecting elements, to be designed very carefully, with many constraints and trade-offs.

Various analytical methods that have been used previously to characterize microwave structures, such as Green's function techniques, conformal mapping, variational methods, spectral domain and mode matching techniques, however, cannot be applied to arbitrary geometries and discontinuities, and also realistic features like finite metallization thickness, etc. cannot be easily accounted for. These closed form solutions are thus very limited in scope and applicability. Moreover, in case of microwave and millimeter wave monolithic ICs, it is next to impossible and impractical to adjust the circuit characteristics once they have been fabricated. Therefore, very accurate numerical characterization techniques become essential and field theory is fortunate to have Finite Difference Method (FDM), Transmission Line Method (TLM), Finite Element Method

(FEM), Method of Moments (MOM), Boundary Element Method (BEM) and Finite Difference-Time Domain (FD-TD) now to its rescue. Also, the advancement of computer technology by leaps and bounds make these techniques even more favorable to the designers.

These approximate methods [1] discretize the Maxwell's equations and convert them into matrix equations that can be solved on digital computers. In the past, there were two factors that had delayed the development of good design tools: limited computer resources, and the nonexistence of appropriate numerical algorithms. The first problem has been resolved today by the availability of high speed digital computers that are capable of performing massive, huge calculations in seconds. The second handicap has been solved satisfactorily by this present work, with the provision of an algorithm for a novel numerical tool for microwave design.

Although the formulations are somewhat the same in all the above, making a tough compromise between versatility, generality, preprocessing, CPU time and storage requirements, **FEM** has been chosen to be the ideal candidate for the job in question.

In various engineering applications, the Finite Element Method has been used with remarkable success in solving two-dimensional scalar type of Boundary Value Problems. Several formulations are possible due to the nature of the Maxwell's equations and the associated Boundary conditions. Various variational approaches have been suggested for the solution of the equations; however, to date, researchers have not agreed on which approaches are the best. Also, little work has been done in extending the FEM to tackle the vector Helmholtz or the curl-curl equation, that too in three dimensions. The important reason is that a stable and a reliable set of Vector Finite Element basis functions, which does not produce spurious modes, is a necessity.

Considering the nodal (scalar or vector) finite element method, which solves for the field values at the nodes, there exist non-physical solutions which creep up. So, in

order to eliminate these parasites, **Vectorial Tangential Finite Elements** have been selected [1,2,7]. The simplest of them solve for the field values at the edges and knowing these, the field values at any other point can be calculated easily and accurately. This means that the field can be defined explicitly everywhere in the region of interest. This simplifies further mathematical manipulations and 'closed form expressions' have been arrived at, thus avoiding troublesome integrations and differentiations. Also, extraction of necessary information from them becomes straightforward, clearly portraying the unsuitability of older finite element techniques.

1.4 Literature Review

The earliest publication publicizing a whole family of finite elements, was by Nédelec [7], in which the edge element was placed on top. A.Bossavit et al. used a primitive form of edge elements in solving the three-dimensional eddy current problems using the magnetic field as the state variable and tetrahedral elements with six degrees of freedom [8]. Their elements were not consistently of a certain degree of approximation, but this had been later overcome by G.Mur [9], who made all his elements consistently linear.

M.Hano [10] solved the closed waveguide problem, filled with various anisotropic media, based on the approximate extremization of a functional, whose Euler Equation is the three-component curl-curl equation derived from Maxwell's equations. He had used rectangular edge elements for solving the inhomogeneous problem and no spurious modes were observed, but needless zero eigenvalues were produced. But, the non-zero eigenvalues (the ω for a given β) displayed a one-to-one correspondence with the guided modes. Later Hano [11] proposed new triangular elements, under the same principle.

Barton and Cendes [12] introduced the new type of vector finite element approximation function, that interpolates to the tangential projection of the magnetic vector potential on each edge of the tetrahedral finite elements. With these new basis func-

tions, continuity of the normal component of the vector potential had been provided only approximately by means of the natural interface condition inherent in the variational procedure. Albanese and Rubinacci [13] exploited the same technique to study eddy current problems in non-magnetic structures but used brick elements instead. J.P.Webb and B.Forghani [14] later applied it to 3-D magnetostatic problems using scalar potentials.

A.Bossavit [15,16] introduced the *Whitney forms* (or) the '*mixed finite elements*' and expressed basic equations in terms of differential forms, instead of vector fields. These simplicial finite elements, be it edge or facet or volume, had been applied to electromagnetic problems, by the author. This paper deals with the mathematics behind these elements - the differential geometry, and the Theory of Differential Forms.

T.Nakata et al. used different types of finite elements in the analysis of 3-D eddy currents [17] and concluded that brick edge elements were the best, in accuracy and in terms of CPU time. A.Kameari [18] studied the above problem, in the modified A-method and showed the applicability and suitability of the elements, by comparing linear 12-edge and quadratic 36-edge brick elements. Tanaka et al. [19] successfully implemented edge elements for Boundary Element Method using vector variables using 4 unknowns(3 edge and 1 normal) per triangle element.

Jin-Fa Lee, described two finite element techniques, the tangential Vector FEM and Transfinite element method [20], for modelling 3-D microwave devices. He had used eight degrees of freedom per triangle in his edge element formulation and that had increased the matrix size enormously. He had also conducted numerical experiments to determine the rate of convergence in using edge elements for the calculation of the dominant resonant frequency in a cavity. He had also used this powerful tool for dielectric waveguides [21] and also for axisymmetric cavity resonators using a hybrid technique, with bilinear functional (yet to be published). He also applied it to structures that contained both electric and magnetic field discontinuities.

Various other authors had published applications of edge elements to 3-D cavities, eddy current problems and non-linear magnetostatics (refer COMPUMAG, JULY 1991).

Zoltan Cendes [22] had discussed in detail the new finite element method structure for vector fields. This structure employed the affine transformation to represent vectors and vectorial operations over a triangular domain, and use of matrix and vector algebra were made extensively throughout this paper. He had derived the 2-D higher order tangential vector elements, consistent with Whitney Forms. This work can be hailed as an extension of recent works done in edge elements and in other tangential and normal vector elements, and this present thesis adopts many of the mathematics behind edge elements from this publication.

So far, in most (if not all) full vectorial formulations, the propagation constant has been given as an input datum and subsequently the operating frequency obtained as an eigenvalue solution. More recently, the methods that had solved for the propagation constant directly, had their own drawbacks: a large number of field components [23,24,25], consideration of the adjoint field which does not correspond to the actual electromagnetic field [26], or the need to estimate the line integral in the variational expression [27].

M.Koshiba and K.Inoue [28] had formulated a simple and most efficient of all edge element methods for the analysis of microwave and optical waveguide problems, using only three components of electric or magnetic fields, and had used triangular elements with just three unknowns per element and this thesis has been based on their literature. An eigenvalue equation that had been derived involved only edge variables in the transversal plane and gave direct solutions to the propagation constant and the corresponding field distribution.

In this present research, based on [22] and [28], use was made of the latest technique involving the least amount of unknown per triangle to solve its own applications. In all

probability, this could be extended to 3-D applications later, using even quadratic shape functions for better approximations.

1.5 Objectives

Current high speed digital circuits have integration levels of several thousand gates. One of the problems encountered with this high level complexity arises from the conductors that interconnect various gates together. Because of the short rise times and fall times of the waveforms in the digital circuits, some of the frequency components of the waveforms extend into the microwave range and for some of the larger interconnects, wave analysis must be used, which must include the effects of coupling, losses and dispersion.

An efficient method for characterizing these high speed interconnects has been proposed, based on curl-curl equations, and has been validated through simple problems. This has been based on the field theory analysis of the electromagnetic field in a 2-D cross-section of passive microwave devices.

This research examined the possible vector wave equations associated with the electric and magnetic field intensity vectors. Faced with the challenge of developing a general purpose analysis tool for the solution of a wide variety of electromagnetic problems, an important and difficult decision had to be made in the choice of the formulation. If enclosed regions or cavities were present, however, difficulties arise from the spurious standing wave solution in the scalar Helmholtz wave equation which does not satisfy the divergence free conditions. In addition, spurious modes are excited whenever the boundary conditions are satisfied in an inexact manner. The Helmholtz formulation, therefore, would require additional conditions to satisfy divergence-free conditions. Also, anisotropic materials cannot be properly treated in this type of formulation. For these reasons, choice of the curl-curl wave equation formulation appeared preferable.

The tangential Vector Finite Element Method, which has been used in [28], unlike the

conventional predecessors, imposes only the tangential continuity of the vector unknown across the elemental boundaries, this being the only necessary essential condition, resulting in reliable solutions. The applications considered have been a rectangular waveguide and eddy-current problem for deterministic case and a dielectric loaded waveguide and a boxed ordinary microstrip for the eigen-value problem, for all of which previous results had been available. The unique and new applications for later study would be the *Valley Microstrip*, and the *Trapezoidal Microstrip*, which to the author's knowledge, has never been analyzed theoretically before and some design guidelines would be set, to highlight their suitability for high speed circuits.

1.6 Novel Contributions

A new variational expression for computing electromagnetic field distributions and for the propagation constant as the eigenvalue has been formulated with transverse electric and magnetic field components for vector analysis of the eigenmodes of the waveguide. Next, as trial functions, linear vector shape functions have been used for the expansion of the transverse fields and complete polynomials for the axial fields. The superiority of this method is that only edge variables in the transversal plane have been used for final computation.

To confirm the validity and effectiveness of the method, eddy-current problem and simple rectangular waveguide, for forced problems, and a shielded ordinary microstrip and a dielectric-loaded waveguide, for eigen-value problems, have been analyzed. The propagation characteristics of both the isotropic and anisotropic microstrip transmission lines have been studied, using this unique vectorial numerical technique, " the Tangential FEM (or) the Edge Element ". This has proved to be a stable tool and also has given a direct solution to the propagation constant and the corresponding field distribution. Moreover, zero eigenvalues do not arise at all in this unique formulation. A simple mesh

generator, being a difficult task when it comes to edge elements, had also been devised.

1.7 Structure of the Thesis

This dissertation has been divided into eight chapters which are outlined below:

Chapter II reviews in brief the numerical technique used. The mathematics behind the edge elements are clearly given and several of its properties illustrated. Its advantages have also been given.

Chapter III deals with the application of edge elements to electromagnetic problems in 2-D. Formulation of the triangular edge elements to compute the dispersion characteristics of planar transmission lines has been presented. The modification needed to apply this technique to deterministic problems has also been stated. It also analyses briefly various matrix techniques used to solve the eigenvalue problem and also the subroutines that had been called for.

Chapter IV discusses all the steps in the original FORTRAN Computer Program "FREDEEM.F" used for edge elements, which had been successfully implemented for various applications.

Chapter V displays and discusses the results achieved from this method, for the different applications analyzed and also compares them with existing results.

Chapter VI contains an overall review and conclusions arrived at, on completion of this research.

Chapter VII states the further developments foreseeable in the near future, some of which are already in progress, using this method.

Chapter 2

The Numerical Technique

2.1 Prelude

Computer techniques have revolutionized the way in which electromagnetic problems have to be analyzed. Antenna and microwave design engineers rely heavily on computer methods to analyze and help evaluate new models and do modifications. Numerical techniques attempt to solve fundamental field equations directly, subject to boundary constraints posed by the geometry. Without making *apriori* assumptions about which field interactions are most significant, numerical tools analyze the entire geometry provided as input. They calculate the solution to a problem based on a full-wave analysis. There are many such techniques available and each is suitable for studying a particular set of problems, and each, in its own way, represents a potentially powerful set of tools for the electromagnetic engineers.

Electrical engineers use FEM to solve complex, nonlinear problems in magnetics, electrostatics and electromagnetics in 2-D and 3-D. Vector problems require more computation than scalar problems, and also spurious solutions known as 'vector parasites' often result in unpredictable, erroneous solutions. However, this research work presented here, has attempted to solve the vector parasite problem.

2.1.1 Why FEM?[29]

The major advantage that FEM has over the other known modelling techniques, that led to the choice of FEM in this work, stems from the fact that the electrical and geometrical properties of each element can be defined independently. This permits the problem to be set up with a large number of small elements in regions of complex geometry and fewer, larger elements in relatively open regions. Thus, it is possible to model configurations that have complicated geometries and many arbitrarily shaped dielectric regions in a relatively efficient manner.

Moment method, another numerical technique, is not very effective when applied to arbitrary configurations with complex geometries or inhomogeneous dielectrics. It is also not well suited for analyzing the interior of conductive enclosures or thin plates with wire attachments on both sides.

Finite Difference Method, suffers from the fact that the problem size can easily get out of hand for some configuration. The grid density is generally determined by the dimensions of the smallest features that need to be modelled. The volume of the grid must be large enough to encompass the entire object and most of the near field. Large objects with regions that contain small complex geometries may require large dense grids. The major restriction in FDM is also that a "structured mesh" with more degrees of freedom, is required.

The primary disadvantage in Transmission Line Method is that voluminous problems which require a fine grid need excessive amount of computation and again TLM also shares most of the disadvantages from FDM.

Boundary Integral Equation Method (BIEM) has a major problem since any structure that involves closed scattering surfaces gives rise to "forbidden" frequencies at which the system is either ill-conditioned or singular. They also work poorly with all but smooth and simple surfaces. So, it was eliminated from consideration [30].

Taking all odds into effect and doing some effective scaling, the fundamental descriptions of all problems to be studied were best suited to be done with Finite Element Method, which has a lack of mesh restriction and are apt to deal with complicated geometries. The normal procedure in a field computation by this powerful numerical method, basically, involves the following steps:

1. Discretization of the field region into a number of node points and finite elements.
2. Derivation of element equation. The unknown field quantity is represented within each element as a linear combination of the shape functions of the element and in the entire domain as a linear combination of the corresponding basis functions. The accuracy of the approximations can be improved either by subdividing the region in a finer way or by using higher order elements.
3. Assembly of element equations to obtain the matrix equations of the overall system. The imposition of the boundary conditions leads to a final system of equations, which is solved by iterative or elimination methods.
4. Postprocessing of the results by plotting graphs, forming tables and finding other desired quantities.

2.1.2 Why Edge? - Why not Nodal Vectorial FEM?[16]

Most current research seems to rely on classical finite elements, obtained by interpolation(linear interpolation, in the simplest case) from the nodal values of vector components. This approach has some appeal, because it extends to vector fields, reliable methods which were originally developed for scalar fields, by the obvious way of considering a vector field as a triplet of scalar fields, in some coordinate system. But there are also inherent difficulties in this method, which has motivated the research study.

Vector fields which represent electromagnetic phenomena have particular properties, which come from physics: field \mathbf{H} , for instance, has tangential continuity across all surfaces, whereas its normal component may have a discontinuity across a material interface. To represent all these components of \mathbf{H} as piecewise-linear, continuous functions of space, as some versions of the FEM would have it, would be clearly wrong. Such representations will be, so to speak, too rigid across interfaces.

On the other hand, the introduction of potentials leads to many difficulties linked with the so-called gauging problem [31]. So, formulations in terms of fields like \mathbf{E} and \mathbf{H} have their partisans. For instance, Ferrari [32] argues strongly in favor of variational formulations in terms of \mathbf{E} and \mathbf{H} directly, underlining in particular, the advantage of their complementarity (due to the symmetry in Maxwell's Equations).

Therefore, there has been a need for special finite elements, well adapted to the representation of vector fields like \mathbf{H} or \mathbf{B} , allowing for their possible discontinuities.

Such finite elements exist, and those that are particularly well adapted to fields like \mathbf{E} and \mathbf{H} are known as '*edge elements*', because their degrees of freedom have to be interpreted as the circulations of the field along mesh-edges, and not as nodal values. The purpose of this thesis is to clearly introduce edge elements (the simplest of all tangential vectorial finite elements) and to show how they could be useful to solve field distribution problems and propagation problems in transmission media.

2.2 Vectorial Finite Elements

Edge elements, a type of tangential vectorial finite element, belong to a more general class of mathematical objects, known as the "*Whitney Differential Forms*". Whitney forms had been described in 1957, long before the use of the finite elements [33]. They were then rediscovered in the finite elements community since 1974, under the name of "*Mixed Elements*" [7] or '*Simplicial finite element*'. Whitney elements of degree p

($p = 0,1,2,3$) have been associated with p -simplices ($p=0$ corresponds to a node, $p=1$ corresponds to an edge, etc). In short, finite element bases can be constructed relative to all kinds of simplices in a simplicial mesh: not only nodes, but to edges, to facets ($p=2$),... Moreover, there have been interesting connections between these different finite elements.

The discussion in this thesis has been confined to just EDGE ELEMENTS, also called the 'Whitney 1-forms'. Edge elements [16] belong to a family of finite element shape-functions which, more generally, assign degrees of freedom to simplices of a given mesh: nodes, edges, facets, tetrahedra ($p=3$). Edge elements were recently developed finite element bases for vector fields, which have this peculiarity that degrees of freedom, instead of being associated, as usual, with nodes of the mesh, are to be interpreted as circulations (of the to-be approached vector field) along the edge of the mesh: their degrees of freedom are edge-based, hence the nick-name of edge elements.

From these remarks, Whitney vector fields of degree 1 (that is, those generated by edge elements) are exactly what is needed in order to represent vector fields like \mathbf{E} , the electric field or \mathbf{H} , the magnetic field in electromagnetic computations, for these fields have precisely the continuity of tangential part across material interfaces.

The circulation of vector fields w_e along edge e (from node i to node j) is equal to 1; and is 0 along all other edges. Also edge elements do not impose more continuity than is actually required [16].

2.3 Mathematical Theory[22]

The structure of electromagnetics parallels that of Whitney forms. The continuity requirement of a scalar variable such as the electric potential is that the variable be continuous but its derivative may jump across inter-element boundaries. The electric field, which is the negative gradient of the potential, satisfies the continuity requirement

that its tangential component be continuous but its normal component may jump across inter-element boundaries. The electric flux, which is obtained by multiplying the electric field by the permittivity, satisfies the continuity requirement that its normal component is continuous but its tangential component may jump across inter-element boundaries. Finally, the divergence of the electric flux is a charge distribution that is a discontinuous scalar.

In the numerical realm, if the potential is approximated by piece-wise continuous polynomials - that is, separate polynomials defined over each finite elements possessing function but not derivative continuity across inter-element boundaries - then to be consistent and to avoid numerical instabilities, the electric field must be approximated by tangential vector finite elements in which the tangential component of the field across the element faces is continuous but the normal component may jump.

2.3.1 The Affine Transformation

As it is well known, homogeneous or barycentric coordinates $(\zeta_i, i=1,2,3)$ are defined over a triangle as follows [34]:

$$X = \Delta F Z \tag{2.1}$$

where

$$X = \begin{bmatrix} 1 \\ x \\ y \end{bmatrix} F = \frac{1}{\Delta} \begin{bmatrix} 1 & 1 & 1 \\ x_1 & x_2 & x_3 \\ y_1 & y_2 & y_3 \end{bmatrix} Z = \begin{bmatrix} \zeta_1 \\ \zeta_2 \\ \zeta_3 \end{bmatrix} \tag{2.2}$$

Also note that

$$\begin{aligned} \zeta_1 + \zeta_2 + \zeta_3 &= 1 \\ x &= \sum_{i=1}^3 x_i \zeta_i \\ y &= \sum_{i=1}^3 y_i \zeta_i \end{aligned}$$

Here $(x_i, y_i), i = 1, 2, 3$ are the three sets of triangle vertex coordinates and

$$\Delta = \sum_{i=1}^3 (x_i y_j - x_i y_k) = 2 A_e \quad (2.3)$$

with $(i, j, k) = \{(1,2,3), (2,3,1), (3,1,2)\}$. The transformation in (2.1) is due to Moebius and is known as the *affine transformation*.

The affine transformation is nonsingular and may be inverted to yield

$$Z = \frac{1}{\Delta} F^{-1} X \quad (2.4)$$

where the elements of the inverse matrix F^{-1} are

$$F^{-1} = \begin{bmatrix} a_1 & b_1 & c_1 \\ a_2 & b_2 & c_2 \\ a_3 & b_3 & c_3 \end{bmatrix} \quad (2.5)$$

Here

$$\begin{aligned} a_i &= x_j y_k - x_k y_j \\ b_i &= y_j - y_k \\ c_i &= x_k - x_j \end{aligned} \quad (2.6)$$

It can be noted that

$$\Delta = \sum_{i=1}^3 x_i b_i = \sum_{i=1}^3 y_i c_i$$

Unit vectors tangent to the element edges are given by

$$\hat{t}_i = \frac{1}{l_i} (c_i \hat{x} - b_i \hat{y}) \quad (2.7)$$

where side i is opposite vertex i , \hat{x} and \hat{y} are the unit vectors in the x and the y directions respectively, and $l_i^2 = b_i^2 + c_i^2$ is the length of side i (see Figure 2.1). Unit normal vectors are given by

$$\begin{aligned} \hat{n}_i &= \hat{t}_i \times \hat{z} = \frac{1}{l_i} (c_i \hat{x} - b_i \hat{y}) \times \hat{z} \\ &= \frac{1}{l_i} [c_i (\hat{x} \times \hat{z}) - b_i (\hat{y} \times \hat{z})] \\ &= -\frac{1}{l_i} (b_i \hat{x} + c_i \hat{y}) \end{aligned} \quad (2.8)$$

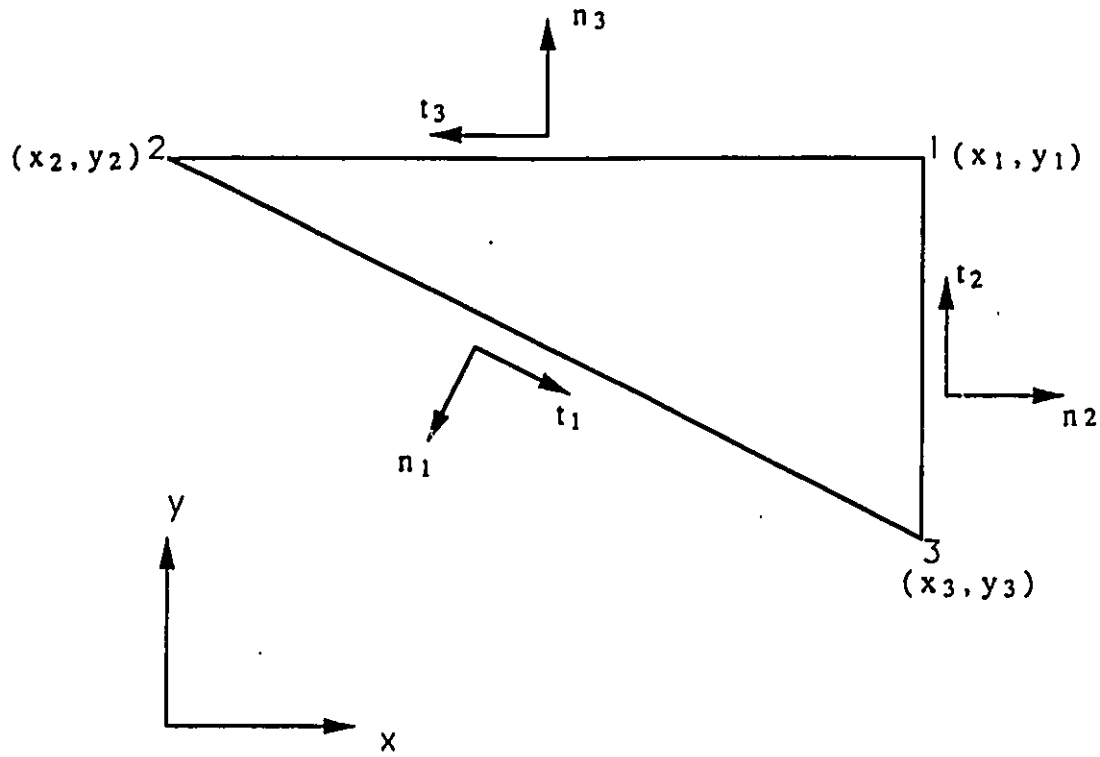


Figure 2.1: The unit tangent and normal vectors on a triangle where side i is opposite vertex i

Writing (2.8) in matrix form gives

$$\hat{N} = -L^{-1} F^{-1} \hat{X} \quad (2.9)$$

where

$$\hat{N} = \begin{bmatrix} \hat{n}_1 \\ \hat{n}_2 \\ \hat{n}_3 \end{bmatrix} \quad L = \begin{bmatrix} l_1 & 0 & 0 \\ 0 & l_2 & 0 \\ 0 & 0 & l_3 \end{bmatrix} \quad \hat{X} = \begin{bmatrix} \hat{0} \\ \hat{x} \\ \hat{y} \end{bmatrix} \quad (2.10)$$

as, from (2.9),

$$\begin{bmatrix} \hat{n}_1 \\ \hat{n}_2 \\ \hat{n}_3 \end{bmatrix} = - \begin{bmatrix} l_1 & 0 & 0 \\ 0 & l_2 & 0 \\ 0 & 0 & l_3 \end{bmatrix}^{-1} \begin{bmatrix} a_1 & b_1 & c_1 \\ a_2 & b_2 & c_2 \\ a_3 & b_3 & c_3 \end{bmatrix} \begin{bmatrix} \hat{0} \\ \hat{x} \\ \hat{y} \end{bmatrix}$$

Also, it can be observed

$$\begin{aligned} L &= L^T \\ L^{-1} &= [L^{-1}]^T = [L^{-T}] \end{aligned}$$

where T stands for the transpose. Even though the parameters a_i are multiplied by zero in equation (2.9), they are included in this equation to preserve all of the columns of the affine matrix F^{-1} . This allows (2.9) to be inverted

$$\hat{X} = -F L \hat{N} \quad (2.11)$$

In a similar way, the unit tangent vectors are written as

$$\hat{T} = L^{-1} G^{-1} \hat{X} \quad (2.12)$$

where G^{-1} is the matrix, similarly given by

$$G^{-1} = \begin{bmatrix} a_1 & c_1 & -b_1 \\ a_2 & c_2 & -b_2 \\ a_3 & c_3 & -b_3 \end{bmatrix} \quad (2.13)$$

Inverting (2.12) gives

$$\hat{X} = G L \hat{T} \quad (2.14)$$

where

$$G = \frac{1}{\Delta} \begin{bmatrix} 1 & 1 & 1 \\ y_1 & y_2 & y_3 \\ -x_1 & -x_2 & -x_3 \end{bmatrix} \quad (2.15)$$

Incidentally

$$\det[G^{-1}] = \det[F^{-1}]$$

From (2.11) and (2.14), the zero 'unit vector' in \hat{X} equals

$$\hat{0} = \sum_i l_i \hat{n}_i = \sum_i l_i \hat{t}_i \quad (2.16)$$

Also, combining the above equations provides $\hat{N} = -L^{-1} F^{-1} G L \hat{T}$ and $\hat{T} = -L^{-1} G^{-1} F L \hat{N}$ where the elements of the product matrices $F^{-1} G$ and $G^{-1} F$ are

$$\begin{aligned}(F^{-1} G)_{ij} &= (a_i + b_i y_j - c_i x_j) / \Delta \\(G^{-1} F)_{ij} &= (a_i + c_i x_j - b_i y_j) / \Delta\end{aligned}\tag{2.17}$$

2.3.2 Angles between the Vectors

The angles between the unit tangent and unit normal vectors (see Figure 2.2) are obtained by using the dot product

$$\hat{N} \cdot \hat{N}^T = \hat{T} \cdot \hat{T}^T = C\tag{2.18}$$

where the matrix C, from definition of scalar products, is given by (see Appendix A.2)

$$C = \begin{bmatrix} 1 & -\cos \theta_3 & -\cos \theta_2 \\ -\cos \theta_3 & 1 & -\cos \theta_1 \\ -\cos \theta_2 & -\cos \theta_1 & 1 \end{bmatrix}\tag{2.19}$$

The negative signs are due to the direction of the signs involved. Here θ_i represents the included angle at vertex i . It is found that

$$\begin{aligned}\hat{N} \cdot \hat{T}^T &= \begin{bmatrix} 0 & -\sin \theta_3 & \sin \theta_2 \\ \sin \theta_3 & 0 & -\sin \theta_1 \\ -\sin \theta_2 & \sin \theta_1 & 0 \end{bmatrix} = [SS] \\ \hat{T} \cdot \hat{N}^T &= \begin{bmatrix} 0 & \sin \theta_3 & -\sin \theta_2 \\ -\sin \theta_3 & 0 & \sin \theta_1 \\ \sin \theta_2 & -\sin \theta_1 & 0 \end{bmatrix} = -[SS] = [SS]^T\end{aligned}\tag{2.20}$$

The proof is given in Appendix A.3 . Equation (2.20) is cast into a simpler form by noting that

$$\sin \theta_i = \frac{h_j}{l_k} = \frac{h_k}{l_j}\tag{2.21}$$

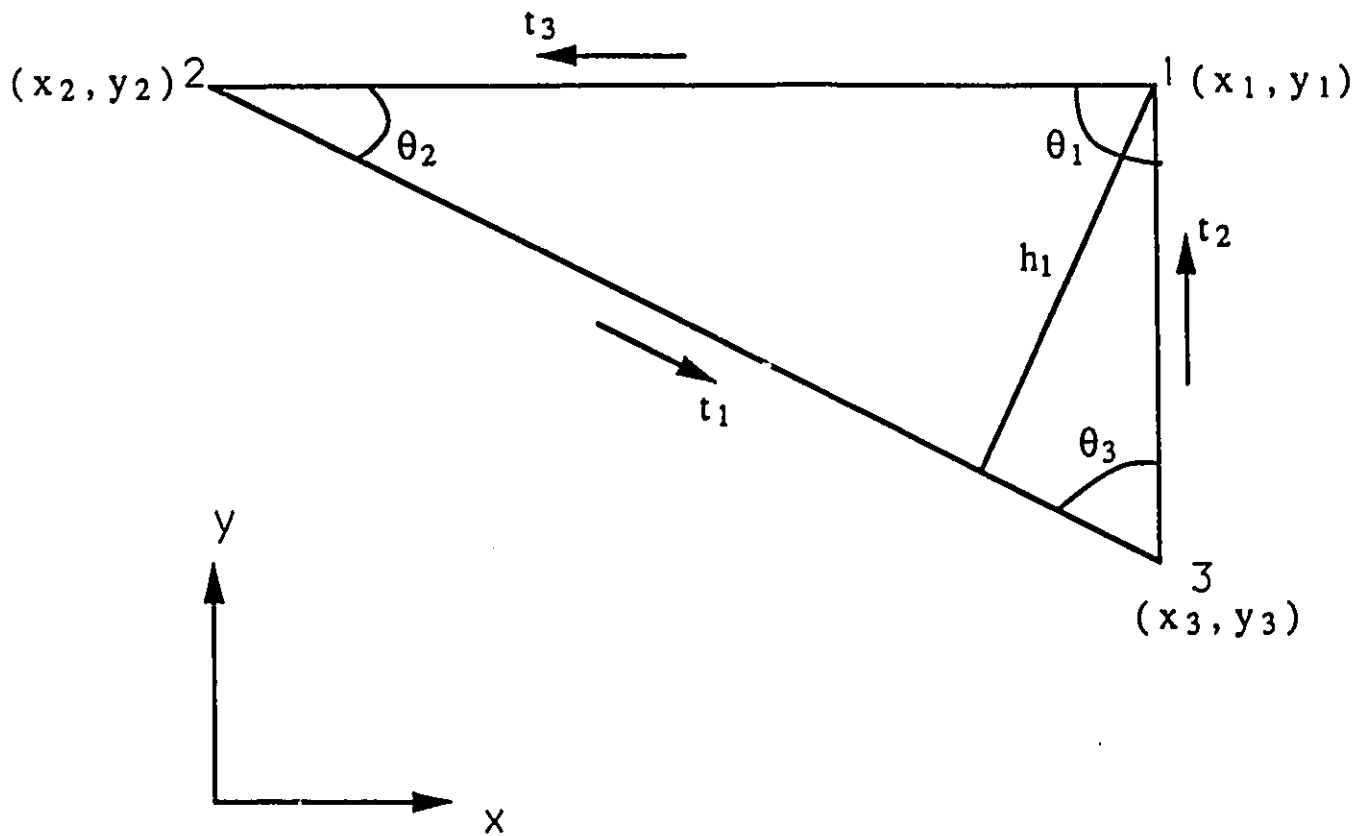


Figure 2.2: The Angles between the tangents and the normals

where h_i is the altitude to vertex i . Thus

$$\begin{aligned}\hat{N} \cdot \hat{T}^T &= \begin{bmatrix} 0 & -\frac{h_1}{l_2} & \frac{h_1}{l_3} \\ \frac{h_2}{l_1} & 0 & -\frac{h_2}{l_3} \\ -\frac{h_3}{l_1} & \frac{h_3}{l_2} & 0 \end{bmatrix} \\ &= \begin{bmatrix} 0 & -h_1 & h_1 \\ h_2 & 0 & -h_2 \\ -h_3 & h_3 & 0 \end{bmatrix} \begin{bmatrix} \frac{1}{l_1} & 0 & 0 \\ 0 & \frac{1}{l_2} & 0 \\ 0 & 0 & \frac{1}{l_3} \end{bmatrix} = H S L^{-1}\end{aligned}$$

Similarly ,

$$\begin{aligned}\hat{N} \cdot \hat{T}^T &= L^{-1} S H \\ \hat{T} \cdot \hat{N}^T &= H S^T L^{-1} = -H S L^{-1} = L^{-1} S^T H = -L^{-1} S H\end{aligned}\quad (2.22)$$

where

$$\begin{aligned}H &= \begin{bmatrix} h_1 & 0 & 0 \\ 0 & h_2 & 0 \\ 0 & 0 & h_3 \end{bmatrix} = H^T \\ S &= \begin{bmatrix} 0 & -1 & 1 \\ 1 & 0 & -1 \\ -1 & 1 & 0 \end{bmatrix}\end{aligned}\quad (2.23)$$

Also, it can be inferred that $S^T = -S$.

2.3.3 Vectors

All fundamental vector operations that would be useful for electromagnetic applications are given here. In matrix algebra, given two matrices $[A]$ and $[B]$,

1. $[A][B] \neq [B][A]$.
2. $[AB]^{-1} = [B]^{-1}[A]^{-1}$.
3. $[A]^{-1} = \frac{\text{adj}[A]}{|A|}$.

A vector in two dimension, \mathbf{v} , is expressed in terms of \hat{X} as

$$\mathbf{v} = v_x \hat{x} + v_y \hat{y} = \hat{X}^T V^{(X)} = V^{(X)T} \hat{X} \quad (2.24)$$

where

$$V^{(X)} = \begin{bmatrix} q \\ v_x \\ v_y \end{bmatrix} \quad (2.25)$$

and q is to be determined. Also

$$\begin{aligned} \det F &= 1 \\ \det G &= 1 \\ F^{-1} &= \text{adj}F \\ G^{-1} &= \text{adj}G \end{aligned}$$

(2.24) can be converted to normal and tangential forms by (2.11) and (2.14). The result is

$$\mathbf{v} = \hat{N}^T V^{(N)} = \hat{T}^T V^{(T)} \quad (2.26)$$

where

$$\begin{aligned} V^{(N)} &= -L F^T V^{(X)} \\ V^{(T)} &= L G^T V^{(X)} \end{aligned} \quad (2.27)$$

(see Appendix A.4 for proofs).

Solving for $V^{(X)}$ from (2.27) gives

$$\begin{aligned} V^{(X)} &= -F^{-T} L^{-1} V^{(N)} \\ V^{(X)} &= G^{-T} L^{-1} V^{(T)} \end{aligned} \quad (2.28)$$

The top row of (2.28) yields

$$q = -\sum_{i=1}^3 \frac{a_i}{l_i} V_i^{(N)} = \sum_{i=1}^3 \frac{a_i}{l_i} V_i^{(T)} \quad (2.29)$$

See Appendix A.5 for proof of (2.29).

By the property of scalar (or) dot products, for any two vectors \mathbf{a} and \mathbf{b} , $\mathbf{a} \cdot \mathbf{b} = |\mathbf{a}| \cdot$ projection of $|\mathbf{b}|$ on $|\mathbf{a}|$ or the vice versa. Thus, the actual components of \mathbf{v} in the three tangential directions to the edges (or simply along the simplex co-ordinates) are actually the projections of all normal components of \mathbf{v} on the tangential components (or) also all projections of all tangential directions on one and the other tangential directions. From (2.26), the components of \mathbf{v} in the three directions tangential to the element edges are:

$$\begin{aligned} \mathbf{v}_t &= \hat{T} \cdot \mathbf{v} = \hat{T} \cdot \hat{N}^T V^{(N)} = H S^T L^{-1} V^{(N)} = L^{-1} S^T H V^{(N)} \\ &= \hat{T} \cdot \hat{T}^T V^{(T)} = C V^{(T)} \end{aligned} \quad (2.30)$$

where \mathbf{v}_t is a vector containing the total components of \mathbf{v} in the three tangential directions. Notice that the components of \mathbf{v}_t are in general not the same as the components of $V^{(T)}$. Referring to Fig. 2.1, it can be seen that the representation of a vector \mathbf{v} in terms of the unit vectors \hat{N} and \hat{T} is not unique. The unique components of the vector \mathbf{v} in the three directions \hat{t}_i are provided by the three components of \mathbf{v}_t .

Substituting (2.27) into (2.30) yields

$$\mathbf{v}_t = -H S^T F^T V^{(X)} = C L G^T V^{(X)} \quad (2.31)$$

It follows that

$$C = -H S^T F^T G^{-T} L^{-1} \quad (2.32)$$

This can also be verified by the expansion of the right hand side.

In a similar way, the components of \mathbf{v} in the directions normal to the element edges are:

$$\mathbf{v}_n = \hat{N} \cdot \mathbf{v} = \hat{N} \cdot \hat{T}^T V^{(T)} = H S L^{-1} V^{(T)} = H S G^T V^{(X)} \quad (2.33)$$

or

$$\mathbf{v}_n = \hat{N} \cdot \hat{N}^T V^{(N)} = C V^{(N)} = -C L F^T V^{(X)} \quad (2.34)$$

which also implies $C = -H S G^T L^{-1} F^{-T}$

Let $D^{-1} = \Delta S F^T$ and $E^{-1} = -\Delta S G^T$. Direct evaluation yields

$$D^{-1} = \begin{bmatrix} 0 & c_1 & -b_1 \\ 0 & c_2 & -b_2 \\ 0 & c_3 & -b_3 \end{bmatrix} \quad E^{-1} = \begin{bmatrix} 0 & b_1 & c_1 \\ 0 & b_2 & c_2 \\ 0 & b_3 & c_3 \end{bmatrix} \quad (2.35)$$

Thus

$$\begin{aligned} \mathbf{v}_i &= -L^{-1} D^{-1} V^{(X)} \\ \mathbf{v}_n &= -L^{-1} E^{-1} V^{(X)} \end{aligned} \quad (2.36)$$

2.3.4 The Gradient

In two dimensions, the gradient operator is written in terms of the vector \hat{X} as

$$\nabla \phi = \hat{X}^T \partial W \phi = \partial W^T \phi \hat{X} \quad (2.37)$$

where

$$\partial W = \begin{bmatrix} w \\ \partial x \\ \partial y \end{bmatrix} \quad (2.38)$$

Here the notation $\partial x \equiv \partial/\partial x$ et cetera is adopted and w is to be determined.

Let

$$\phi = \sum_{i=1}^3 \alpha_i(x, y) \phi_i$$

By definition of simplex coordinates,

$$\Delta \zeta_i = a_i + b_i x + c_i y$$

and so

$$\begin{aligned} \frac{\partial \zeta_i}{\partial x} &= \frac{b_i}{\Delta} \\ \frac{\partial \zeta_i}{\partial y} &= \frac{c_i}{\Delta} \end{aligned}$$

Applying the chain rule gives

$$\begin{aligned}
 \frac{\partial \phi}{\partial x} &= \sum_{i=1}^3 \frac{\partial \alpha_i}{\partial x} \phi_i = \sum_{i=1}^3 \frac{\partial \alpha_i}{\partial \zeta_i} \frac{\partial \zeta_i}{\partial x} \phi_i \\
 &= \frac{1}{\Delta} \sum_{i=1}^3 b_i \frac{\partial(\alpha_i \phi_i)}{\partial \zeta_i} \\
 &= \frac{1}{\Delta} \sum_{i=1}^3 b_i \frac{\partial \phi}{\partial \zeta_i}
 \end{aligned}$$

that is,

$$\partial x = \frac{1}{\Delta} \sum_{i=1}^3 b_i \partial \zeta_i \quad \text{and, also} \quad \partial y = \frac{1}{\Delta} \sum_{i=1}^3 c_i \partial \zeta_i \quad (2.39)$$

Also,

$$w = \frac{1}{\Delta} \sum_{i=1}^3 a_i \partial \zeta_i$$

Thus it can be written,

$$\partial W = \frac{1}{\Delta} F^{-T} \partial Z \quad (2.40)$$

where

$$\partial Z = \begin{bmatrix} \partial \zeta_1 \\ \partial \zeta_2 \\ \partial \zeta_3 \end{bmatrix} \quad (2.41)$$

Substituting (2.40) into (2.37) gives

$$\nabla \phi = \hat{X}^T \partial W \phi = \hat{X}^T \frac{1}{\Delta} F^{-T} \partial Z \phi = \hat{X}^T \Delta^{-1} F^{-T} \partial Z \phi \quad (2.42)$$

To express $\nabla \phi$ in terms of the unit normal vectors, (2.11) can be used to give

$$\nabla \phi = -\hat{N}^T L^T F^T \Delta^{-1} F^{-T} \partial Z \phi = -\hat{N}^T \frac{L}{\Delta} \partial Z \phi = -\hat{N}^T H^{-1} \partial Z \phi \quad (2.43)$$

where $h_i l_i = \Delta$ or $L/\Delta = 1/H$. Thus, the gradient is expressed "naturally" (i.e. as partials of homogeneous coordinates) in terms of the unit normals to the sides of the element.

The gradient is given in terms of the unit tangent to the element edges by substituting (2.14) into (2.42). The result is

$$\begin{aligned}
\nabla \phi &= \hat{T}^T L^T G^T \Delta^{-1} F^{-T} \partial Z \phi = \hat{T}^T \frac{L}{\Delta} G^T F^{-T} \partial Z \phi \\
&= \hat{T}^T H^{-T} G^T F^{-T} \partial Z \phi \\
&= \hat{T}^T H^{-1} G^T F^{-T} \partial Z \phi
\end{aligned} \tag{2.44}$$

as $H^{-1} = [H^{-1}]^T = H^{-T}$. The components of $\nabla \phi$ in the directions tangential to the element edges are obtained by taking the dot product of (2.43) with \hat{T} .

$$\begin{aligned}
\nabla \phi_t &= \hat{T} \cdot \nabla \phi = -\hat{T} \cdot \hat{N}^T H^{-1} \partial Z \phi \\
&= -H S^T L^{-1} H^{-1} \partial Z \phi = -L^{-1} S^T H H^{-1} \partial Z \phi \\
&= -L^{-1} S^T \partial Z \phi = L^{-1} S \partial Z \phi
\end{aligned} \tag{2.45}$$

Similarly, the components of ϕ in the normal direction are

$$\begin{aligned}
\nabla \phi_n &= \hat{N} \cdot \nabla \phi = \hat{N} \cdot \hat{T}^T H^{-1} G^T F^{-1} \partial Z \phi \\
&= L^{-1} S H H^{-1} G^T F^{-1} \partial Z \phi = L^{-1} S G^T F^{-1} \partial Z \phi \\
&= -\hat{N} \cdot \hat{N}^T H^{-1} \partial Z \phi = -C H^{-1} \partial Z \phi
\end{aligned} \tag{2.46}$$

2.3.5 The Divergence

In two dimensions, the divergence of the vector \mathbf{v} is given as

$$\nabla \cdot \mathbf{v} = \partial X^T V^{(X)} = \frac{\partial}{\partial x} v_x + \frac{\partial}{\partial y} v_y \tag{2.47}$$

where

$$\partial X = \begin{bmatrix} 0 \\ \partial x \\ \partial y \end{bmatrix} \tag{2.48}$$

Using (2.35), (2.39) and (2.41) gives

$$\partial X^T = \partial Z^T E^{-1} / \Delta \tag{2.49}$$

Thus

$$\nabla \cdot \mathbf{v} = \partial Z^T \Delta^{-1} E^{-1} V^{(X)} \quad (2.50)$$

In terms of $V^{(T)}$, this yields from (2.28),

$$\nabla \cdot \mathbf{v} = \partial Z^T \Delta^{-1} E^{-1} G^{-T} L^{-1} V^{(T)} \quad (2.51)$$

Using (2.35), it can found that

$$\nabla \cdot \mathbf{v} = -\partial Z^T \Delta^{-1} \Delta S L^{-1} V^{(T)}$$

as

$$E^{-1} G^{-T} = -\Delta S \quad (2.52)$$

Thus, (2.51) becomes

$$\nabla \cdot \mathbf{v} = -\partial Z^T S L^{-1} V^{(T)} \quad (2.53)$$

It is interesting to note that the divergence operator expressed in terms of unit tangent vectors is

$$\text{div}^{(T)} = (\nabla \cdot \hat{T})^{(T)} = -\partial Z^T S L^{-1} \quad (2.54)$$

as $\mathbf{v} = \hat{T}^T V^{(T)}$, while the transpose of the tangential components of the gradient operator, from (2.45) is given by

$$\nabla \phi_t = -L^{-1} S^T \partial Z \phi$$

Thus

$$\text{grad}^{(T)T} = -(L^{-1} S^T \partial Z)^T = -\partial Z^T (L^{-1} S^T)^T = -\partial Z^T S L^{-T} = -\partial Z^T S L^{-1} \quad (2.55)$$

as $L^{-T} = L^{-1}$. Thus, as expected, *the adjoint of the gradient is equal to the divergence.*

$$\text{grad}^{(T)T} = \text{div}^{(T)}$$

To write the divergence in terms of $V^{(N)}$, (2.28) can be substituted into (2.50). This gives

$$\nabla \cdot \mathbf{v} = -\partial Z^T \Delta^{-1} E^{-1} F^{-T} L^{-1} V^{(N)} = -\partial Z^T K L^{-1} V^{(N)} \quad (2.56)$$

where $K = E^{-1} F^{-T} / \Delta$. The elements of K are

$$K_{ij} = (b_i b_j + c_i c_j) / \Delta \quad (2.57)$$

But, according to Silvester and Ferrari [34](Pg 110, Eqn.5.07),

$$(b_i b_j + c_i c_j) = \begin{cases} -\Delta \cot \theta_k & \text{if } i \neq j \\ \Delta (\cot \theta_j + \cot \theta_k) & \text{if } i = j \end{cases}$$

Using this cotangent identity, K may be written as

$$K = \begin{bmatrix} \cot \theta_2 + \cot \theta_3 & -\cot \theta_3 & -\cot \theta_2 \\ -\cot \theta_3 & \cot \theta_1 + \cot \theta_3 & -\cot \theta_1 \\ -\cot \theta_2 & -\cot \theta_1 & \cot \theta_1 + \cot \theta_2 \end{bmatrix} \quad (2.58)$$

2.3.6 The Curl

The curl operator is similar to the divergence operation in two dimensions.

$$\nabla \times \mathbf{v} = \hat{z} \partial Y^T V^{(X)} = \hat{z} \frac{\partial}{\partial x} v_y - \frac{\partial}{\partial y} v_x \quad (2.59)$$

where

$$\partial Y = \begin{bmatrix} 0 \\ -\partial_y \\ \partial_x \end{bmatrix} \quad (2.60)$$

as $\partial z = 0$ in two dimensions. It can be written as

$$\nabla \times \mathbf{v} = -\hat{z} \partial Z^T D^{-1} V^{(X)} \quad (2.61)$$

Using (2.28) and recognizing that $D^{-1} F^{-T} = \Delta S$ and that $D^{-1} G^{-T} = \Delta K$ allows one to write (2.61) in terms of unit normal and tangent vectors (also note that $\Delta/L = H$)

$$\begin{aligned} \nabla \times \mathbf{v} &= \hat{z} \partial Z^T D^{-1} F^{-T} L^{-1} V^{(N)} \\ &= \hat{z} \partial Z^T \Delta S L^{-1} V^{(N)} = \hat{z} \partial Z^T S H V^{(N)} \\ &= -\hat{z} \partial Z^T D^{-1} G^{-T} L^{-1} V^{(T)} \\ &= -\hat{z} \partial Z^T \Delta K L^{-1} V^{(T)} = -\hat{z} \partial Z^T K H V^{(T)} \end{aligned} \quad (2.62)$$

2.3.7 The Laplacean

Using (2.53) and (2.44) it can be found that

$$\begin{aligned}\nabla \cdot \nabla \phi &= \partial Z^T S L^{-1} H^{-1} G^T F^{-T} \partial Z \phi = -\Delta^{-1} \partial Z^T S G^T F^{-T} \partial Z \phi \\ &= -\Delta^{-1} \partial Z^T (-E^{-1}/\Delta) F^{-T} \partial Z \phi = \Delta^{-1} \partial Z^T K \partial Z \phi\end{aligned}\quad (2.63)$$

Thus the relationship of the Laplacean operator to the triangle cotangents [34] is derived directly from the affine transformation.

Compatibility : The finite element solution of electromagnetic field problems requires that the approximation functions satisfy the proper continuity conditions across element boundaries. Finite elements satisfying the proper continuity conditions are said to be *compatible*. For the 1-form elements, or edge elements, compatibility requires that the tangential components of the vector field be continuous while for 2-form (facet) elements, the normal components must be continuous.

Unisolvence : Unisolvence means that the finite element basis functions must be linearly independent to provide a unique solution of the operator equation. To get correct solutions, the linear independence of the approximating functions must be ensured.

Unisolvence requires that the only non-trivial solution of $\nabla \times \mathbf{v} = 0$ is $\mathbf{v} = -\nabla \phi$ for some ϕ . Thus, if $\nabla \times \mathbf{v} = 0$ and $\mathbf{v} \neq -\nabla \phi$ then $\mathbf{v} = 0$ may be the only solution.

2.4 The Vector Wave Equation

At this point, there is a need to determine how the elements derived above are used in finite element analysis. To make the analysis concrete, the variational solution of the vector wave equation is examined. The medium is assumed to be linear, stationary and source free and the analysis is performed in frequency domain.

The vector curl-curl wave equation is

$$\nabla \times \frac{1}{\mu} \nabla \times \mathbf{E} = \frac{k^2}{\mu} \mathbf{E} \quad (2.64)$$

where $k^2 = \omega^2 \mu \epsilon$. Inside a material medium, the permittivity ϵ is determined by the electrical properties of the medium and the permeability μ by the magnetic properties of the medium. It will be shown that the variational functional, for linear materials,

$$\mathcal{F}(\mathbf{E}) = \int \frac{1}{\mu} (\nabla \times \mathbf{E})^2 d\Omega - \int \frac{k^2}{\mu} \mathbf{E}^2 d\Omega \quad (2.65)$$

may be used to solve (2.64) provided the tangential component of \mathbf{E} is made continuous.

The continuity requirements of the electric field (magnetic field can be solved likewise) at the interface are expressed mathematically as

$$\mathbf{1}_n \cdot \mathbf{D}_1 = \mathbf{1}_n \cdot \mathbf{D}_2$$

$$\mathbf{1}_n \times \mathbf{E}_1 = \mathbf{1}_n \times \mathbf{E}_2$$

where \mathbf{D} is the electric flux, \mathbf{E} is the electric field intensity, and $\mathbf{1}_n$ is the unit vector normal to the interface. It is assumed that there is neither surface charge density nor surface current density. To minimize $\mathcal{F}(\mathbf{E})$, let $\mathbf{E} = \mathbf{E}_{ex} + \beta \xi$ where \mathbf{E}_{ex} is the exact solution of the wave equation (2.64), β is a small real number and ξ is an arbitrary vector function, which satisfies all essential boundary conditions. The first variation of $\mathcal{F}(\mathbf{E})$ is

$$\begin{aligned} \delta \mathcal{F}(\mathbf{E}) &= \left. \frac{\partial \mathcal{F}(\mathbf{E}_{ex} + \beta \xi)}{\partial \beta} \right|_{\beta=0} \\ &= \int \frac{1}{\mu} (\nabla \times \xi) \cdot (\nabla \times \mathbf{E}_{ex}) d\Omega - \int \frac{k^2}{\mu} \xi \cdot \mathbf{E}_{ex} d\Omega \end{aligned} \quad (2.66)$$

By integrating the vector identity

$$\nabla \cdot (\mathbf{a} \times \mathbf{b}) = (\nabla \times \mathbf{a}) \cdot \mathbf{b} - \mathbf{a} \cdot (\nabla \times \mathbf{b}) \quad (2.67)$$

that is,

$$\mathbf{b} \cdot (\nabla \times \mathbf{a}) = \nabla \cdot (\mathbf{a} \times \mathbf{b}) + \mathbf{a} \cdot (\nabla \times \mathbf{b})$$

it can be found that

$$\oint (\mathbf{a} \times \mathbf{b}) \cdot d\mathbf{S} = \int [(\nabla \times \mathbf{a}) \cdot \mathbf{b} - \mathbf{a} \cdot (\nabla \times \mathbf{b})] d\Omega \quad (2.68)$$

Thus (2.66) is converted into

$$\begin{aligned}
\delta\mathcal{F}(\mathbf{E}) &= \int \xi \cdot \left[\nabla \times \frac{1}{\mu} \nabla \times \mathbf{E}_{ex} - \frac{k^2}{\mu} \mathbf{E}_{ex} \right] d\Omega \\
&+ \int \nabla \cdot \left[\xi \times \frac{1}{\mu} \nabla \times \mathbf{E}_{ex} \right] d\Omega \\
&= \int \xi \cdot \left[\nabla \times \frac{1}{\mu} \nabla \times \mathbf{E}_{ex} - \frac{k^2}{\mu} \mathbf{E}_{ex} \right] d\Omega \\
&+ \oint \left[\xi \times \frac{1}{\mu} \nabla \times \mathbf{E}_{ex} \right] \cdot dS \\
&\text{(by divergence theorem)} \tag{2.69}
\end{aligned}$$

Since \mathbf{E}_{ex} satisfies (2.64) exactly, which is the Euler's equation, the first volume integral drops out. So, one is concerned only with the second closed integral which must be evaluated on all surface - interior and exterior - of the finite-element mesh.

$$\delta\mathcal{F}(\mathbf{E}) = \oint \left[\xi \times \frac{1}{\mu} \nabla \times \mathbf{E}_{ex} \right] \cdot dS = -j\omega \oint (\xi \times \mathbf{H}) \cdot dS \tag{2.70}$$

due to the fact that $\nabla \times \mathbf{E}_{ex} = -j\omega \mathbf{B} = -j\omega \mu \mathbf{H}$. Finally, setting the first variation of $\mathcal{F}(\mathbf{E})$ equal to zero yields

$$\oint (\xi \times \mathbf{H}) \cdot dS = 0 \tag{2.71}$$

(2.71) provides the natural boundary conditions for the functional.

2.4.1 Interface Conditions

At interfaces, as previously stated, the electric field \mathbf{E} satisfies the condition that its tangential component is continuous

$$\hat{n} \times \mathbf{E}_1 = \hat{n} \times \mathbf{E}_2 \tag{2.72}$$

while the flux $\mathbf{D} = \epsilon \mathbf{E}$ satisfies the condition that its normal component is continuous

$$\begin{aligned}
\hat{n} \cdot \mathbf{D}_1 &= \hat{n} \cdot \mathbf{D}_2 \\
\hat{n} \cdot \epsilon_1 \mathbf{E}_1 &= \hat{n} \cdot \epsilon_2 \mathbf{E}_2
\end{aligned} \tag{2.73}$$

For the magnetic field \mathbf{H} , the corresponding interface conditions are the tangential component of \mathbf{H} is continuous and the normal component of the magnetic flux \mathbf{B} is continuous

$$\hat{n} \times \mathbf{H}_1 = \hat{n} \times \mathbf{H}_2 \quad (2.74)$$

$$\hat{n} \cdot \mathbf{B}_1 = \hat{n} \cdot \mathbf{B}_2$$

$$\hat{n} \cdot \mu_1 \mathbf{H}_1 = \hat{n} \cdot \mu_2 \mathbf{H}_2 \quad (2.75)$$

(2.75) is expressed in terms of \mathbf{E} by using Faraday's law. This yields, from the magnetic flux continuity,

$$\hat{n} \cdot \nabla \times \mathbf{E}_1 = \hat{n} \cdot \nabla \times \mathbf{E}_2 \quad (2.76)$$

Adopting an (n, τ, λ) local orthogonal system, where n is the normal to the interface, and τ and λ are parallel (i.e. tangential) to the interface (see Appendix A.6), (2.76) becomes

$$\left(\frac{\partial \mathbf{E}_\lambda}{\partial \tau} - \frac{\partial \mathbf{E}_\tau}{\partial \lambda} \right)_1 = \left(\frac{\partial \mathbf{E}_\lambda}{\partial \tau} - \frac{\partial \mathbf{E}_\tau}{\partial \lambda} \right)_2 \quad (2.77)$$

Notice that (2.77) involves only the tangential components and the tangential derivatives of \mathbf{E} . It can thus be concluded that the *continuity of the normal component of magnetic flux \mathbf{B} is ensured by setting the tangential component of the electric field \mathbf{E} to be continuous*. A corollary of this is that *continuity of the normal component of electric flux \mathbf{D} is ensured by setting the tangential component of the magnetic field \mathbf{H} to be continuous*. The tangential component of the magnetic field in terms of the electric fields can be expressed by using Faraday's Law. The result would be

$$\hat{n} \times \frac{1}{\mu_1} (\nabla \times \mathbf{E}_1) = \hat{n} \times \frac{1}{\mu_2} (\nabla \times \mathbf{E}_2) \quad (2.78)$$

From the tangential continuity requirements, (2.74) or (2.78) can be written down in components as

$$\frac{1}{\mu_1} \left(\frac{\partial \mathbf{E}_\tau}{\partial n} - \frac{\partial \mathbf{E}_n}{\partial \tau} \right)_1 = \frac{1}{\mu_2} \left(\frac{\partial \mathbf{E}_\tau}{\partial n} - \frac{\partial \mathbf{E}_n}{\partial \tau} \right)_2 \quad (2.79)$$

$$\frac{1}{\mu_1} \left(\frac{\partial \mathbf{E}_n}{\partial \lambda} - \frac{\partial \mathbf{E}_\lambda}{\partial n} \right)_1 = \frac{1}{\mu_2} \left(\frac{\partial \mathbf{E}_n}{\partial \lambda} - \frac{\partial \mathbf{E}_\lambda}{\partial n} \right)_2 \quad (2.80)$$

Provided that (2.79) and (2.80) are satisfied, (2.73) will surely be satisfied.

2.4.2 Natural Interface Conditions

Evaluating (2.71) by components yields

$$\oint (\xi_\tau \mathbf{H}_\lambda - \xi_\lambda \mathbf{H}_\tau) dS = 0 \quad (2.81)$$

In terms of the electric field \mathbf{E} this is

$$\oint \left[\xi_\tau \frac{1}{\mu} \left(\frac{\partial \mathbf{E}_\tau}{\partial n} - \frac{\partial \mathbf{E}_n}{\partial \tau} \right) - \xi_\lambda \frac{1}{\mu} \left(\frac{\partial \mathbf{E}_n}{\partial \lambda} - \frac{\partial \mathbf{E}_\lambda}{\partial n} \right) \right] dS = 0 \quad (2.82)$$

(i) On exterior boundaries, if the tangential components of \mathbf{E} are set equal to a given value, then ξ_τ and ξ_λ are zero and (2.82) is satisfied.

(ii) On the other hand, along boundaries where ξ_τ and ξ_λ are arbitrary, a solution is automatically obtained for \mathbf{E} that satisfies

$$\hat{n} \times \mathbf{H} = 0 \quad (2.83)$$

(iii) On interior boundaries, if the continuity of the tangential component of \mathbf{E} is imposed, then

$$\begin{aligned} \xi_{\tau_1} &= \xi_{\tau_2} = \xi_\tau \\ \xi_{\lambda_1} &= \xi_{\lambda_2} = \xi_\lambda \end{aligned} \quad (2.84)$$

and (2.82) yields

$$\begin{aligned} & \int \xi_\tau \left[\frac{1}{\mu_1} \left(\frac{\partial \mathbf{E}_\tau}{\partial n} - \frac{\partial \mathbf{E}_n}{\partial \tau} \right)_1 - \frac{1}{\mu_2} \left(\frac{\partial \mathbf{E}_\tau}{\partial n} - \frac{\partial \mathbf{E}_n}{\partial \tau} \right)_2 \right] dS \\ & - \int \xi_\lambda \left[\frac{1}{\mu_1} \left(\frac{\partial \mathbf{E}_n}{\partial \lambda} - \frac{\partial \mathbf{E}_\lambda}{\partial n} \right)_1 - \frac{1}{\mu_2} \left(\frac{\partial \mathbf{E}_n}{\partial \lambda} - \frac{\partial \mathbf{E}_\lambda}{\partial n} \right)_2 \right] dS = 0 \end{aligned} \quad (2.85)$$

Since ξ_r and ξ_λ are arbitrary on interior boundaries, (2.85) yields exactly the required interface conditions (2.79) and (2.80).

In view of the above analysis, specifying the continuity of the normal components of electric or magnetic fields is *not* required in the finite element solution of the vector wave equation. As discussed in [12], this is also true in the magnetostatic and eddy current cases. In fact, imposing continuity on the normal component of the field is wrong with finite elements of polynomial order less than 5 since it is then impossible to have tangentially continuous 1-form vectors or derivative-continuous finite elements with an arbitrary mesh. Tangential vector finite elements provide correct solutions because the continuity of the normal component of the electric field is *not* specified, so that the discontinuity in the normal component is correctly produced by the natural boundary conditions in the variational principle.

The magnetic wall condition is $\mathbf{H}_{tang} = 0$, or, in terms of the electric field, $curl \mathbf{E}_{tang} = 0$. Using the finite element method based on the curl-curl equation for \mathbf{E} , there is no need to impose this boundary condition explicitly. The computed field will satisfy it approximately - to about the same accuracy as it satisfies the curl-curl equation itself. On the other hand, using the finite element method to solve the curl-curl equation for \mathbf{H} , the condition \mathbf{H}_{tang} must be imposed explicitly in advance.

The electric wall using the magnetic field formulation is the dual of the magnetic wall using the electric field formulation. The conducting wall condition is $\mathbf{E}_{tang} = 0$, or, in terms of the electric field, $curl \mathbf{H}_{tang} = 0$. Using the finite element method based on the curl-curl equation for \mathbf{H} , there is no need to impose this boundary condition explicitly. The computed field will satisfy it approximately - to about the same accuracy as it satisfies the curl-curl equation itself. On the other hand, using the FEM to solve the curl-curl equation for \mathbf{E} , the condition \mathbf{E}_{tang} must be imposed explicitly in advance.

2.5 Spurious Modes

“ Spurious modes ” have plagued the computation of resonant modes in cavities for years [35]. The problem consists of solving a curl-curl equation with a null right-hand side, that is, as in an eigenvalue problem. But when this equation is solved by conventional methods, like nodal vectorial elements, a numerical check of this equality shows that two kinds of numerical eigenmodes can be distinguished: those for which the divergence is effectively small (and decreases with the grain of the mesh) and those for which it is large, which are therefore unacceptable as physical solutions. One often says that the ‘spectrum’ is ‘polluted’ by these spurious modes, and the metaphorical way of referring to them (a ‘ plague ’, a ‘ curse ’, etc.) eloquently shows what a nuisance they may be and so either they must be eradicated or at least frightened away. Actually, even though they are still to be fully explained to which causes that they are related to, all these solutions have been proposed : the spurious modes can be sorted out by monitoring their divergence, or kept at bay by penalizing the divergence, or by using the equation $\text{div } \mathbf{B} = 0$ to reduce by one third the number of unknowns, by using divergence-free element bases, etc. None of these solutions seems to be fully efficient in practice.

Spurious solutions (or) vector parasites, the incorrect solutions generated by poor approximations of the null space of the curl operator, are supposed to be prevented from appearing by the “ tangentially continuous ” vector finite elements. These modes are formed with conventional Cartesian finite elements because polynomials of order less than five do not in general satisfy the proper compatibility conditions between elements. The other type of spurious modes may be due to incorrect solutions formed by linearly dependent approximation functions and is discussed in detail in [22].

2.6 Advantages and Comparisons

The primary advantages of the use of edge elements are:

- it imposes only the continuity of the tangential components of the electric and magnetic fields, as is required physically.
- does not over-prescribe the continuity of the normal components.
- the interfacial boundary conditions are automatically obtained through the natural boundary conditions in the variational process.
- Dirichlet boundary condition can be easily set along the element edges (like $E_{tan} = 0$ on a perfect electric conductor).
- divergence is zero ; the unwanted, divergent solutions are not present and there is no need to enforce a gauge by a penalty function.
- can handle material interfaces with combined permittivity and permeability.

When the merit of edge elements is plotted versus the cost of the solution [12], which is taken to be proportional to the size of the required matrix, the new tangential finite elements require only 60% of the work to achieve an approximation of a given accuracy compared with the traditional approach. Also, in terms of degrees of freedom, the two methods are equally effective in approximating the field.

But as is evident, the edge element method requires more number of unknowns, it being a hybrid method. Thus information regarding all the nodes and edges have to be stored and hence storage requirements are higher. Mesh generation is not a easy task and compared to a nodal FEM, this requires more computational time for the same number of nodes.

In summary, this chapter deals with the mathematical concepts, based on transformations to provide a powerful tool, in vector finite elements. The finite elements that

interpolate to either the tangential or the normal components of vector fields were also derived. The method presented in here has the flexibility that it can be extended to three dimensions.

Chapter 3

Application to Transmission Lines

3.1 Finite Element Formulation

Consider a dielectric waveguide with a diagonal permittivity tensor and assume that the electromagnetic field in the waveguide varies as $\exp[j(\omega t - \beta z)]$, where t is the time, z is the propagation direction, ω is the angular frequency, and β is the propagation constant in the z direction. The medium in general can be assumed to be linear, stationary, source-free but could be non-homogeneous and non-isotropic and the analysis is in frequency domain.

From Maxwell's equations in point form written in frequency domain, in the absence of conduction current and charges,

$$\nabla \times \mathbf{E} = -j\omega \mathbf{B}$$

$$\nabla \times \mathbf{H} = j\omega \mathbf{D}$$

$$\nabla \cdot \mathbf{D} = 0$$

$$\nabla \cdot \mathbf{B} = 0$$

the following wave equation can be derived, for non-magnetic material:

$$\nabla \times ([p] \nabla \times \phi) - k_o^2 [q] \phi = 0 \quad (3.1)$$

with

$$[p] = \begin{bmatrix} p_x & 0 & 0 \\ 0 & p_y & 0 \\ 0 & 0 & p_z \end{bmatrix} \quad (3.2)$$

$$[q] = \begin{bmatrix} q_x & 0 & 0 \\ 0 & q_y & 0 \\ 0 & 0 & q_z \end{bmatrix} \quad (3.3)$$

where k_o is the free-space wavenumber, ϕ denotes either fields \mathbf{E} or \mathbf{H} , and the components of $[p]$ and $[q]$ are given by

$$\begin{aligned} p_x &= p_y = p_z = 1, \\ q_x &= \epsilon_{rx} = n_x^2, \\ q_y &= \epsilon_{ry} = n_y^2, \\ q_z &= \epsilon_{rz} = n_z^2 \text{ for } \phi = \mathbf{E} \end{aligned} \quad (3.4)$$

$$\begin{aligned} q_x &= q_y = q_z = 1, \\ p_x &= \frac{1}{\epsilon_{rx}} = \frac{1}{n_x^2}, \\ p_y &= \frac{1}{\epsilon_{ry}} = \frac{1}{n_y^2}, \\ p_z &= \frac{1}{\epsilon_{rz}} = \frac{1}{n_z^2} \text{ for } \phi = \mathbf{H} \end{aligned} \quad (3.5)$$

Here, $\epsilon_{rx}, \epsilon_{ry}, \epsilon_{rz}$ are the relative permittivities in the x, y, z directions, respectively, and n_x, n_y, n_z are the refractive indices in the x, y, z directions, respectively. Here only an electrically anisotropic medium has been analyzed. It can be noted that a medium can be both electrically and magnetically anisotropic.

As seen in the earlier chapter, the variational energy functional for (3.1) is given by

$$\mathcal{F}(\phi) = \int_{\Omega} \int [(\nabla \times \phi)^* \cdot ([p] \nabla \times \phi) - k_o^2 [q] \phi^* \cdot \phi] dx dy \quad (3.6)$$

where Ω is the waveguide cross section and the asterisk $*$ denotes complex conjugate. From the functional, it can be seen that both $\nabla \times \phi$ and ϕ need to be square integrable. Therefore, the solution must be sought from the function space $L^2_{curl}(\Omega)$, which is defined by

$$L^2_{curl} = \{\phi \in L^2(\Omega) : \nabla \times \phi \in L^2(\Omega)\}$$

where $L^2(\Omega)$ is the linear space of square-integrable vector fields defined on the problem domain Ω .

A stationary energy functional can be constructed for either of the three components of \mathbf{E} or \mathbf{H} field vectors. In Cartesian coordinates, this functional is specialized to linearly polarized travelling waves and solution of this functional can be accomplished by linear edge finite element method which reduces the functional to a matrix form. The solution of the given curl-curl equation can be achieved by minimizing the associated functional.

3.1.1 Triangular Edge Finite element

The electromagnetic fields have to be tangentially continuous across material interfaces. Herewith, the edge element has been applied to the inhomogeneous waveguiding problems and a triangle has been used as the finite element, this being the most fundamental because two triangles can easily make a quadrilateral.

The six nodes described in the triangular edge element consist of three corner and three side points, as shown in Fig.3.1. The corner points 1 to 3 are for the axial component ϕ_z (E_z or H_z), while the side points 4 to 6 are for the tangential component ϕ_t (E_t or H_t).

The transverse components of the field now may be approximated in terms of edge unknowns and the azimuthal (axial) components in terms of the nodal unknowns. There is no inconsistency in this type of decomposition since ϕ_z is tangential to all boundary surfaces in the plane of interest and the condition that $\phi_z = 0$ on the conducting surfaces

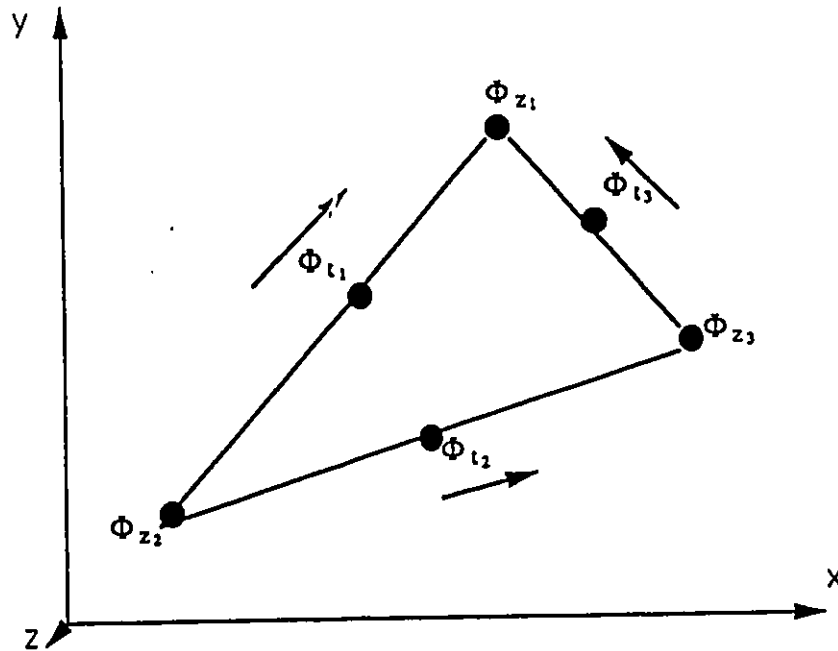


Figure 3.1: Triangular Edge Element

is easily satisfied. Similarly, since the edge unknowns represent the projection of the electric field onto a given edge of the triangular element, the condition

$$\hat{i} \cdot \phi_t = 0$$

is also easily satisfied, where as usual \hat{i} is the unit vector tangential to the conductor surface. An advantage of the application of the edge element technique is that due to the use of ϕ_t as a state variable, the Dirichlet boundary condition for the electric field can be enforced, without difficulty, on the perfect conductor surfaces.

The axial (or) the longitudinal component ϕ_z is approximated by a complete polynomial of first order:

$$\phi_z = j \{N(x, y)\}^T \{\phi_z\}_e = j \{N\}^T \{\phi_z\}_e \quad (3.7)$$

with

$$N = \begin{bmatrix} \zeta_1 \\ \zeta_2 \\ \zeta_3 \end{bmatrix} = \frac{1}{2A_e} \begin{bmatrix} a_1 & b_1 & c_1 \\ a_2 & b_2 & c_2 \\ a_3 & b_3 & c_3 \end{bmatrix} \begin{bmatrix} 1 \\ x \\ y \end{bmatrix} \quad (3.8)$$

where $\{\phi_x\}_e$ is the nodal axial-field vector for each element. $\{N\}$ is the ordinary shape function vector for the linear triangular element, ζ_i 's ($i = 1,2,3$) are the area coordinates (or simplex coordinates), and, the area of the triangular element, A_e , and the coefficients are given by [34]

$$2A_e = \begin{vmatrix} 1 & 1 & 1 \\ x_1 & x_2 & x_3 \\ y_1 & y_2 & y_3 \end{vmatrix} \quad (3.9)$$

$$a_i = x_j y_k - x_k y_j \quad (3.10)$$

$$b_i = y_j - y_k \quad (3.11)$$

$$c_i = x_k - x_j \quad (3.12)$$

Here x_i, y_i ($i = 1,2,3$) are the Cartesian coordinates of the corner points 1 to 3 of the triangle and the subscript i, j, k always progress modulo 3, i.e., cyclically around the three vertices of the triangle.

The transverse components ϕ_x (E_x or H_x) and ϕ_y (E_y or H_y) are approximated by a linear function of y and x , respectively:

$$\phi_x = \{U(y)\}^T \phi_e = \{U\}^T \phi_e \quad (3.13)$$

$$\phi_y = \{V(x)\}^T \phi_e = \{V\}^T \phi_e \quad (3.14)$$

with

$$\{U\} = \begin{bmatrix} \bar{a}_1 + \bar{c}_1 y \\ \bar{a}_2 + \bar{c}_2 y \\ \bar{a}_3 + \bar{c}_3 y \end{bmatrix} \quad (3.15)$$

$$\{V\} = \begin{bmatrix} \bar{b}_1 - \bar{c}_1 x \\ \bar{b}_2 - \bar{c}_2 x \\ \bar{b}_3 - \bar{c}_3 x \end{bmatrix} \quad (3.16)$$

where $\{\phi\}_e$ is the edge variables in the transversal place of each element. $\{U\}$ and $\{V\}$ are the shape function vectors for the triangular edge element, and the coefficients $\bar{a}_i, \bar{b}_i, \bar{c}_i$ are given by

$$\begin{aligned} \bar{a}_i = & -[(y_{k+3} \cos \theta_{k+3} - x_{k+3} \sin \theta_{k+3}) \sin \theta_{j+3} \\ & -(y_{j+3} \cos \theta_{j+3} - x_{j+3} \sin \theta_{j+3}) \sin \theta_{k+3}] / \Delta \end{aligned} \quad (3.17)$$

$$\begin{aligned} \bar{b}_i = & -[(y_{j+3} \cos \theta_{j+3} - x_{j+3} \sin \theta_{j+3}) \cos \theta_{k+3} \\ & -(y_{k+3} \cos \theta_{k+3} - x_{k+3} \sin \theta_{k+3}) \cos \theta_{j+3}] / \Delta \end{aligned} \quad (3.18)$$

$$\bar{c}_i = -(\cos \theta_{j+3} \sin \theta_{k+3} - \cos \theta_{k+3} \sin \theta_{j+3}) / \Delta \quad (3.19)$$

with

$$0 \leq \theta_{i+3} = \tan^{-1}\{(y_i - y_j) / (x_i - x_j)\} < \pi \quad (3.20)$$

(the angles measured in radians). One can assume any random direction of the edge variables. There is the only condition that any edge shared by two triangles must have the same directions, and of course the same magnitude. In (3.20), the range for the angles has been defined. Here, the directions of the edge variables change according to the state of the element-division. So, in Fig. 3.1., the direction of the ϕ_{i_2} sometimes becomes from direction 3 to 2.

$$\begin{aligned} \Delta = & -\sum_{i=1}^3 (y_{i+3} \cos \theta_{i+3} - x_{i+3} \sin \theta_{i+3}) \\ & \cdot (\cos \theta_{j+3} \sin \theta_{k+3} - \cos \theta_{k+3} \sin \theta_{j+3}) \end{aligned} \quad (3.21)$$

Here x_{i+3}, y_{i+3} ($k = 1, 2, 3$) are the Cartesian coordinates of the side points 4 to 6 of the triangle.

Note that the tangential component, $\phi_t = \phi_x \cos \theta + \phi_y \sin \theta$, is continuous along the interelement boundaries and is constant on each side of the triangles. That is, the tangential component along the common side is same in sign and magnitude, namely continuous, and not the transverse components.

Proof: Let it be assumed

$$\begin{aligned}\phi_x &= \alpha_1 + \alpha_2 y \\ \phi_y &= \alpha_3 - \alpha_2 x\end{aligned}\tag{3.22}$$

because the mesh would be refined so high, that it can be assumed that along the x-direction, there is variation only with reference to y and along y-direction, there is variation only with reference to x.

Thus,

$$\begin{aligned}\phi_{x_1} &= \alpha_1 + \alpha_2 y_{i+3} \\ \phi_{x_2} &= \alpha_1 + \alpha_2 y_{j+3} \\ \phi_{x_3} &= \alpha_1 + \alpha_2 y_{k+3}\end{aligned}\tag{3.23}$$

and

$$\begin{aligned}\phi_{y_1} &= \alpha_3 - \alpha_2 x_{i+3} \\ \phi_{y_2} &= \alpha_3 - \alpha_2 x_{j+3} \\ \phi_{y_3} &= \alpha_3 - \alpha_2 x_{k+3}\end{aligned}\tag{3.24}$$

Also,

$$\begin{aligned}\phi_{t_1} &= \phi_{x_1} \cos \theta_{i+3} + \phi_{y_1} \sin \theta_{i+3} \\ \phi_{t_2} &= \phi_{x_2} \cos \theta_{j+3} + \phi_{y_2} \sin \theta_{j+3} \\ \phi_{t_3} &= \phi_{x_3} \cos \theta_{k+3} + \phi_{y_3} \sin \theta_{k+3}\end{aligned}\tag{3.25}$$

Putting (3.23) and (3.24) into (3.25),

$$\begin{aligned}\phi_{t_1} &= (\alpha_1 + \alpha_2 y_{i+3}) \cos \theta_{i+3} + (\alpha_3 - \alpha_2 x_{i+3}) \sin \theta_{i+3} \\ &= \alpha_1 \cos \theta_{i+3} + \alpha_2 (y_{i+3} \cos \theta_{i+3} - x_{i+3} \sin \theta_{i+3}) \\ &\quad + \alpha_3 \sin \theta_{i+3}\end{aligned}$$

and similarly

$$\begin{aligned}
\phi_{t_2} &= \alpha_1 \cos \theta_{j+3} + \alpha_2 (y_{j+3} \cos \theta_{j+3} - x_{j+3} \sin \theta_{j+3}) \\
&\quad + \alpha_3 \sin \theta_{j+3} \\
\phi_{t_3} &= \alpha_1 \cos \theta_{k+3} + \alpha_2 (y_{k+3} \cos \theta_{k+3} - x_{k+3} \sin \theta_{k+3}) \\
&\quad + \alpha_3 \sin \theta_{k+3}
\end{aligned} \tag{3.26}$$

Let

$$\begin{aligned}
e_i &= \cos \theta_{i+3} \\
f_i &= (y_{i+3} \cos \theta_{i+3} - x_{i+3} \sin \theta_{i+3}) \\
g_i &= \sin \theta_{i+3}
\end{aligned}$$

Thus,

$$\begin{aligned}
e_1 \alpha_1 + f_1 \alpha_2 + g_1 \alpha_3 &= \phi_{t_1} \\
e_2 \alpha_1 + f_2 \alpha_2 + g_2 \alpha_3 &= \phi_{t_2} \\
e_3 \alpha_1 + f_3 \alpha_2 + g_3 \alpha_3 &= \phi_{t_3}
\end{aligned} \tag{3.27}$$

Thus

$$\det = \begin{bmatrix} e_1 & f_1 & g_1 \\ e_2 & f_2 & g_2 \\ e_3 & f_3 & g_3 \end{bmatrix}$$

After due expansion, it can be observed that

$$\det = \Delta$$

that is given in (3.21). (3.27) is a set of linear algebraic equations with three unknowns.

It can be solved by Cramer's rule to yield

$$\begin{aligned}
\alpha_1 &= (\phi_{t_1} \bar{a}_i + \phi_{t_2} \bar{a}_j + \phi_{t_3} \bar{a}_k) \\
\alpha_2 &= (\phi_{t_1} \bar{c}_i + \phi_{t_2} \bar{c}_j + \phi_{t_3} \bar{c}_k) \\
\alpha_3 &= (\phi_{t_1} \bar{b}_i + \phi_{t_2} \bar{b}_j + \phi_{t_3} \bar{b}_k)
\end{aligned}$$

Therefore

$$\begin{aligned}\phi_x &= \alpha_1 + \alpha_2 y = \{U\}^T \{\phi_t\}_e \\ \phi_y &= \alpha_3 - \alpha_2 x = \{V\}^T \{\phi_t\}_e\end{aligned}$$

which are just (3.13) and (3.14).

Note:

- The directions of the edge variables change according to the state of element division, in this definition. That is, if $(y_i - y_j) / (x_i - x_j) \geq 0$, then the direction is from Node j to Node i . Or, if $(y_i - y_j) / (x_i - x_j) < 0$, then the direction is from Node i to Node j .
- The tangential component ϕ_t , and not the *transverse component*, along the common side between triangles, is the same in sign and magnitude, namely continuous, iff locally both triangles assume the same direction along the common side.

3.1.2 Finite-element Discretization

Dividing the waveguide cross section into a number of edge elements, the transverse components ϕ_x , ϕ_y and the axial component ϕ_z in each element can be expanded as

$$\phi = [N]^T \phi_e \quad (3.28)$$

with

$$\phi_e = \begin{bmatrix} \{\phi_t\}_e \\ \{\phi_z\}_e \end{bmatrix} \quad (3.29)$$

$$[N] = \begin{bmatrix} \{U\} & \{V\} & \{0\} \\ \{0\} & \{0\} & j\{N\} \end{bmatrix} \quad (3.30)$$

where $\{0\}$ is a null, zero vector. It sums up to six unknowns per triangle, three each of axial and transverse components.

Since the propagation constant in the z direction is β , each component of ϕ is proportional to $\exp\{-j\beta z\}$. Therefore, ∇ may be written as $(\nabla_t - j\beta\hat{z})$ where ∇_t is equal to $\hat{x}\partial/\partial x + \hat{y}\partial/\partial y$ and $\hat{x}, \hat{y}, \hat{z}$ are the unit vectors in the x, y, z directions, respectively.

Therefore

$$\nabla \times = (\nabla_t - j\beta\hat{z}) \times = \begin{bmatrix} 0 & j\beta & \frac{\partial}{\partial y} \\ -j\beta & 0 & -\frac{\partial}{\partial x} \\ -\frac{\partial}{\partial y} & \frac{\partial}{\partial x} & 0 \end{bmatrix} \equiv [\mathcal{D}]$$

Thus,

$$\nabla \times \phi = [\mathcal{D}][N]^T \phi_e = [B]^T \phi_e$$

where

$$[B] = ([\mathcal{D}][N]^T)^T = \begin{bmatrix} j\beta\{V\} & -j\beta\{U\} & \{V_z\} - \{U_y\} \\ j\{N_y\} & -j\{N_x\} & 0 \end{bmatrix} \quad (3.31)$$

Substituting (3.28) into the functional in (3.6), from the variational principle, the following eigenvalue problem is obtained:

$$[K]\phi - k_o^2[M]\phi = 0 \quad (3.32)$$

with

$$\begin{aligned} [K] &= \begin{bmatrix} [K_{tt}] & [K_{tz}] \\ [K_{zt}] & [K_{zz}] \end{bmatrix} \\ &= \sum_c \int_c \int [B]^* \cdot [p][B]^T dx dy \end{aligned} \quad (3.33)$$

$$\begin{aligned} [M] &= \begin{bmatrix} [M_{tt}] & [0] \\ [0] & [M_{zz}] \end{bmatrix} \\ &= \sum_c \int_c \int [N]^* \cdot [q][N]^T dx dy \end{aligned} \quad (3.34)$$

where $\{\phi\}$ is the global field vector and the submatrices of $[K]$ and $[M]$ are given by

$$[K_{tt}] = \sum_c \int_c \int [p_x \beta^2 \{V\} \{V\}^T + p_y \beta^2 \{U\} \{U\}^T + 4p_z \{U_y\} \{U_y\}^T] dx dy \quad (3.35)$$

$$[K_{tz}] = [K_{zt}]^T = \sum_c \int_c \int [p_x \beta \{V\} \{N_y\}^T + p_y \beta \{U\} \{N_x\}^T] dx dy \quad (3.36)$$

$$[K_{zz}] = \sum_e \int_e \int [p_x \{N_y\} \{N_y\}^T + p_y \{N_x\} \{N_x\}^T] dx dy \quad (3.37)$$

$$[M_{tt}] = \sum_e \int_e \int [q_x \{U\} \{U\}^T + q_y \{V\} \{V\}^T] dx dy \quad (3.38)$$

$$[M_{zz}] = \sum_e \iint q_z \{N\} \{N\}^T dx dy \quad (3.39)$$

Here, as observed,

$$\{N_x\} \equiv \partial\{N\}/\partial x,$$

$$\{N_y\} \equiv \partial\{N\}/\partial y,$$

$$\{U_y\} \equiv \partial\{U\}/\partial y,$$

$$\{V_x\} \equiv \partial\{V\}/\partial x$$

(3.32) is an eigenvalue problem that solves for frequency, when the propagation constant is given. But it is interesting to have to solve for β , when the ω is provided. Thus, after some rearrangement, the (3.32) can be rewritten as

$$[K_{tt}]' \{\phi_t\} - \beta [K_{tz}]' \{\phi_z\} - \beta^2 [M_{tt}]' \{\phi_t\} = 0 \quad (3.40)$$

$$-\beta [K_{zt}]' \{\phi_t\} + [K_{zz}]' \{\phi_z\} = 0 \quad (3.41)$$

with now,

$$[K_{tt}]' = \sum_e \int_e \int [q_x k_o^2 \{U\} \{U\}^T + q_y k_o^2 \{V\} \{V\}^T - 4p_z \{U_y\} \{U_y\}^T] dx dy \quad (3.42)$$

$$[K_{tz}]' = [K_{zt}]' = \sum_e \int_e \int [p_x \{V\} \{N_y\}^T + p_y \{U\} \{N_x\}^T] dx dy \quad (3.43)$$

$$[K_{zz}]' = \sum_e \int_e \int [q_z k_o^2 \{N\} \{N\}^T - p_x \{N_y\} \{N_y\}^T - p_y \{N_x\} \{N_x\}^T] dx dy \quad (3.44)$$

$$[M_{tt}]' = \sum_e \int_e \int [p_x \{V\} \{V\}^T + p_y \{U\} \{U\}^T] dx dy \quad (3.45)$$

K_{tt} and M_{tt} are matrices involving only edge contributions and K_{zz} involves only nodal contributions. But the matrices K_{tz} and K_{zt} involve both the edge and nodal contributions and this is the only matrix which accounts for the nonsymmetry of the eventual

resultant matrices. Note that the submatrices in (3.42) to (3.45) are different from those in (3.35) to (3.39).

Substituting (3.41) into (3.40), to get rid of longitudinal components, by writing it in terms of the transversal components, the following final eigenvalue problem is obtained:

$$[K_{tt}]' \{\phi_t\} - \beta^2 [\tilde{M}_{tt}] \{\phi_t\} = 0 \quad (3.46)$$

with

$$[\tilde{M}_{tt}] = [M_{tt}]' + [K_{tz}]' [K_{zz}]'^{-1} [K_{zt}]'. \quad (3.47)$$

Note that (3.47) would give a solution directly for the propagation constant β and the corresponding field distribution ϕ , and involves only the edge variables in the transversal plane ϕ_t . Incidentally, $\beta^2 = \kappa_e k_0^2$, where κ_e is called the effective dielectric constant. This effective dielectric constant is more commonly used in all literatures as this is a less sensitive parameter than the propagation constant itself. But it is important to point out that, although the initial matrices are sparse, the price paid for this (3.47) is: a matrix inversion has to be performed and the sparsity of the matrices are destroyed. The Dirichlet boundary conditions (both ϕ_t and ϕ_z) are set as soon as (3.40) and (3.41) are obtained in order to accurately make (3.46). The boundary conditions of all three components must be taken care of in order to obtain the physically exact solutions (to restrict physically the electromagnetic field) and that is why the boundary conditions even for ϕ_z has to be considered, making this method a hybrid one involving both edge and node variables.

The integrals necessary to construct the element matrices for the resonant-problem are all closed form expressions and are given in Appendix B.

3.1.3 Deterministic problems

If the propagation constant is 0, that is when the structure is at cutoff or at resonance, a forced problem is obtained, which is just a modification of (3.46) :

$$[K_{tt}]' \{\phi_t\} = \{0\}$$

Here, the ϕ_t has to be solved for after some matrix manipulations are done to add contribution to the right hand side and reduce the order of the matrix. This is simple, as only a sparse matrix is involved.

Also a non-resonant problem can be got when β is known beforehand, by analytical formulae, in which case (3.46) becomes

$$([K_{tt}]' - \beta^2 [\tilde{M}_{tt}]) \{\phi_t\} = \{0\}$$

which transforms, after boundary conditions are set, into

$$[A]\{\phi_t\} = [B]$$

which is a system of linear equations, and has to be solved for the fields. Hence, as observed, for the deterministic problems, the field distributions have been solved as the unknowns directly. The solvers, for both real and complex matrices have been taken from the library routine package called LINPACK.

A generalized finite element approach utilizing the edge unknowns in conjunction with nodal unknowns has been presented, for both deterministic problems and eigenvalue problems. This approach may be readily modified for use in design problems, which are of great interest in the development of electronic packaging techniques. The method proves to be versatile and lends itself to many applications.

3.2 Matrix methods

The main characteristics of a propagation or dynamic problem is that the response of the system under consideration changes with time. Hence, it can be implied that there exists no unique solution for the response of the system, be it dynamic or steady state. Eigenvalue problems arise in both steady state and dynamic analysis and the main characteristic of an eigenvalue problem is that there is no unique solution to the response of the system.

The stationary points of the function $\mathcal{F}\{\phi\}$ in (3.6) correspond to the solutions of the generalized eigenmatrix equation (3.46). This might be rewritten as

$$[A]x = \lambda[B]x$$

where $\lambda = \beta^2$, $[A] = [K_{tt}]'$ and $[B] = [\tilde{M}_{tt}]$. Here both $[A]$ and $[B]$ are indefinite matrices, and $[A]$ is sparse and symmetric and $[B]$ is dense and non-symmetric. The matrix is referred to as dense since the percentage of zero elements or its distribution is such as to make it uneconomic to take advantage of their presence. The resonant modes of the problem could be computed more or less in the order of dominance, with the more dominant mode corresponding to the larger eigenvalue.

Some interesting properties about matrices are given here, before the methods used to solve the eigenvalue problem are given:

- The eigenvalues are the roots of the characteristic polynomial - $\det ([A] - \lambda [B])$.
- A matrix and its transpose have the same eigenvalues.
- The eigenvectors are not unique, as they are normalized to some constant. That is, an eigenvector is only defined within a multiple of itself.
- The inverse of a symmetric matrix is always symmetric.

- The product of two symmetric matrices is symmetric, if and only if they are commutative, i.e. $[A][B] = [B][A]$.
- If $[B]$ is symmetric, then $[A][B][A]^T$ is symmetric, where $[A]$ need not necessarily be symmetric.
- A real matrix in general can have complex eigenvalues, only when it is non-symmetric.
- If $[A]$ and $[B]$ are real matrices, only when $[B]$ is non-singular, can the generalized eigenvalue problem be transformed into $[B]^{-1}[A]x = \lambda x$. When $[B]$ is singular though, this is *not* valid, as there is not a complete set of eigenvalues.
- For a matrix $[A]$ with real elements, the eigenvectors, if complex, can be expressed as complex conjugate pairs.

In (3.46), a variety of factors enter into the determination of the most efficient algorithm for its solution. There is no single algorithm that always provides an efficient solution. The most important are:

- Eigenvalues and eigenvectors may be required or the eigenvalues only.
- The *complete* set of eigenvalues and/or eigenvectors may be required or only a comparatively small number (that is only the first two modes).
- For very large matrices (for higher orders), the economy of storage may well be the paramount consideration in the selection. A matrix is called small when all its elements are equally and rapidly accessible; otherwise, it is large.
- The results may be required to only a modest accuracy or high precision may be vital.

A package of FORTRAN programs given the acronym EISPACK is a systematized collection of subroutines [36] which compute the eigenvalues and/or eigenvectors for all classes of matrices. The subroutines based mainly upon Algol procedures published by Wilkinson and Reinsch [37], have been adapted and thoroughly tested on several machines, and are based on algorithms which are numerically stable.

Due to unsymmetry, the eigenvalues are in general complex. The complex eigenvalue pairs are stored in consecutive elements of the array, with that member of the pair with positive imaginary part first, in all these routines. And then, it is also impossible to design equally satisfactory algorithms for the nonsymmetric cases when compared to the symmetric cases [38]. There are two reasons for this: First, the eigenvalues of the nonsymmetric matrix can be very sensitive to small changes in the matrix elements ('*ill-conditioned*'). Second, the matrix itself can be defective, so that there is no complete set of eigenvectors. It is emphasized that these difficulties are intrinsic properties of certain nonsymmetric matrices, and no numerical procedure can "cure" them. The best is to have procedures which do not exacerbate such problems.

The presence of rounding errors can only make the situation worse. With finite-precision arithmetic, one cannot even design a foolproof algorithm to determine whether a given matrix is defective or not. Thus current algorithms generally try to find a *complete* set of eigenvectors, and rely on the user to inspect the results. If many eigenvectors are almost parallel, the matrix is probably defective. The sensitivity of eigenvalues to rounding errors during the execution of some algorithms can be reduced by the procedure of *balancing*. The errors in the eigensystem found by a numerical procedure are generally proportional to the Euclidean norm of the matrix, that is, to the square root of the sum of the squares of the elements. The idea of balancing is to use similarity transformations to make corresponding rows and columns of the matrix have comparable norms, thus reducing the overall norm of the matrix while leaving the eigenvalues

unchanged. A symmetric matrix is already balanced. It is recommended that a non-symmetric matrix be balanced always, as it can substantially improve the accuracy of the eigenvalues computed for a badly balanced matrix. The operation of 'balancing' includes two distinct functions: permutation of the rows and columns of the matrix to display any isolated eigenvalues, and the equilibration of the remaining of the matrix.

The best algorithm for finding all eigenvalues and eigenvectors of a real, general matrix is based on a combination of a reduction to Hessenberg form using the pair of procedures *elmhes* and *eltran* followed by the QR algorithm *hqr 2*. If the procedure *balanc* has been used, the eigenvectors of the original matrix are recovered from those of the balanced matrix using the procedure *balbak*. If the eigenvalues only are required, then *hqr* is used in place of *hqr 2*.

In *elmhes*, considerable advantage can be taken of the presence of zero elements in the matrix, and if the matrix is very sparse *elmhes* is strongly recommended. When the matrix has multiple eigenvalues corresponding to linear divisors, *hqr 2* determines fully independent vectors. *hqr 2* is very economical on storage.

There is no procedure for finding selected eigenvalues, but when all eigenvalues have been computed using *hqr*, eigenvectors corresponding to a small number of selected eigenvalues (i.e. first two or three modes) may be found using the procedure *invt*. As is usual with inverse iteration, the speed and accuracy of *invt* are very satisfactory for well separated eigenvalues and the procedure provides an elegant solution to the problem. For coincident and pathologically close eigenvalues the procedure is aesthetically less satisfying. If more than 25% of the eigenvectors are wanted, it is almost invariably more satisfactory to use *hqr 2*.

In the problems analyzed, ill-conditioning has sometimes been encountered as one problem and the subroutines utilized were the most optimum for the resultant matrices, although not the best. Thus the results obtained still suffered from inherent flaws due

to the limitations of the subroutines used in solving for the inverse of the matrix and for solving the eigen-value problem.

Chapter 4

Description of the Computer Program

For every edge in the finite element discretized region Ω , there is only one degree of freedom: ϕ_t . For every node in the finite element discretized region Ω , there is only one degree of freedom: ϕ_z . The final system of equations produced after the assembly of the contributions from each edge were stored in a $NE \times NE$ matrix, where NE is the total number of edges. The final system of equations produced after the assembly of the contributions from each node were stored in a $NO \times NO$ matrix, where NO is the total number of nodes. If the Dirichlet boundary conditions for both edges and nodes were imposed, then the number of unknowns become fewer.

The program for the edge element formulation has been written in FORTRAN under UNIX environment and tested on DEC 2100/3100 workstations. It has been appropriately named FREDEEM.F, an abbreviation for 'FREquency Domain Edge Element Method'. When the unknown variables are complex, they would require twice the memory of the real variables. It has been preferred to use double precision variables, to minimize the errors introduced by round-off and discretization, and thus the memory requirement simply for the coefficients of the systems of equations had been $16 NE^2$ and $16 NO^2$ bytes, for edges and nodes respectively.

The body of the program could be broken into Five major parts :

1. *Parameter Input* - All the physical and geometrical dimensions of the structure being analyzed (width, permittivity, etc) were given as input or read in from an Input file alongwith the frequencies of observation and an Output file was also opened for storing the solutions later.
2. *Co-ordinate Generator* - It does computations on the input that has been given to it, does some calculations and generates the co-ordinates corresponding to all the nodes in the structure.
3. *Node & Edge Generator* - It works on the coordinates and identifies the nodes and edges locally for each and every triangle and has been originally created for this purpose. It can be further modified for automatic and adaptive mesh generator. It is generalized only to rectangular geometry, with modifications to include regular geometries like circular structures, but it is preferable (although tedious) to use a DATA statement for complex, irregular structures.
4. *Forcing the Boundary Conditions* - In this particular part, the nodes and edges that fall on the boundaries were identified and set as Dirichlet Boundary conditions to the problem. Incidentally, the beauty here is that the value of the forced boundary need not be known for the nodes as long it is known to be a forced boundary node. But the edge requires information about whether it is a Dirichlet boundary or not, and if it is, its value too. The reason behind which the nodal Dirichlet value need not be known is because they are for intermediate calculations and the whole nodal part of the hybrid method gets eliminated as the final equation is set up by some algebraic manipulations.
5. *Numerical Formulation* - It had used the technique given in Chapter 3 to create all the matrices there, with a good amount of algebraic arithmetic involved. It

had calculated the contributions of each transversal edge variable and each axial node variable and summed it over the surface of each triangular element, and then combined them to generate the global coefficient matrix, at each frequency. Simple, original subroutines have been written to compute the transpose of a matrix, to multiply and add two matrices and a general inverse routine has been called for, GAUSSJ, from the library of routines, be it for dense or sparse, symmetric or nonsymmetric matrix and for any definiteness of the matrix.

6. *Solution and Output* - The deterministic problem, were solved by subroutines from the LINPACK library, for both real and complex matrices. The eigenvalue problem, stored in matrix form has been reduced and solved by subroutines from EISPACK library. The output eigenvalues (the propagation factors) were sorted out in descending order and the eigenvectors (the transversal edge variables) for selective eigenvalues, useful for calculating the transverse components of fields, were produced as outputs.

The final system of matrices were not symmetric, and regardless of the way the edges were numbered, there has been uniqueness in the solutions obtained. Convergence of the solutions, by means of various applicable subroutines, has been found to be satisfactory. The basic, general program for a typical rectangular cross-section has been provided in Appendix C.

Chapter 5

Results and Discussions

A general purpose computer program in FORTRAN, "FREDEEM.F" has been written in frequency domain for two-dimensional applications in cartesian coordinates, to implement the preceding analysis, for both deterministic problems and eigenvalue problems. The element size have been chosen conveniently in such a way that the outer lines coincide with the boundaries and all geometrical discontinuities include nodes and edges. The electric conductors are perfectly conducting walls, namely electric walls. So, ϕ_t and ϕ_z on all outer conductors and the strip (if any) have to be set to zero. All structures analyzed were assumed to be non-magnetic, that is, the magnetic permeabilities of all regions are the same as free-space. Concentration has been given on transmission lines that would be of interest in electrical interconnects and hence such structures have been discussed theoretically. Edge elements can be well suited for dielectric materials because they imply the tangential continuity of the electric field across the interfaces and take account of the discontinuity of their normal component. Eigenvalue problems have been discussed in more detail, as a deterministic problem is just a modification of the former. A property of any finite element method is the convergence of the solution increases as the problem size decreases and this is applied to edge elements too.

5.1 Deterministic Problems:

To illustrate applications to deterministic problems, simple situations like eddy-current problems (finite conductivity) and rectangular waveguides have been analyzed. The forced problem always has a known source of excitation and a particular known propagation constant β . Thus, the final set of matrix equations to be solved would be algebraic and LINPACK routines have been used as solvers.

5.1.1 Test Problem : Parallel Plate Waveguide

The parallel plate waveguide (Fig.5.1.) has been analyzed in H-field. One assumes that both plates are perfect conductors, separated by $W = 0.01$ m and that the plate dimension D in the y -direction is very large so no field vectors have any y -dependence - that is, $\partial/\partial y = 0$ as $D \gg W$. This latter assumption can be physically justified when the fields are confined between the plates and when consequently there are negligible fringing fields outside the edges at $y = 0$ and $y = D$.

The transverse magnetic (TM) waves to be analyzed have only the H_y , E_x and E_z field components. The solutions of the wave equation is expected to represent waves propagating in the z -direction. All the field components have been known to vary only along x -direction in a sinusoidal or cosinusoidal way. Applying the boundary conditions that E_z is zero at the two conductors, gives the guidance condition

$$k_x W = m \pi$$

where m is any integer, which is incidentally identical to the boundary condition for TE waves[39]. When $m = 0$, the TM_0 mode is excited, which is better known as the TEM mode, whose cutoff frequency is zero.

For our test example, the TM_1 mode has been forced ($m = 1$) and the normalized

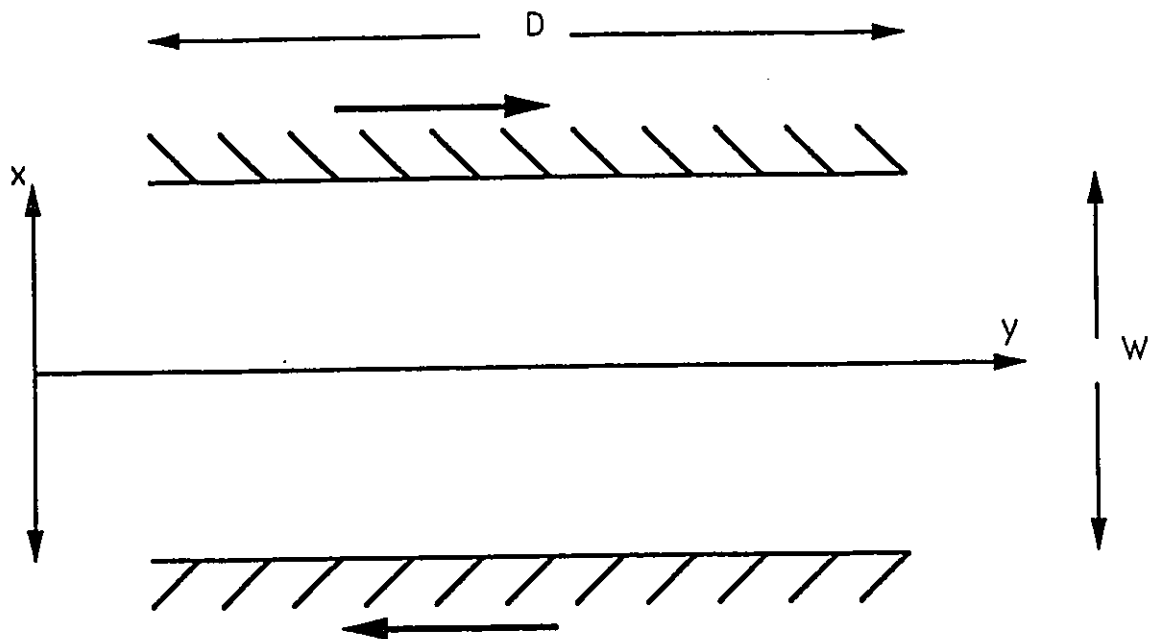


Figure 5.1: Test Geometry : Parallel Plate Waveguide.

H-field component has been given below:

$$H_y = \cos k_x x$$

According to the physical criteria, the boundary conditions for the edges on the conductors for the normalized H-field has been set to +1 at $x = 0$ and -1 at $x = W$. The simulated plot has also been compared with the analytical results in Fig.5.2. The results agree exactly with the analytical results, even when the 2-D algorithm was simulating the 1-D problem. Only for more rectangles along y-direction than in the x-direction is the solution exact, because of the assumption of the shape functions for the transverse components. A bad choice in discretization gives unsatisfactory results and the mesh size has been seen to be proportional to length D. The mesh divisions had 400 triangles with 630 edges and 231 nodes and the cutoff frequency of the TM_1 mode for the given

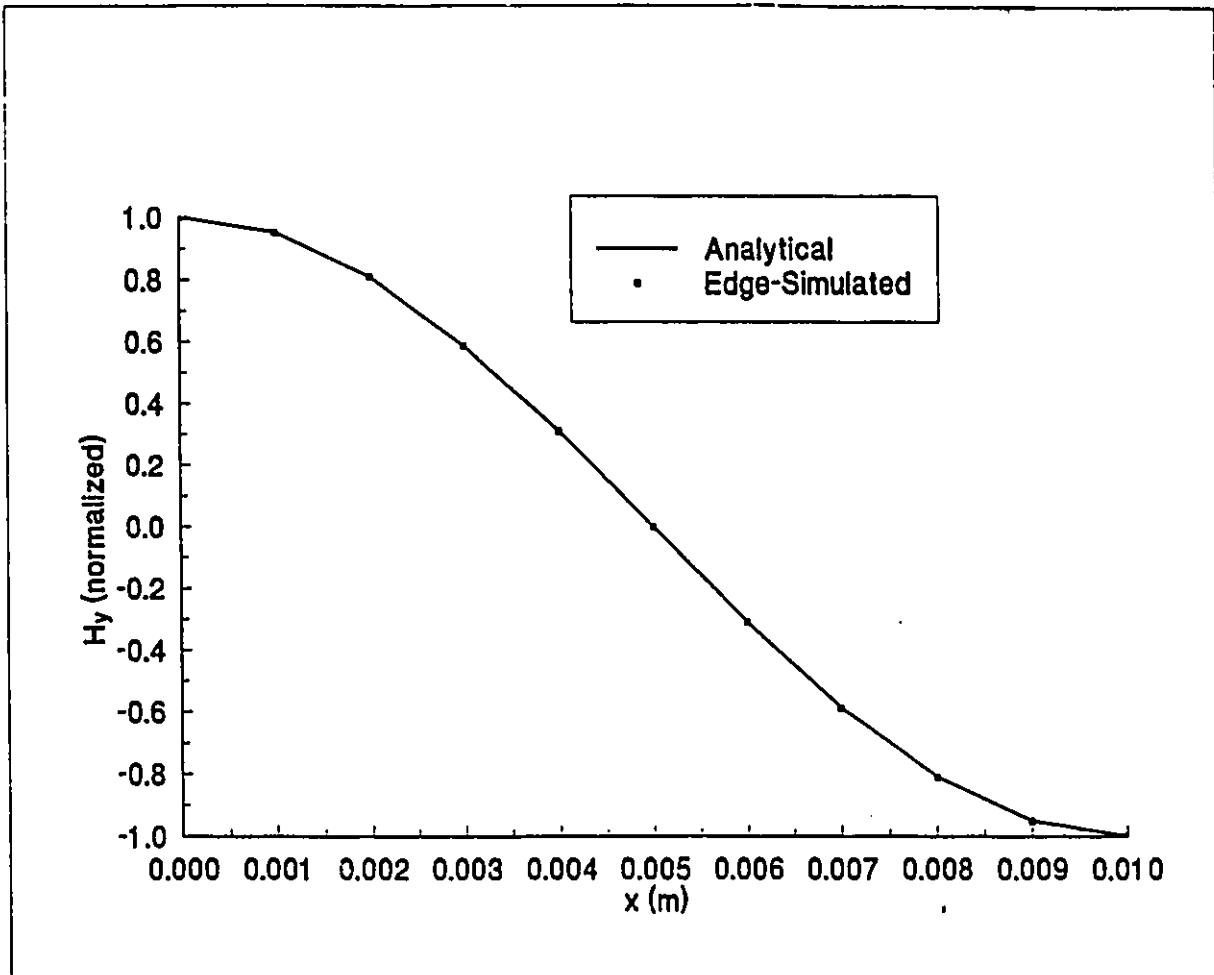


Figure 5.2: TM_1 mode for Parallel Plate Waveguide

dimension was 14.9898 GHz.

5.1.2 Rectangular Waveguide

The rectangular waveguide of width W and height B (Fig.5.3.) has been excited to simulate the TE mode. If a region of space is bound by a perfect electric conductor, with no magnetic currents flowing in its surface, then it can be solved by E field formulation as has been done here. The source has been put in the middle of the waveguide and has been normalized to 1.0, to simulate the dominant TE_{10} mode at cutoff ($\beta = 0$). The cut-off frequencies for the first mode, for the dimensions $W = 0.003$ m and $B = W/2$ is found by the relation $f_c = c_0 k_c / 2\pi$ where c_0 is the velocity of light in free-space

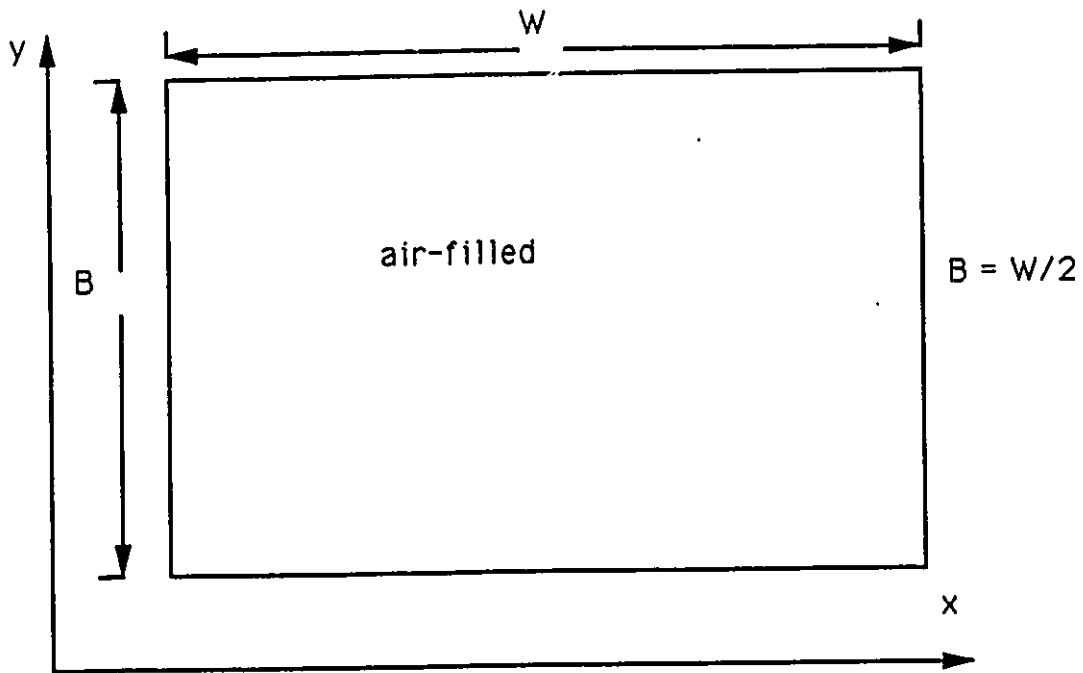


Figure 5.3: Rectangular air-filled waveguide

and k_z can be found to be 1047.1975. There had been 360 triangles, 603 edges and 244 nodes in total for this problem and the reciprocal condition was in the order of $1E-4$. The results by simulation and by analytical means for the normalized field E_y has been shown in Fig.5.4. There were more divisions along x because the variation is only along that direction in this case, and the whole structure has been analyzed. The dominant mode here has been simulated very well, as seen from the smoothness of the 3-D contour and also the exact match with the analytical formula given by $E_y = \cos \pi x/W$. If the shape functions had been assumed to be sinusoidal functions here and also in the previous case, the results would be much better, even at lower discretizations.

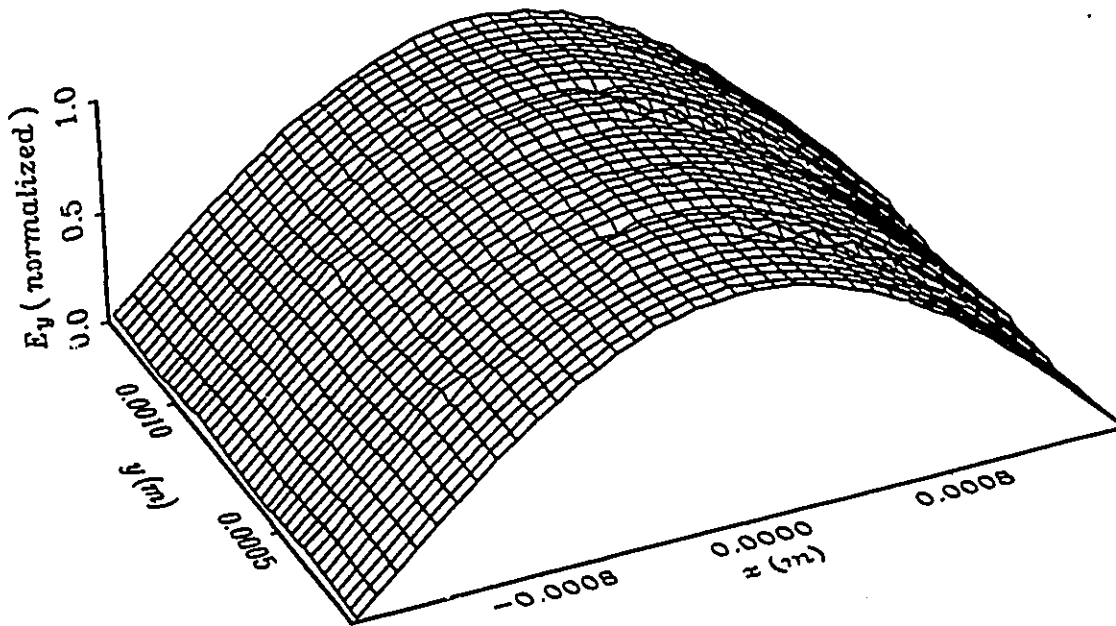
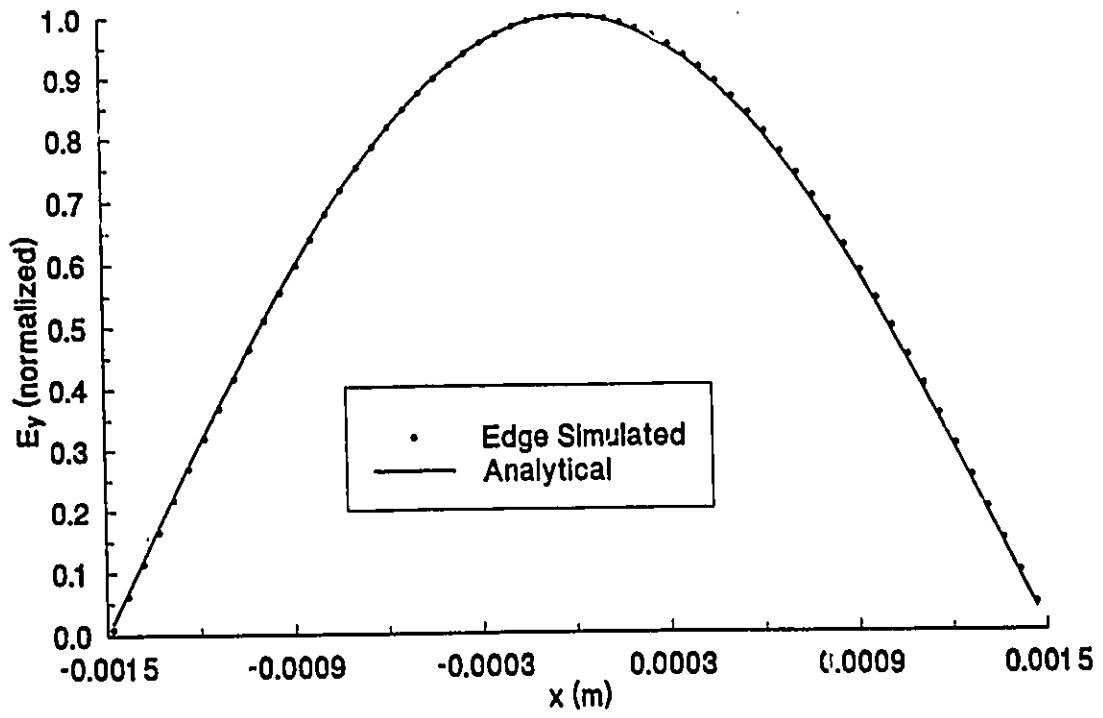


Figure 5.4: TE_{10} mode - E_y field for Rectangular Waveguide

5.1.3 Eddy Current problem

The treatment of the eddy-current problem is based on the solution of differential equations derived from Maxwell's equations under the general assumption that the displacement current density, $\partial D/\partial t$, in conducting media may be neglected for frequencies lower than those of the optical spectrum[40]. It is to be noted that neglecting the displacement current is not equivalent to neglecting the charge density on the interface between the regions having different conductivities. The field formulation uses directly the field vectors, which for a linear medium, is

$$\nabla \times \nabla \times \mathbf{H} = -\mu \sigma \partial \mathbf{H} / \partial t$$

which in the time harmonic case,

$$\nabla \times \nabla \times \mathbf{H} + j \omega \mu \sigma \mathbf{H} = 0$$

and is sometimes called the diffusion equation[41]. In the given general formulation, $k_0^2 = -j \omega \mu \sigma$ and a complex problem has to be dealt with here. The weakness inherent in this formulation when used in the node-based conventional FEM is that it is inconvenient to apply to regions where the permeability changes discontinuously. The edge element method presented here to solve this 1-D Eddy current problem (Fig. 5.5.), can take this into account easily in its implementation.

The skin depth is an important parameter of eddy current problems. It describes the skin effect of an electromagnetic field in a conductor. The conductivity is used to characterize different materials and to measure the thickness of a conductive coating on a metal substrate. The metal plates must be thin enough so that the depth of penetration is comparable to the measured thickness. When the skin depth is very small (at very high frequency), a very finer discretization is needed to obtain a satisfactory solution and consequently much computing time is required. Sometimes an excessive numerical error may be produced when the mesh is inappropriate, as is evident from edge element

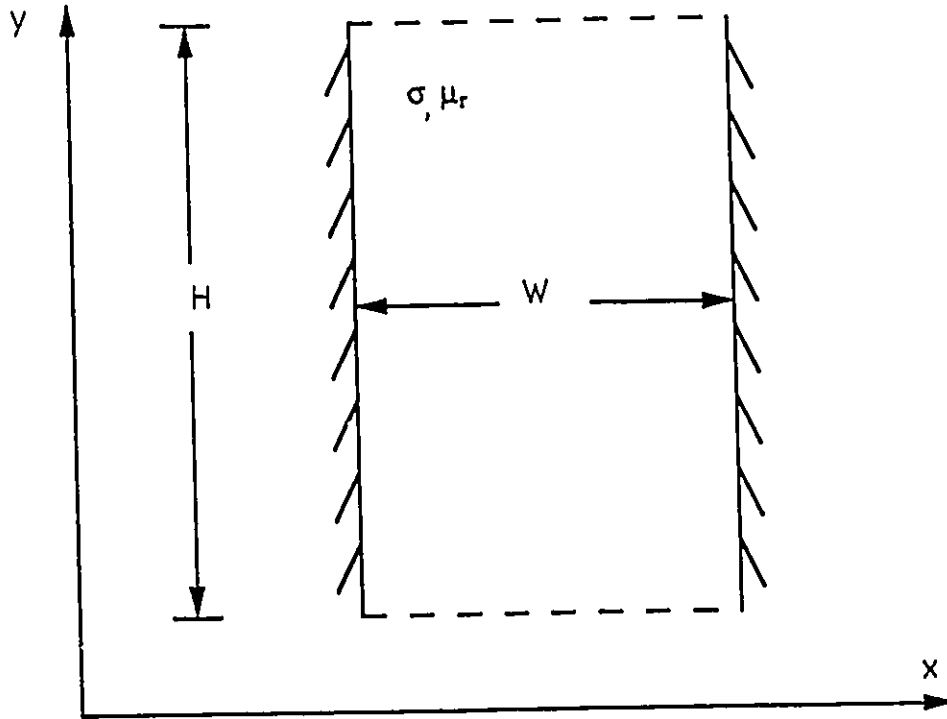


Figure 5.5: Eddy Current Problem

solution at higher frequency. Even a quarter of the problem was solved, to allow for finer meshes but still due to the maximum limit of the computer capabilities, the error has been clearly portrayed at higher frequencies and also it is the same as what was got due to a half structure. Somewhat a forced-adaptive mesh generation has been used here.

The formulation has been done in H-field and the value of the magnetic field (being proportional to the surface current density) has been normalized to 1.0 on both conductor boundaries and was analyzed at various frequencies. The conductor used is copper with conductivity $\sigma = 5.8 \times 10^7 \text{U/m}$, the thickness of the conductor is 0.02 m and due to symmetry only the upper half plane has been discretized into triangles. The relevant equations for the eddy current problem to show how the electromagnetic field distributes in a conductor are given below:

$$\nabla \times \nabla \times \mathbf{H} - k_0^2 \mathbf{H} = 0$$

$$\begin{aligned}
\mathbf{H}|_{x=-w} &= 1.0 = \mathbf{H}|_{x=+w} \\
k_0^2 &= -\gamma^2 \\
\gamma^2 &= j\omega\mu\sigma = (1+j)/\delta \\
\delta &= \sqrt{\frac{2}{\omega\mu\sigma}}: \text{skin depth}
\end{aligned}$$

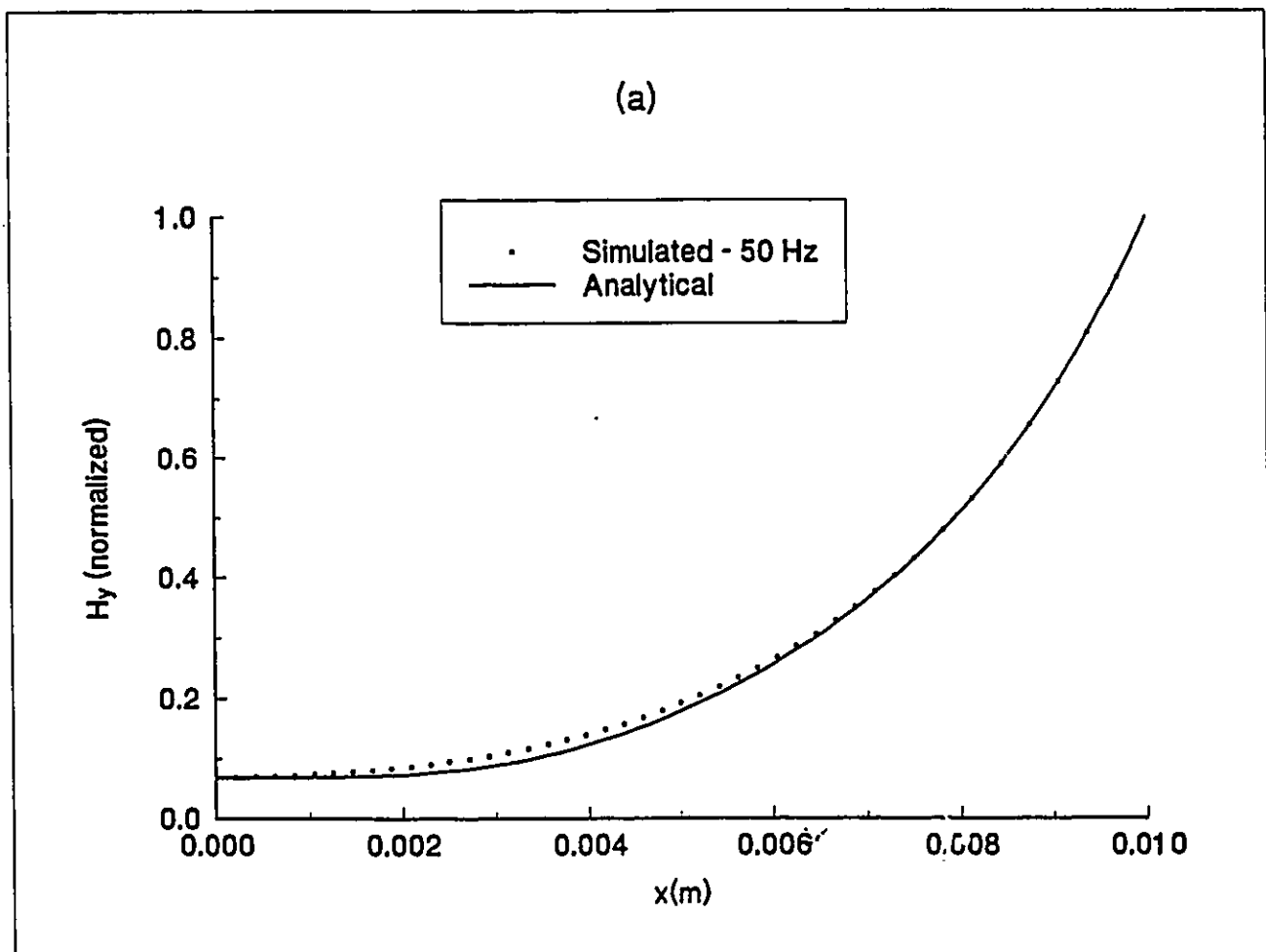
where \mathbf{H} is the magnetic complex field strength. The normalized analytical solution to this is given by

$$\mathbf{H} = \mathbf{H}_v(x) = \frac{\cosh \sqrt{j\omega\mu\sigma} x}{\cosh \sqrt{j\omega\mu\sigma} W}$$

The results got has been compared with the analytical solutions and they appear to agree very well but at progressively higher frequencies (50,500,5K,50K - all in Hz), due to lack of finer mesh and better computers, the edge element method's prediction seems unsatisfactory, especially at the regions of maximum slope, typical of any numerical technique (Fig.5.6.). There is another important consideration here that the complex matrix when inverted, by the use of routines from LINPACK, seems to have some conditioning problems.

The difference between the analytical and simulated results are of the same order for 50 Hz and 500 Hz, but this order increases for higher frequencies, clearly portraying the unsuitability of the analytical formula without any modifications. The skin depth at those frequencies respectively are 2.9554 mm, 0.9346 mm, 0.2955 mm and 0.0935 mm. The total number of nodes and edges used were 352 and 576 respectively, for all the cases but they have been individually discretized differently. The rule of the thumb is that the finite element length should be atleast a tenth of the skin depth but this condition is difficult to meet at higher frequencies. Also, as the frequency increases, it is no more advisable to neglect wholly the effect of the displacement current and the whole formulae has to be modified. The discrepancy between the analytical results and the simulated results can be thus accounted for by the above factors.

Some of the interesting applications of eddy current problems are in power generation and conversion which deals with magnetic levitation, electromagnetic launching and biomedicine and also in information processing which in turn deals with nondestructive testing methods and extraction of information from them. The numerical solution would also be greatly improved, if the interpolation function had been chosen as a hyperbolic function instead of a linear or even a parabolic function. Apart from a number of simple two-dimensional problems like this, inhomogeneous and nonlinear problems as well as problems involving complicated geometries cannot be solved analytically and thus one has to rely heavily on accurate numerical methods like edge elements.



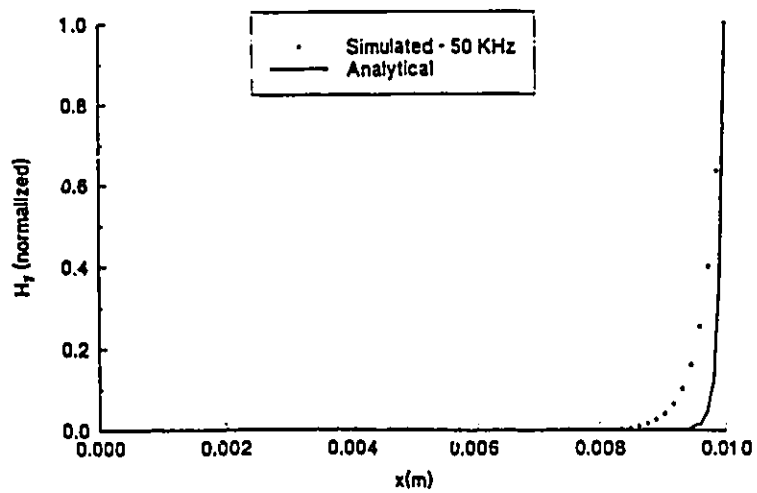
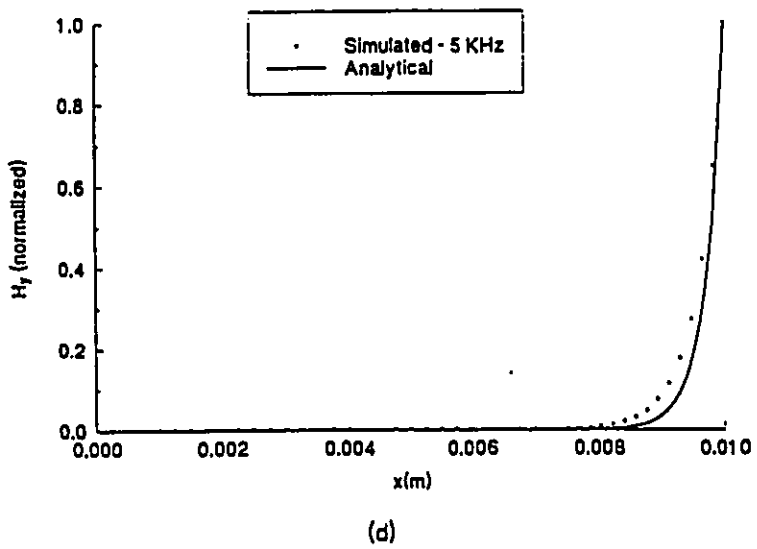
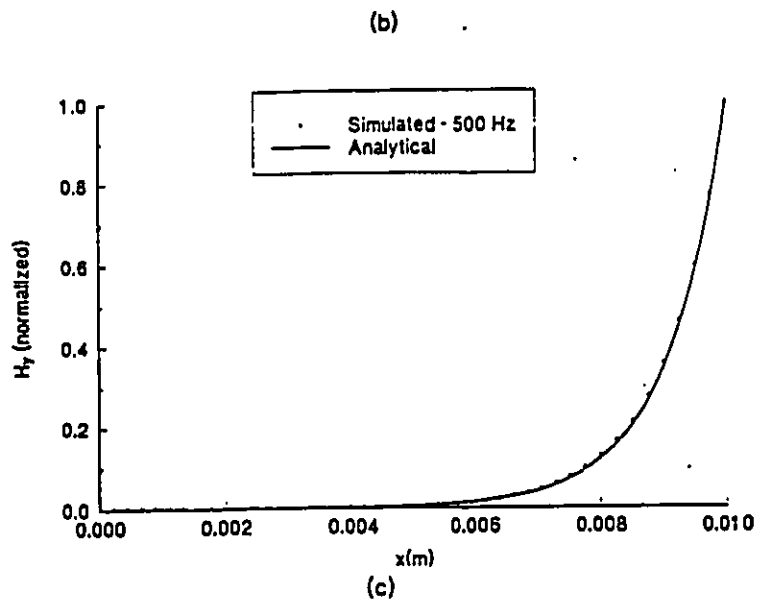


Figure 5.6: Comparison between the analytical and simulated results for eddy current problem (a) 50 Hz (b) 500 Hz (c) 5 KHz and (d) 50 KHz.

5.2 Eigenvalue Problems:

Usually, in the formulations that have been done so far, the propagation constant had been known and provided as input and the frequency computed. The generalized eigen equation would then be of the form,

$$[S] \{e\} = k^2 [T] \{e\}$$

where the matrices $[S]$ and $[T]$ were usually real, semi-definite and most importantly, symmetric and sparse. Hence iterative methods like Lanczos algorithm could be used to solve for the eigenvalues.

But, the formulation outlined in this work, inputs the frequency which has been taken as a known quantity and the propagation constant has been solved for. The resulting system of equations is then of the general form,

$$[S] \{e\} = \beta^2 [T] \{e\}$$

where the matrices $[S]$ and $[T]$ are again real but indefinite. Also $[S]$ was found to be sparse and symmetric, whereas $[T]$ was eventually dense and unsymmetric, because an inverse of a sparse matrix had made the matrix dense and multiplying two symmetric matrices had given rise to the unsymmetry. So, due to the loss of the sparsity and symmetry of the standard eigenvalue problem arrived at ($[T]$ being non-singular), choice of routines to solve these set of equations, as highlighted in the earlier chapter, had been very difficult and Lanczos algorithm had proved not to be a much better choice. Also the Lanczos algorithm has to be extended for indefinite cases and modified to handle the unsymmetric case too. Hence the famous QR algorithm had to be used for unsymmetric eigenvalue problem solution. The major advantage, compared to the former formulation, is that there does not exist zero eigenvalues here.

Also for a real, unsymmetric and indefinite matrix system, mathematically the eigenvalues are supposed to be generally complex. Since only the propagating modes has been

of interest in this study, the complex propagation constants with non-zero imaginary parts had been ignored. Also, of the remaining, propagation constants with negative real parts had been filtered off. Of the remainder, in the absence of spurious solutions, the highest β should correspond to the lowest propagating mode. That is, for a given frequency, the dominant mode must have the largest value of β .

If the formulation had been perfect, there should be no other non-physical values of the propagation constant mixed with these highest values. This is a major limitation in two-dimensions as the method is not purely edge but rather a hybrid edge-node method and hence the inherent spuriousness of the nodal finite element method still exists. Also if the boundary conditions are not met properly by the method, spurious modes would creep in too. This could possibly be eliminated in three-dimensional cases, as the node which represents the longitudinal fields could be simulated by edges of the tetrahedral in the third direction. Also, as β decreases, the field complexity becomes greater and accuracy therefore worsens.

5.2.1 Test Geometry : Air-filled Rectangular Waveguide

The whole structure (Fig.5.9.) has been analyzed for dispersion characteristics in E field (Fig.5.8.) and only dominant mode was of interest and after applying all the symmetry conditions, a half structure was analyzed too with the same results. They were also compared with the analytical solutions for each mode and they matched very well. But the half waveguide after giving the exact dominant mode, when tried for the second order mode, simulated it slightly approximately because of the fact that higher order mode would need better mesh refinement. Throughout the simulation at all frequencies, for the given dimension, there appeared multiple eigenvalues corresponding to the free space value which had been suppressed out. Both had 400 triangles, 630 edges and 231 nodes in their discretization and the width was 1.0 m and height 0.5 m. The most important

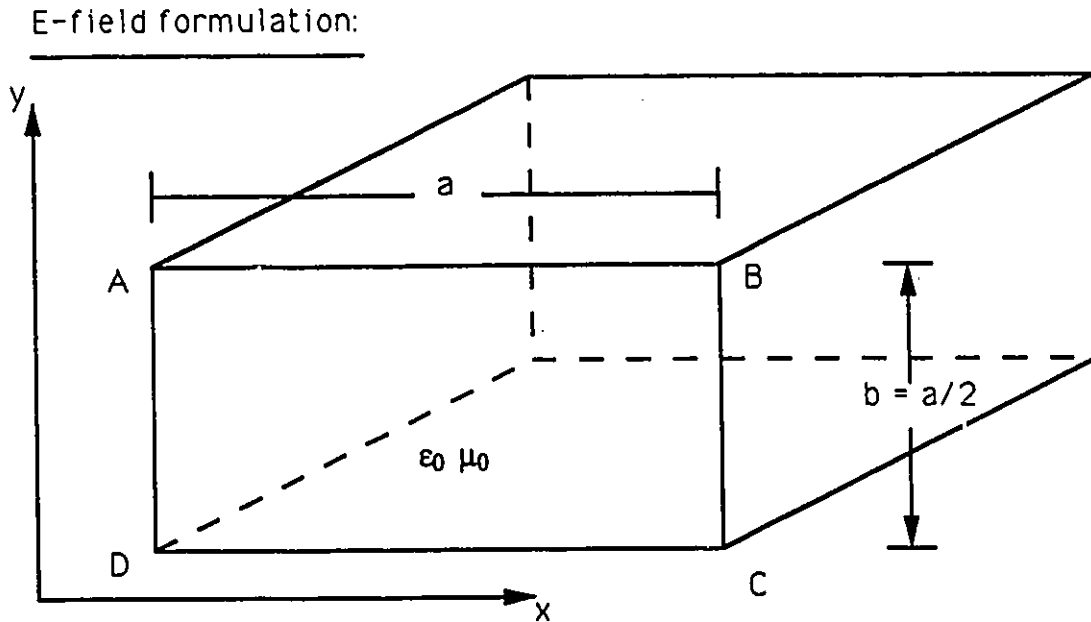


Figure 5.7: Test Geometry : Rectangular cavity

conclusion here has been that the lowest set of eigenvalues corresponded with the highest set of modes, and they were unique for each frequency. The total number of eigenvalues obtained with the present method was equal to the final order of matrices to be solved, which is equal to the total number of unknown edges. The complex eigenvalues with non-zero imaginary parts are definitely nonphysical, as they are not bounded real numbers which correspond to the propagating mode. Thus only the purely real eigenvalues were considered for the dispersion characteristics.

5.2.2 Dielectric-loaded waveguide

First, the presence of inhomogeneous material implies that in general the normal component of the field must be discontinuous at the interface between the two materials. For cartesian formulations typically all components must be discontinuous across such

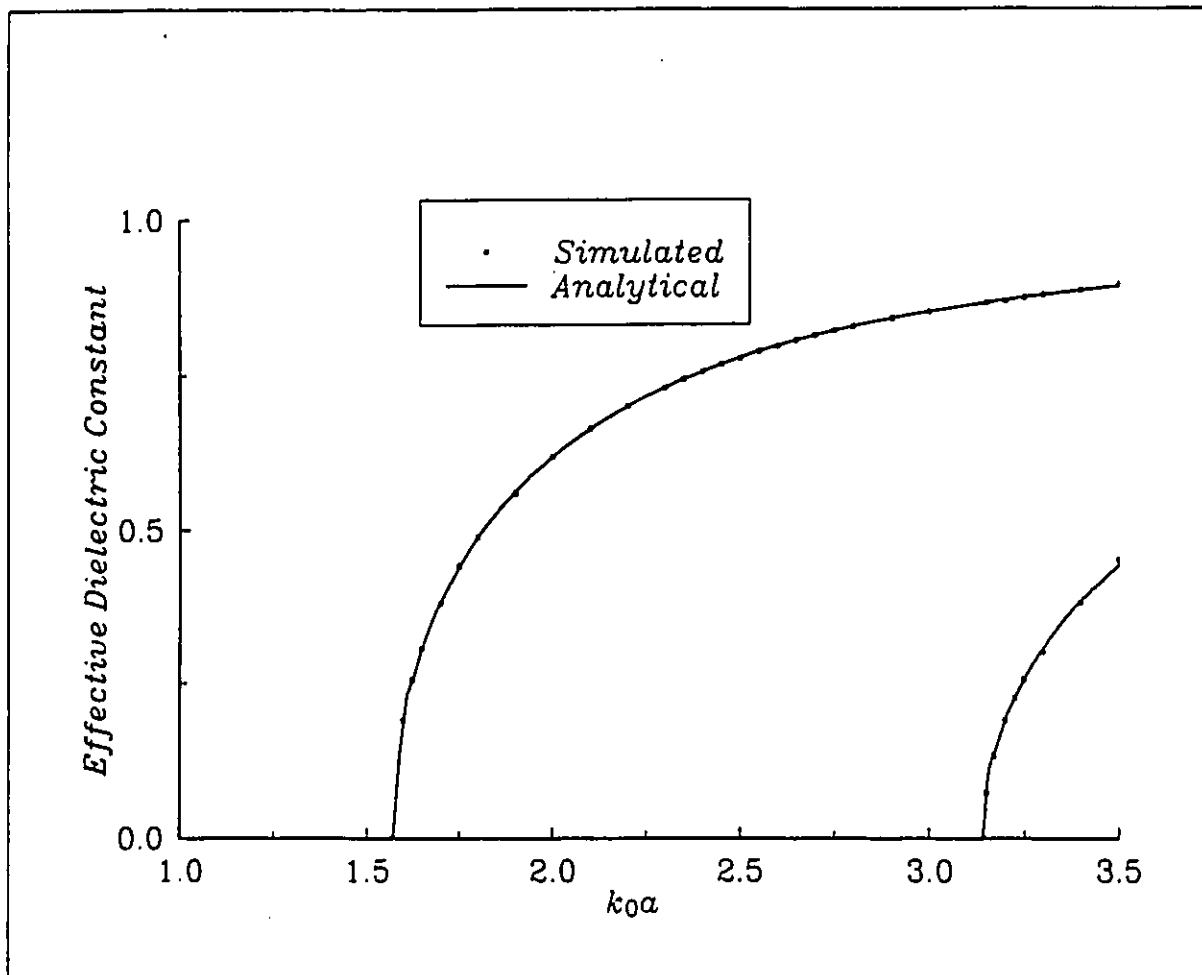


Figure 5.8: Modal analysis diagram for simple cavity problem

an interface. Edge elements, unlike the conventional nodal FEM, formulate this problem in terms of the field components tangential to an edge of the element, guaranteeing continuity of only these components, allowing the normal component to jump at material interfaces, and making the specifications of electromagnetic boundary conditions easy. As known, the discontinuity of the normal component at material interfaces is not automatic but must be explicitly enforced.

For the analysis of inhomogeneous structures, uniform in the z -direction (longitudinal) it is advantageous to decompose the fields into LSE (Longitudinal Section Electric) and LSM (Longitudinal Section Magnetic) solutions because they can fulfill the interface condition at the dielectric boundaries independently, wherever there are *no* metallic strips. Coupling occurs only in the planes containing the metallic strips.

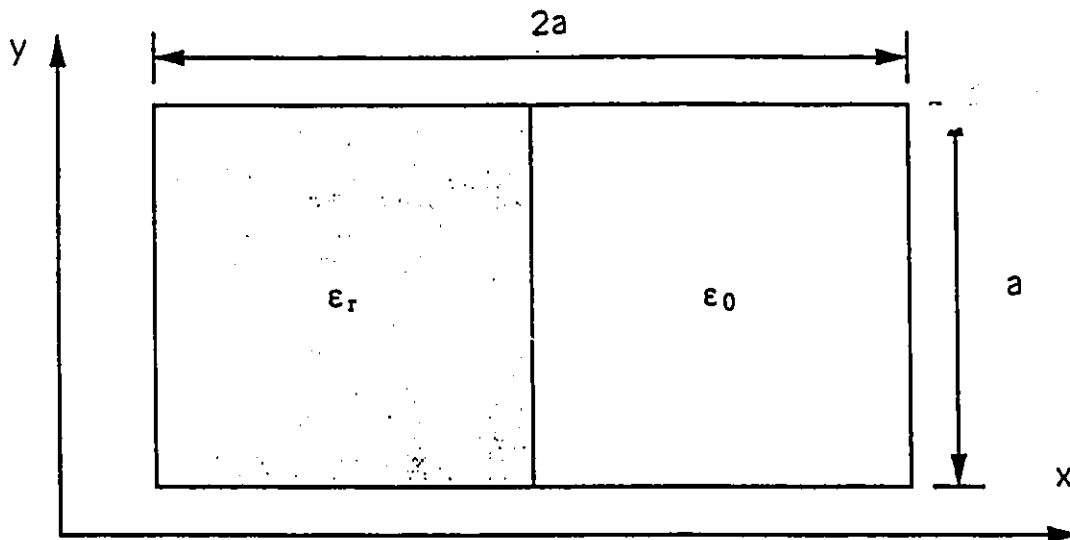


Figure 5.9: Dielectric waveguide : An Optical structure

For an abrupt discontinuity in permittivity, in an inhomogeneous medium, there is an abrupt change in field E as well. In such cases, although it could be advantageous to solve for the H field, due to the presence of conductors at the boundaries, the problem has been solved in E field. The normal modes of the dielectric waveguides are grouped in two families, E_{pq}^y and E_{pq}^z [42]. The main field components of the first family are E_y and H_x , where the subscripts p and q denote the number of extrema of the electric and magnetic field in the x and y directions, respectively. The lowest order E^y mode of the dielectric waveguides is the E_{11}^y mode in which E_y is symmetric about the center of the width of the waveguide.

The dielectric waveguide investigated here has a cross-section of $a \times 2a$, where $a = 1.0$ m and bounded by a perfect conductor. Half of the waveguide has been filled with dielectric material whose relative permittivity and permeability equal to 2.25 and 1

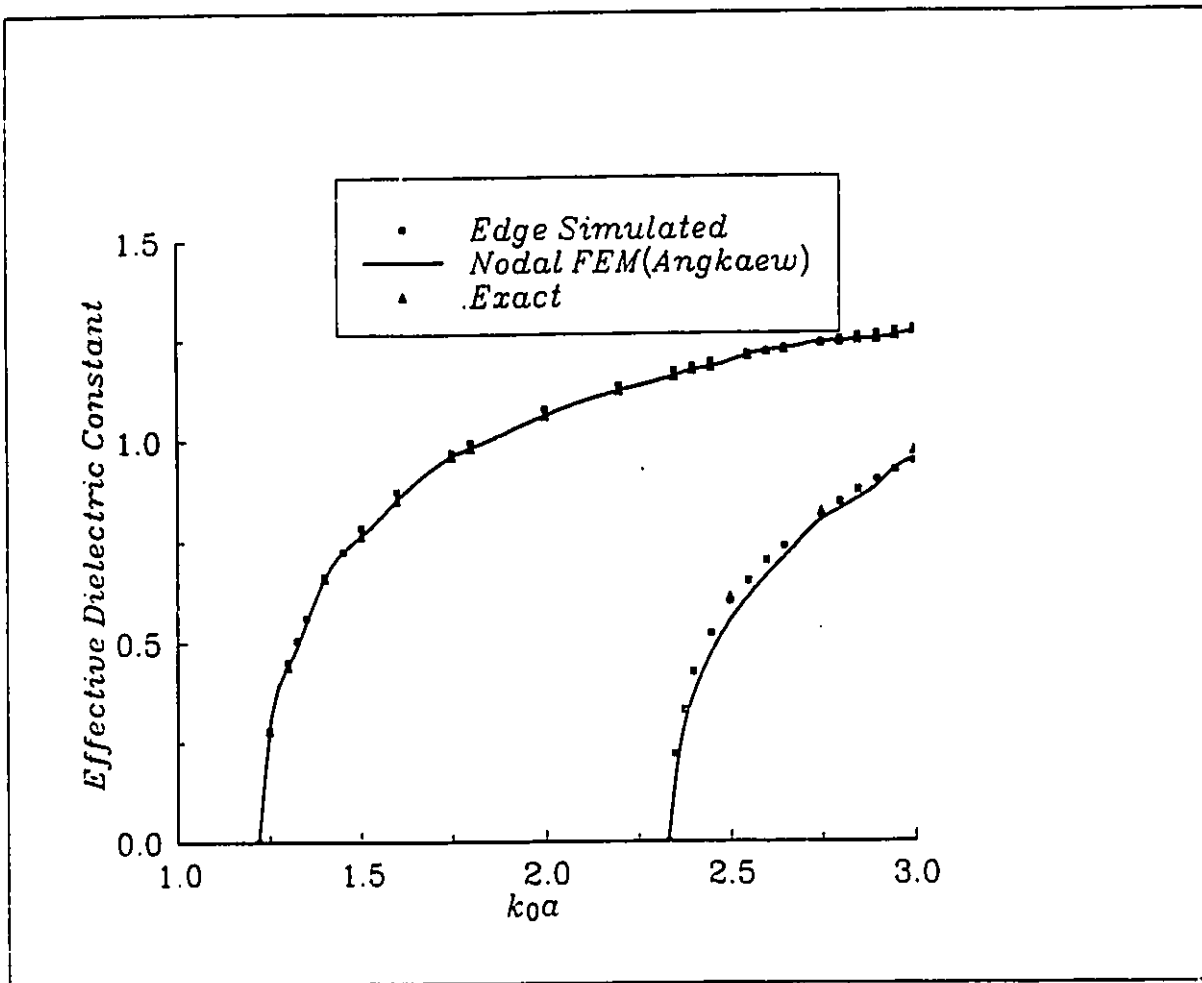


Figure 5.10: Comparison between the edge-simulated and published results -. Dielectric loaded waveguide

respectively and the other half has been assumed to be vacuum. The dispersion characteristics were plotted (Fig.5.10.) and compared with that of T. Angkaew[23] for the full structure, and the resulting few non-physical modes have been easily discriminated as they appear as three different values of normalized propagation constants. Also, as in the homogeneous case discussed earlier, in this inhomogeneous case too the lower β s correspond to the higher modes. In case of the fundamental mode as well as the second order mode, the edge element analysis agreed exactly with the nodal FEM solutions of Angkaew[23]. The higher order modes, after about $k_0a = 2.3$, obviously cannot be reproduced so well because of an insufficient number of elements in the mesh at these short wavelengths. However the accuracy in the higher order modes can be improved

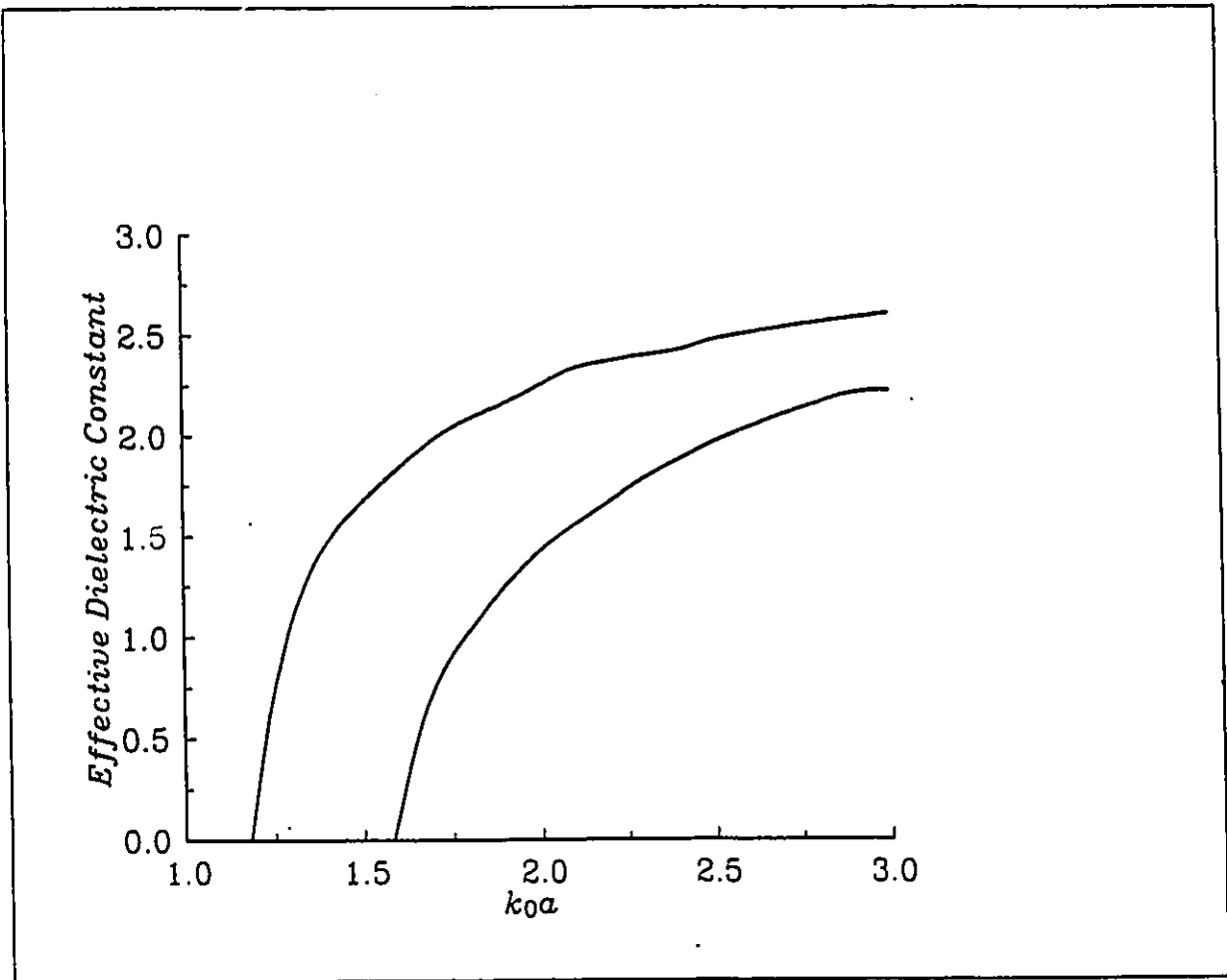


Figure 5.11: Effective Dielectric constant of Dielectric Waveguide of permittivity 8.5

by increasing the number of elements or using quadratic shape functions instead of the linear ones used here. Plotting the $\omega - \beta$ diagram for higher order modes requires considerable computation time if treated separately. The permittivity was increased to 8.5 from 2.25 and this indicated that the frequency at which the dominant and higher order modes begin to appear is lower for a guide filled with dielectric substrate which has larger dielectric constant(Fig.5.11). The convergence of the results also improved when the mesh was refined from 513 edges to 630 edges. Also use of Lanczos algorithm gives the same values for the propagating modes, but the only advantage observed here was that it suppresses some unwanted repetitive solutions.

5.2.3 Microstrip Transmission Lines[43]

One of the main requirements for a transmission structure to be suitable as a circuit element in monolithic integrated circuits is that the structure should be 'planar' in configuration. A planar configuration implies that the characteristics of the element can be determined by the dimensions in a single plane. As for example, the width of the microstrip line on a dielectric substrate can be adjusted to control its impedance.

A microstrip (Fig.5.12) makes it convenient for use in MICs where discrete lumped devices (active or passive) are to be mounted in the circuit but the presence of the air-dielectric interface modifies the mode of propagation in the microstrip to a non-TEM hybrid mode. It may be pointed out that it is only the fringing components E_x and H_x at the dielectric-air interface that lead to the non-TEM nature of the microstrip mode. Since these fringing field components are much smaller than the main field (within the substrate below the strip), the departure from the TEM behavior should be small and thus a full-wave analysis of the microstrip can be supported. As the microstrip configuration is not capable of supporting a pure TEM mode, the hybrid modes supported by microstrips cannot be fully described in terms of static capacitances and inductances. Therefore, one has to introduce time varying E and H fields and solve the wave equation to determine the propagation constant (this does not necessitate any quasi-static assumption). Also, the shielded microstrip line is an important problem which has sharp edges, and is one for which a scalar analysis is inadequate.

First a shielded microstrip line (Fig.5.12) has been analyzed and this is just another two-medium waveguide with a metal conductor inside of width 1.27 mm and thickness $t = 0$ mm. The lossless conditions require that the permittivity and the permeability tensors be Hermitian. The whole shielded line had a width 12.7 mm and height of 12.7 mm and the dielectric ($\epsilon_r = 8.875$) height was 1.27 mm. $E_{tan} = 0$ on the strip(if present) and on all the four conductor sides and the half microstrip had been solved in

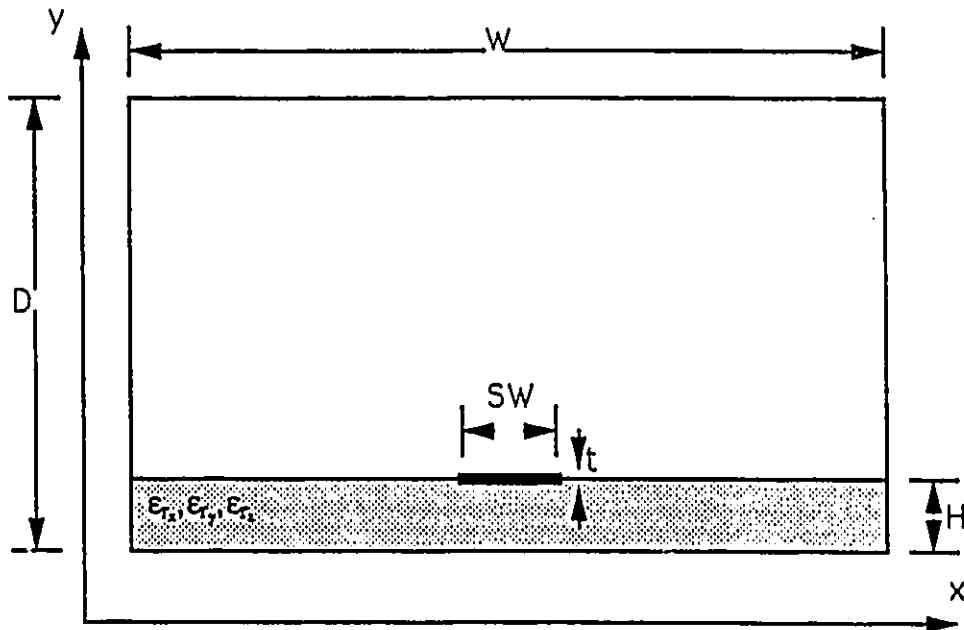


Figure 5.12: Ordinary Shielded Microstrip

E-field with magnetic wall symmetry at the center, which allows only one half cross-section to be discretized into edge elements. The initial meshes were refined to check convergence and finally the total number of elements were 364, the number of nodes were 210 and the total number of edges were 573. The introduction of a metallic strip causes severe problem as would be evident subsequently. The whole half-section has been divided into two different discretization as shown in Fig.5.13, the second one being more dense around the strip and in the dielectric. Both give rise to some spurious solutions and also approximated the needed value to some degree of convergence. The reasons for these many unwanted modes, although being due to the introduction of the conductor inside, unfortunately cannot be reasoned out with surety. The strip being the culprit can be evident from the fact that if just a metal has been introduced within an empty rectangular waveguide, there are many of these modes which come out as

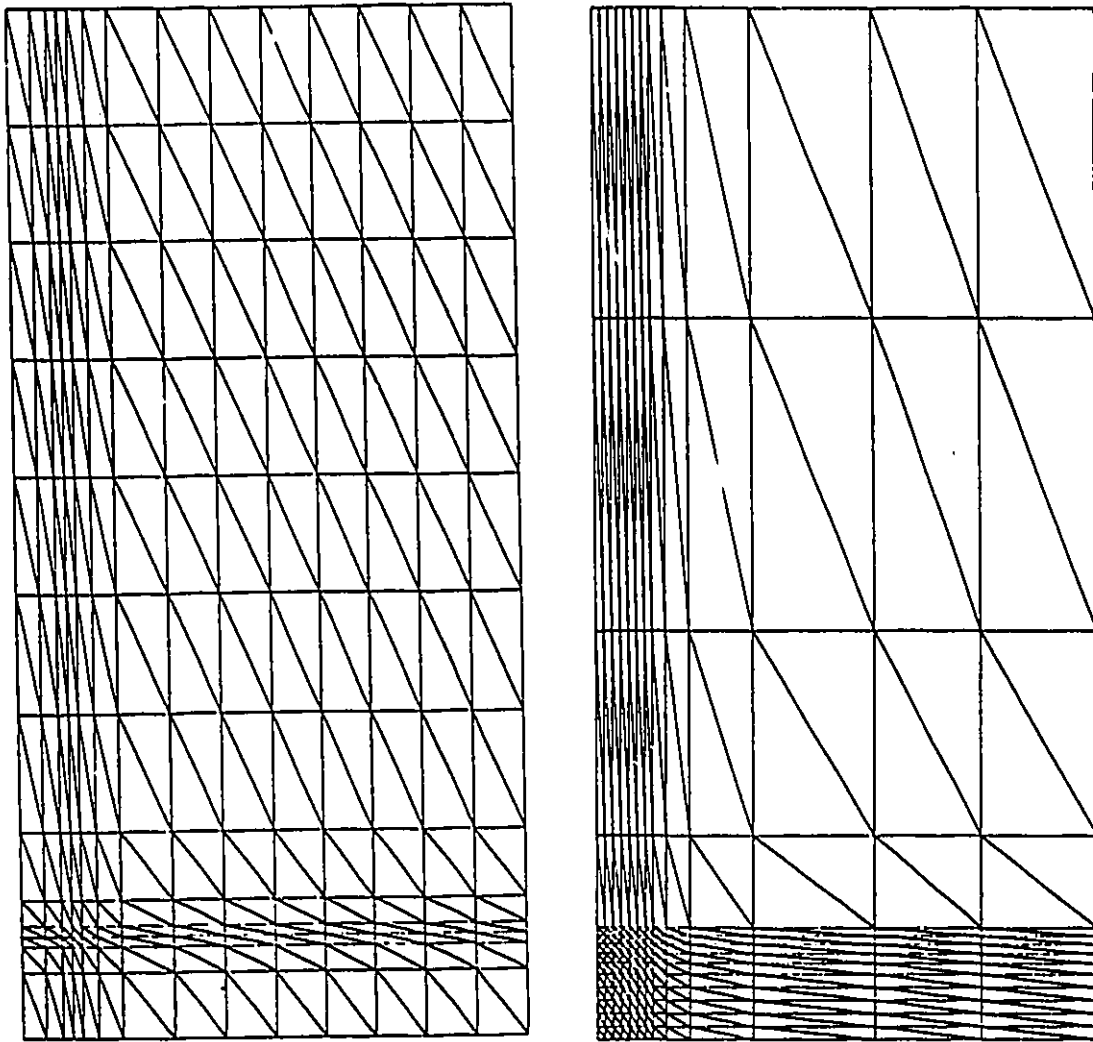


Figure 5.13: Microstrip problem discretization - two possible ways

solutions alongwith the needed one (which are exact) and they are also easily eliminated because the field distribution is easily known for such a problem. The propagation characteristics for the first two modes of a microstrip on an isotropic substrate with $\epsilon_r = 8.875$ has been plotted (Fig.5.14) making use of the first discretization as there had been no marked difference in the $f - \beta$ plots between the two. The first mode has been compared with both singular integral equation approach of Mittra and Itoh[44] and nodal FEM supplemented with singular trial functions of Webb[45] and the second mode has been compared with spectral domain approach of Mirshekar-Syahkal and Davies[46] and nodal FEM using covariant projection quadrilateral elements of Miniowitz and Webb[47]

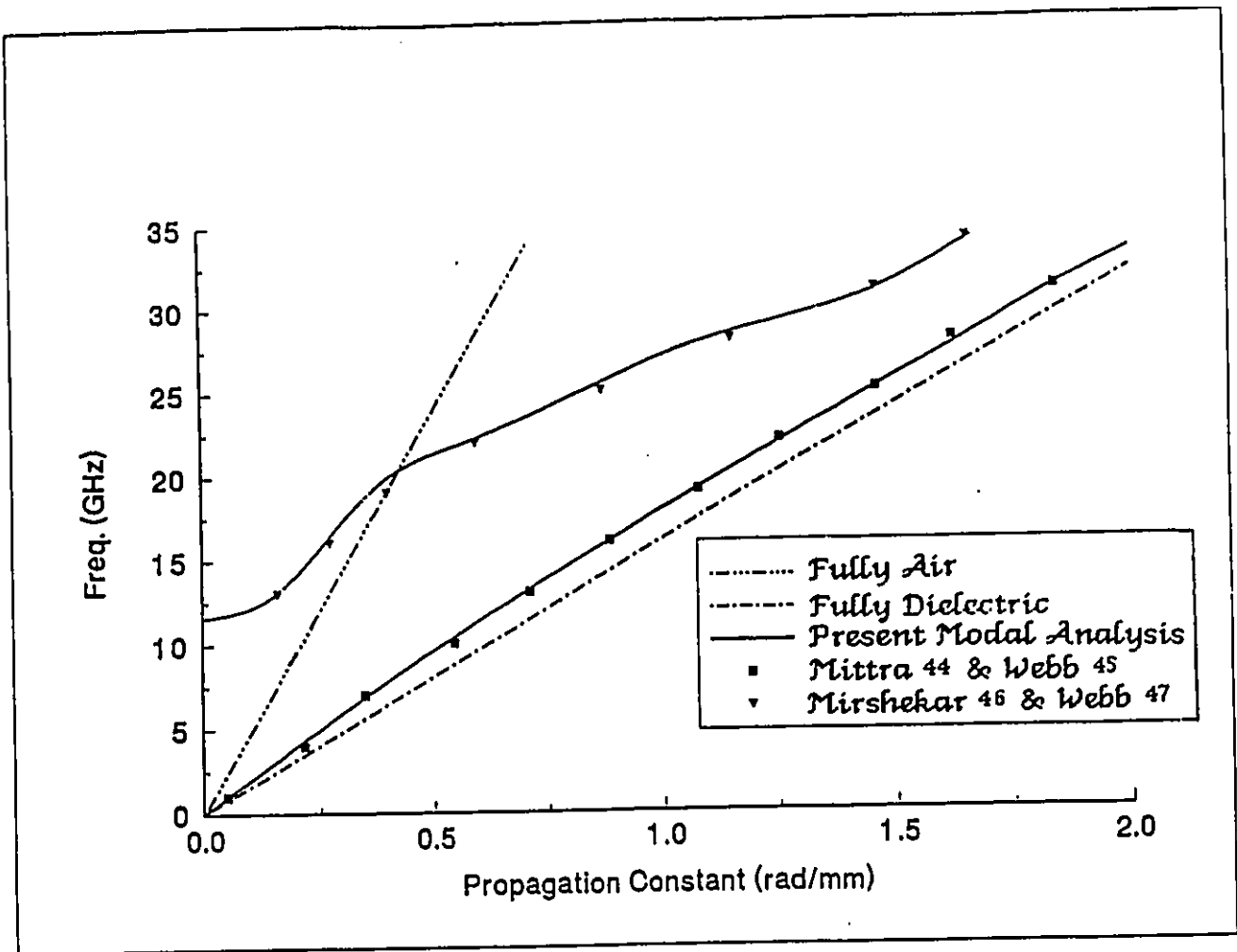


Figure 5.14: Dispersion Characteristics - Isotropic case

and present results agree well with these previously reported ones. But the choice of eigenvalues to compare themselves with the previous known results is time-consuming as the field distributions were checked for the eigenvalues chosen and were found to be approximating the field distribution of a microstrip. The LSE and LSM modes had gradually changed to stripline modes when the center conductor appeared. It is evident that with increasing frequencies, the dispersion curves for the lowest order mode become parallel to the dielectric-filled TEM transmission line. Thus, for higher frequency, the normalized guide wavelength for the lowest order mode approaches the inverse of square root of the permittivity, this being the ratio of guide wavelength in the dielectric filled TEM transmission line to that in the air filled line.

At higher frequencies, existence of enclosures causes propagation of higher order

modes. At higher frequencies, more and more energy propagates inside the substrate and below the strip. The presence of air-dielectric interface modifies the mode of propagation in the microstrip to a non-TEM hybrid mode. Most of the energy in the dominant hybrid mode is concentrated in the dielectric substrate under the center strip, where longitudinal components are relatively weak. Because the plane of symmetry makes so little difference to the higher order modes, these modes are strongly associated not with the strip but rather with the dielectric-air interface. The field singularity near the edge of the strip, where variation is most rapid, has been accounted for by means of finer element division near the edges as well as the dielectric - air interface. The number of elements would have to be higher to obtain a well-convergent solution.

Offering similarity with the crystals, when two of the three parameters are equal, in anisotropic medium, it is termed as uniaxial. Here, there is a two-dimensional degeneracy; the principle axis that exhibits this anisotropy is called the optic axis. Some of the substrates used for microstrip circuits exhibit anisotropy in permittivity, like sapphire (single crystal) and Epsilam-10 (ceramic loaded resin). In both these cases, the substrates are manufactured such that one of the principle axis of the permittivity tensor is perpendicular to the dielectric interface. In the case of anisotropic microstrip, the y-axis is the optic axis, and for uniaxial case $\epsilon_{r_x} = \epsilon_{r_z}$.

- Sapphire : $\epsilon_{r_x} = \epsilon_{r_z} = 11.6$ and $\epsilon_{r_y} = 9.4$.
- Epsilam-10 : $\epsilon_{r_x} = \epsilon_{r_z} = 15.0$ and $\epsilon_{r_y} = 10.0$.

Here sapphire substrate anisotropic microstrip substrate has been analysed for dispersion (Fig.5.15) and compared quite well with Webb[45] and this had the same characteristics as the isotropic case.

Also larger the refractive index, the slower is the wave velocity inside the medium, this being a strong design factor in optical fibers. For increasing frequency, effective

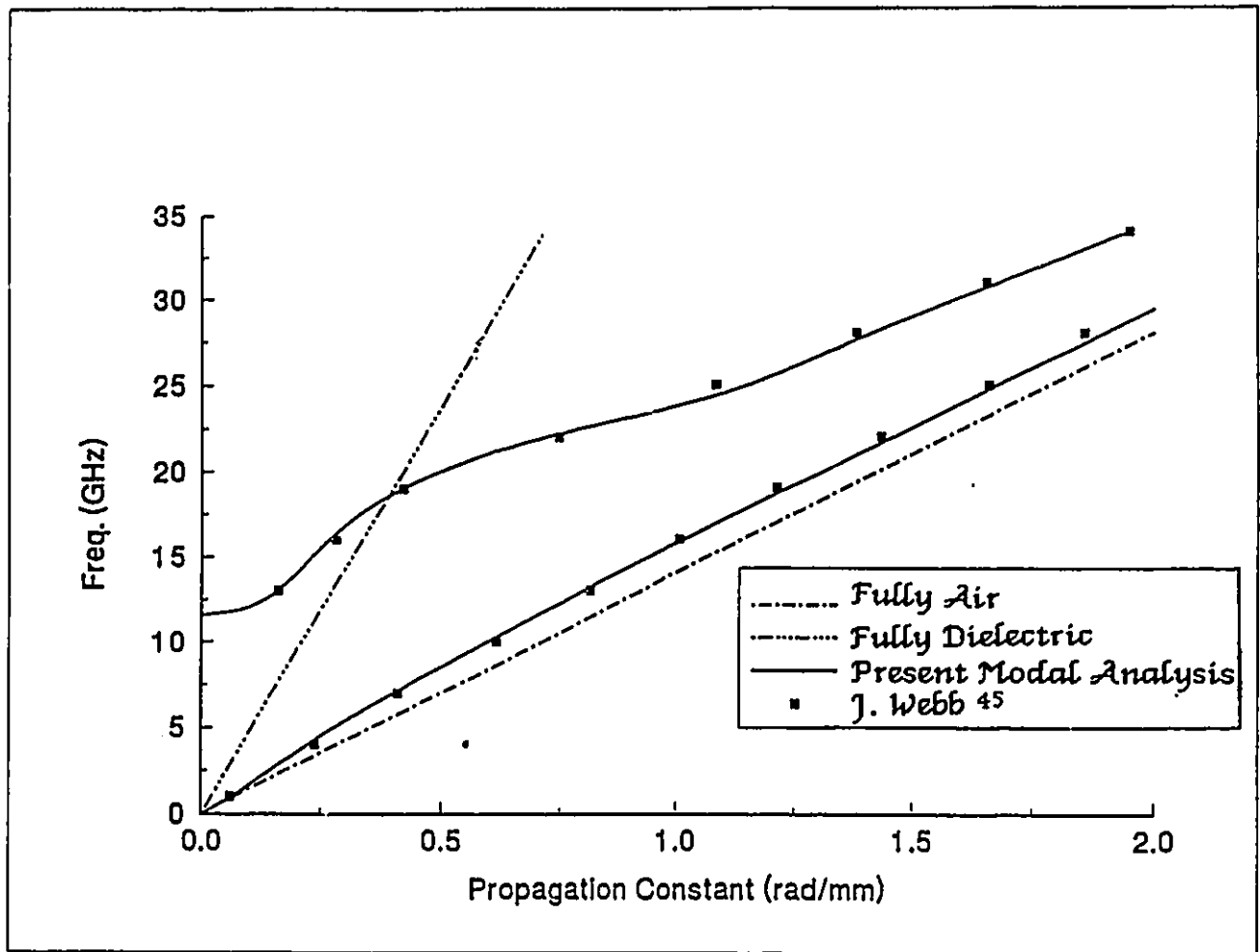


Figure 5.15: Dispersion Characteristics - Anisotropic case

dielectric constant for the microstrip increases (Fig.5.16). An increase in effective dielectric constant implies that the fields are getting concentrated below the strip which also amounts to a decrease in effective width of the microstrip.

Discrepancies between the edge element curve and the exact or compared curves can be due to :

- Insufficient number of elements being used, especially at higher frequencies.
- The shape functions, which are linear within each elements, do not fit the exact solution.
- Round-off errors being present.
- The presence of singularities degrading the accuracy of the numerical approxima-

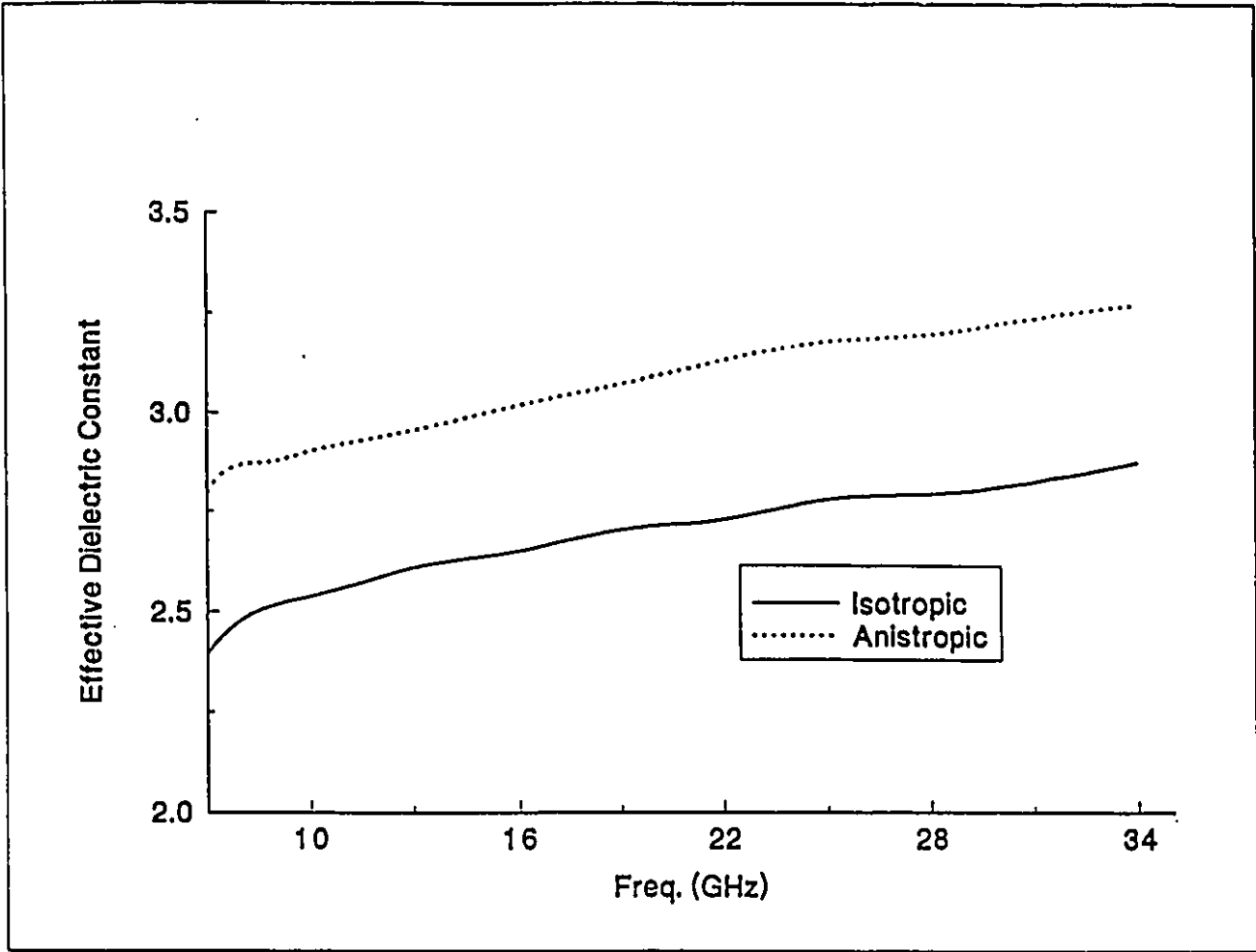


Figure 5.16: Effective Dielectric constant - Dominant mode.

tions and thus slowing down the convergence.

- Residual errors caused by premature terminations of the iterations used to evaluate the eigenvalues.

It should be noted that as the degeneracy of the eigenvalues increases, the matrix becomes increasingly ill-conditioned and numerical solution is correspondingly less accurate[48].

Spurious solutions, as discussed earlier, are solutions which do not automatically satisfy the divergence free condition implied by the Maxwell's equation and also can be one which do not satisfy the boundary conditions properly. The number of these unwanted numerical fields is particularly high in the case of waveguides with strips and is shown to be relevant on how the continuity conditions are imposed on the transversal

fields between the materials. It has been observed that discretized fields with continuous tangential components, being inherently divergence-free, suppress the spurious modes which even in this two-dimensional formulation is quite true as atleast the spurious modes can be easily separated from the needed modes. One good way to check for spurious modes is to plot the field distribution at cut off (when the propagation constant is zero) and thus to have an idea of the actual field distribution. Also, they do not satisfy the rigidly imposed boundary condition and they do not have any low-frequency cutoff, thus making them non-unique[49].

These spurious solutions can be observed to be just mathematical solutions of the eigenvalue problem and do not represent the physical solutions. Moreover, the number of such modes which occur in the output varies with the number of degrees of freedom in the finite element model. The conclusions out of this research on these spurious solutions in 2-D has been that (a) they do not mix with the physical modes in homogeneous structures, (b) they do mix with the real eigenmodes but can be easily separated from them in non-homogeneous structures, but (c) they mix and are difficult to filter out from the actual solutions in structures where metallic conductors(or any sharp edges) were present.

Also, in ridged waveguides and cavity problems, the singularity of the fields near sharp edges implies special adjustment to take the corners of the boundary into account. Once a conducting strip had been introduced, things get worse and so far studies done through edge elements have been confined to dominant modes and unfortunately higher order modes have not been investigated. Any work done on the higher order modes in cavity problems, through vectorial tangential finite elements so far have not been with conducting strips inside and this work has attempted to analyze them. Spurious modes are still known to exist which after careful comparison with other methods give good results, but nevertheless, the edge elements seem to be promising to solve complicated

problems in high frequency applications. Also the spurious solutions could be possibly eliminated by the proper use of singular trial functions near the edges.

Summarizing, the electromagnetic boundary value problems treated in this thesis have been those associated with :

- homogeneous, isotropic waveguides.
- inhomogeneous, isotropic waveguides.
- homogeneous, anisotropic waveguides.
- inhomogeneous, anisotropic waveguides.
- axisymmetric resonant cavities.

Although this present work had been intended to demonstrate the new approach, it can be hoped that this method can be used to solve many other practical microwave and optical problems.

Chapter 6

Conclusions

The conventional finite element method with node based elements is much less reliable and not readily applicable to regions containing discontinuous boundaries in shape and material. In this thesis, a two-dimensional formulation of the finite element method using all the three components of either the electric or magnetic fields has been developed, to solve either for the dispersion characteristics and the electromagnetic field distribution directly, in an arbitrary region containing conducting and dielectric materials, when the boundary conditions are properly known and met. The main intent of this work has been to explore the feasibility of analyzing various types of new high speed electrical interconnects. Since only lossless medium has been considered ($\sigma = 0$), except in eddy current problems, only the displacement current (in eddy current problem, the conduction current) has been considered in arriving at the neat curl-curl equation, rather restricting the solution to high frequencies but which could be afforded in all applications considered[50].

A new numerical procedure has been presented for the full-wave analysis of dielectric waveguides, cavity resonators and microstrip transmission lines. In this procedure, a novel vector finite element had been proposed for the electromagnetic field computation, using triangular elements to treat arbitrarily shaped waveguides. The energy functional

has been developed and solved by edge finite element method. The bounded region of interest has been discretized using second order triangles and the fields functions has been defined by first order linear shape functions. All the integrals has been derived to algebraic formulae and the program ' FREDEEM.F ' has been written in frequency domain to solve for either field values.

Unlike conventional nodal finite element method, tangential vectorial finite elements imposes only the tangential continuity of the electric or magnetic field across element boundaries. In this way, the new method not only matches the underlying physical requirements but also provides reliable numerical solution. Also the newly derived eigenvalue problem does not produce zero eigenvalues which are present in $[S] \{e\} = k^2 [T] \{e\}$. Also, its specialty lies in the fact that it involves only the edge variables in the transversal plane and provides a direct solution of β . But the present method suffers from the disadvantage that it requires large and dense matrices for computation and thus effectively needs more computer storage and CPU time than the ordinary FEM.

The homogeneous Neumann conditions have to be chosen as a natural boundary conditions and the homogeneous Dirichlet boundary conditions are the forced boundary conditions. The Neumann conditions have been considered automatically in the variational treatment and that is why they are called Natural Boundary Conditions. The convergence has been checked by increasing the number of elements and values of dimensions for the influence of the artificial boundaries to be negligible.

The system of equations generated by finite element method is sometimes an ill-conditioned system, especially field singularities are present. The reciprocal condition is a measure of the ill-condition or nearness to singularity of a matrix and it is proportional to the frequency again. Thus, even with sufficiently available memory resources, at very high frequency the results would not be that reliable; however, the results had been good with sufficient resolution to the physical ones. Also, due to the non availability of suitable

routines for this type of matrix eigenvalue problems, the need for a highly efficient matrix solver for large, dense and generally complex generalized eigenvalue problems has been a severe handicap here.

The maximum size of an element has been determined by the frequency in question. When mesh size increases, spatial and frequency dispersion occurs. The size was restricted because the amount of available memory fixed the upper limit on the number of nodes or edges on any problem[50]. Hence, it is very important to pay proper attention to the discretization of the problem into finite elements. The element size should be atleast one order of magnitude smaller than the skin depth in the conducting region and signal shortest wavelength(highest frequency) in non-conducting region.

Various structures, which included the microwave and optical waveguides, have been analyzed and numerical results compare well with those obtained elsewhere by other methods. From these structures, the generality of the present analysis can be demonstrated. It has also been inferred that there is still the existence of spurious modes which can be easily identified, the automatic mesh generation would be very difficult in edge elements and there has been severe limitation in the speed and dynamic memory of the computer. Due to a better field resolution and fulfillment of continuity condition, the new edge elements give better convergence and accuracy than the traditional FEM. The confidence gained from this study would enable us in future to use this versatile vectorial finite element technique to treat other guiding structures, which have not been analyzed elsewhere. Also since the analysis has worked out very well for one-dimensional and two-dimensional cases, it could be extrapolated that it would work well in three-dimension, where it would be purely an edge element method and other peers in this area have demonstrated its best utility only in 3-D.

Chapter 7

Further Developments

Attenuation in a transmission line or waveguide can be caused by either dielectric loss or conductor loss. Attenuation caused by conductor loss depends on the field distribution in the guide, and so must be evaluated separately for each type of transmission line or waveguide. But if the line or guide is completely filled with a homogeneous dielectric, the attenuation due to lossy dielectric can be calculated from the propagation constant and this result will apply to any guide or line with a homogeneous dielectric filling. Thus, as an extension to this work, finite conductivity and complex permittivity could be introduced in the region to make it lossy and analyzed for conductor and dielectric losses, in frequency domain.

Finite thickness can be introduced, which is supposed to increase the capacitance and thus decrease the impedance. It is known that the fringing fields are larger for narrower strips. Also line parameters and characteristic impedances and their variations to the width of the strip and permittivity of dielectric region could be extracted and comparison made. Also the crosstalk, distortion of pulses and coupling phenomena could be possibly analyzed even better with edge elements. The study of edge elements could be further extended to three dimensions, where it offers better promises, using tetrahedral elements. Time-domain analysis suitable for digital designers, although a herculean task, could

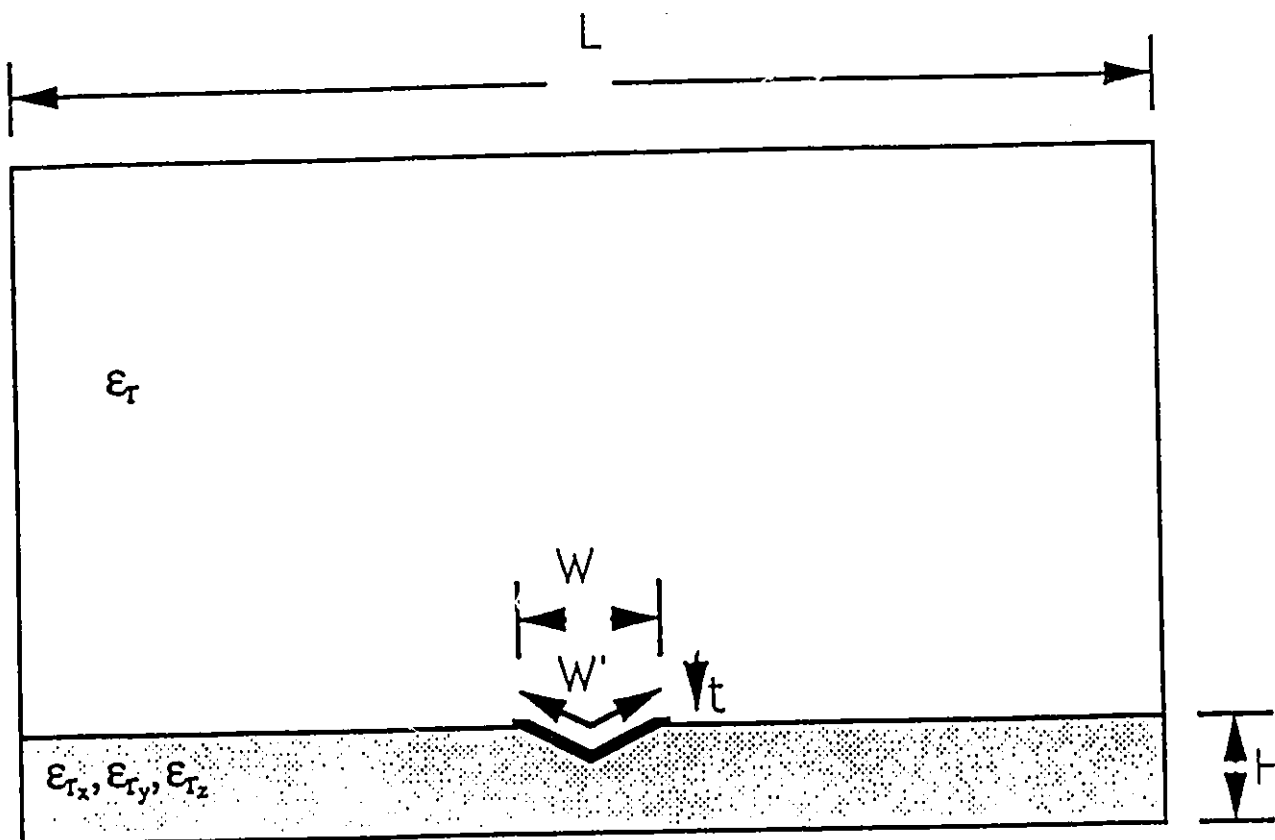


Figure 7.1: Valley (or) Groove Microstrip

be done and S-parameters for discontinuities could be determined and compared with experimental results and this would prove good for industrial applications of high speed interconnections.

A valley microstrip line and a trapezoidal microstrip line which had been fabricated by using multilayer MMIC technologies, had been proposed and its performance experimentally investigated by [51,52]. Insertion loss of the valley microstrip line (Fig.7.1) is smaller than that of conventional microstrip lines having the same width of strip conductor.

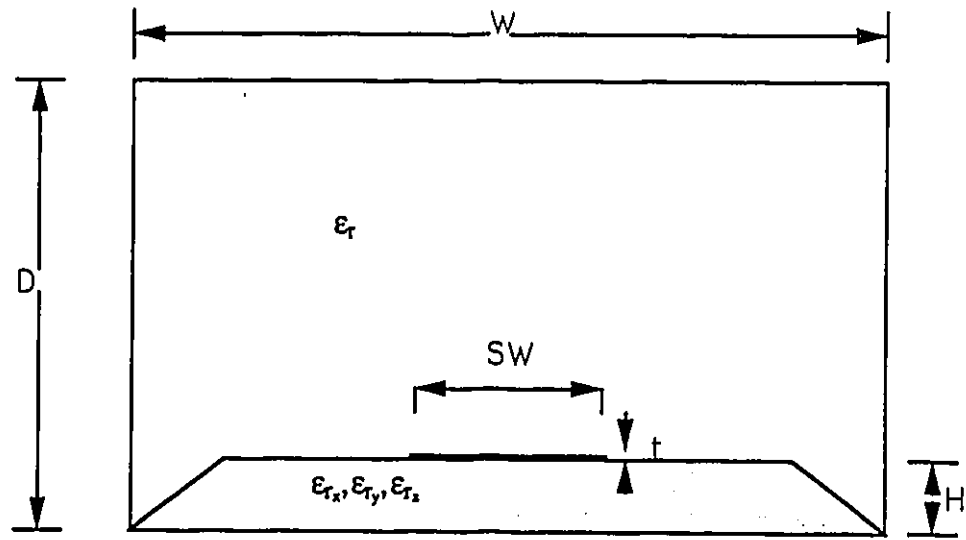
Reducing insertion loss is normally accomplished by increasing the width of the strip conductor in a ordinary microstrip, but as a result, the circuit size becomes very

large. But the new valley and trapezoidal microstrip structure eliminates the current concentration at both edges of the strip conductor. Since the distance between the ground plane and the center of the valley microstrip conductor is smaller than that between the ground plane and the edge of the conductor, the concentration of current is dispersed between the three points, i.e., the center and both edges of the valley microstrip conductor. Also, the length, W' , along the valley microstrip conductor is wider than the conductor width, W . Therefore, the dispersion degree of current in the valley microstrip conductor becomes higher than in the microstrip conductor if the width of the valley microstrip conductor nearly equal to the width of the microstrip conductor for the same characteristic impedance. These two effects reduce the conduction loss of the valley microstrip line. The insertion loss of the valley microstrip is about 20 % less than the ordinary microstrip lines with the same conductor width.

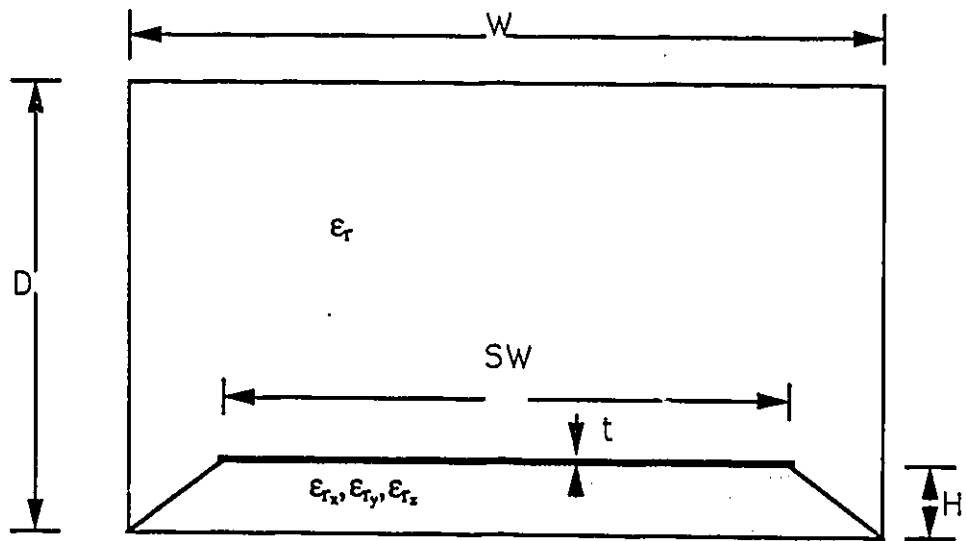
The effect of the current distribution in the trapezoidal microstrip conductor (Fig.7.2) is slightly less pronounced than in the valley microstrip conductor. Although the width of the trapezoidal microstrip line is 20 % greater than that of the ordinary microstrip lines with an overlay, the transmission line loss of the trapezoidal lines is 30 % less.

Thus both valley and trapezoidal microstrips, in all its variations, have the potential to reduce the size of multi-layered MMICs and might be very useful as high speed interconnects. Thus, these two new lines can be analyzed thoroughly for propagation, dispersion, delays and S-parameters. Also these different electrical interconnects lines can be compared with optical interconnects, and effective design guide lines brought about which might proves their usefulness as high speed interconnects.

It has become also increasingly clear that single-stranded optical fiber cables (Fig.7.3) will eventually replace copper based coaxial cables or twisted pairs at high data rate communication lines and it is highly essential therefore to analyze the propagation constants and field intensity distribution of the dominant mode in arbitrarily shaped inhomoge-



(a)



(b)

Figure 7.2: Trapezoidal Microstrip : (a) Partial Fill-in, and (b) Full Conductor.

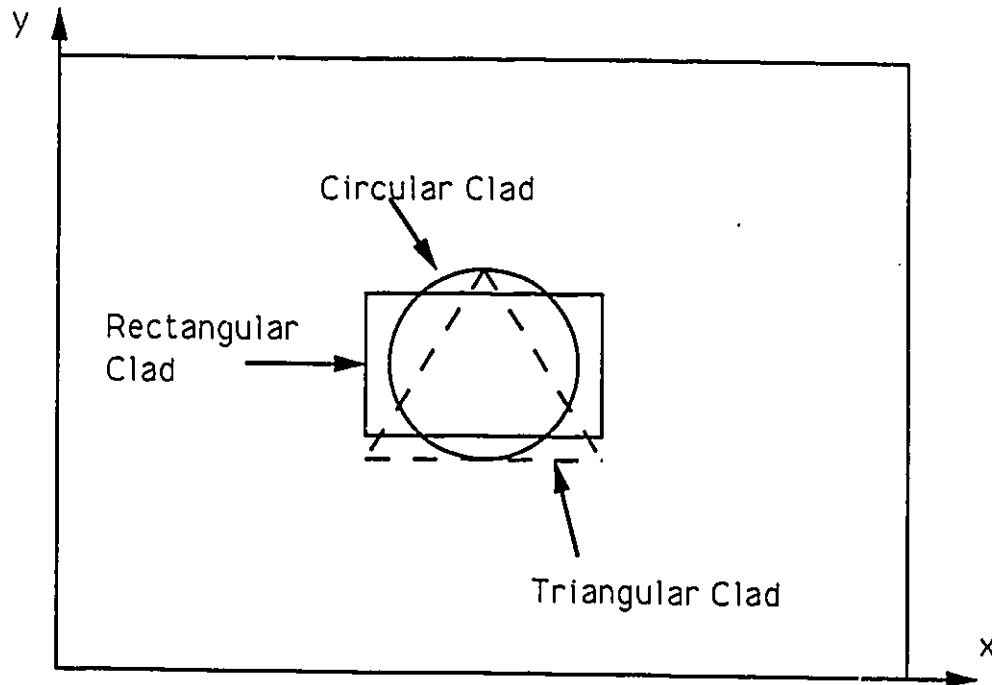


Figure 7.3: Various possible Optical fiber structures.

neous fibers. This edge finite element method is especially suited for problems involving complicated geometries and variable index of refraction and could be used to obtain the propagation characteristics of step-index fibers and other optical waveguiding structures. This is necessary to establish how many modes the structure can support, the information about the first two modes particularly and how small changes in dimensions or refractive indices could result in the whole structure being at cut-off or supporting more than desired.

Such optical waveguides, which are just dielectric waveguides, can be distinguished from metallic waveguides with the fact that there is no conducting surfaces[53]. The conducting surfaces are impractical at optical frequencies and the guiding action is different at these frequencies. Also, although metal waveguides shall be preferred, optical

waveguides can be still be used at microwave frequencies too. But the guiding action of reflections at dielectric boundaries and the detailed analysis of optical waveguides is very complicated added to the fact that the FEM at these shortest wavelength has to be dealt with properly. The advantages that these carry are low transmission losses, large frequency bandwidth, smaller size and weight, flexible cables, no EMI, signal transmission security, easy integration and low potential cost. Main areas of applications of optical waveguides would be in long distance communication by land or under sea, medicine and optical interconnects based on the theory of integrated optics.

Also, this approach can be applied easily to realistic geometries including active media and to magnetic anisotropic waveguides (like the ferrite loaded waveguide) and to the whole class of other non-reciprocal microwave components.

Definitions and Notations

Sparse Matrix : An $m \times n$ matrix A will be said to be sparse if and only if each row of the matrix contains at most a few entities which are not zero.

Real Symmetric Matrix : An $n \times n$ matrix A is real symmetric if and only if A is real and it is equal to its transpose. That is $A^T = A$.

Hermitian Matrix : An $n \times n$ matrix A is Hermitian if and only if $A^H = A$ where H is the Hermitian transpose. That is, for each, $1 \leq i, j \leq n$, $a_{ij} = a_{ji}^*$. Therefore, the diagonal entries of any Hermitian matrix must be real.

Upper Hessenberg Matrices : A $n \times n$ matrix H is an upper Hessenberg Matrix if and only if all of its entries below the main subdiagonal are zero. That is, if $H \equiv (h_{ij})$, then

$$h_{ij} \equiv \begin{cases} 0 & \text{for } i > (j + 1) \\ \text{and for } 1 \leq i, j \leq n. \end{cases}$$

Triangular Matrices : An $n \times n$ matrix A is upper triangular if and only if all the nonzero entries of A are on or above the main diagonal of A . An $n \times n$ matrix A is lower triangular if and only all the nonzero entries of A are on or below the main diagonal of A .

Skew Symmetric Matrix : An $n \times n$ matrix $A \equiv (a_{ij})$ is skew symmetric if and only if A is real and $A^T = -A$. That is

$$\text{for } 1 \leq i, j \leq n : a_{ij} = -a_{ji}$$

In particular, the diagonal entries of any skew symmetric matrix must all be zero, and any skew symmetric matrix of odd order must be singular.

Adjoint of a Matrix : If A is an $n \times n$ matrix, then its adjoint $\text{Adj}(A)$ is defined by

$$\text{Adj}(A)(A) = (A)\text{Adj}(A) = \det(A)I_n$$

If A is nonsingular so that $\det(A) \neq 0$, then the inverse of A , that is $A^{-1} \equiv \text{Adj}(A)/\det(A)$.

Spectrum of a Matrix : The set of eigenvalues of any given $n \times n$ matrix A is called the spectrum of A . If a matrix has all real eigenvalues, then the extreme eigenvalues of A are defined as those eigenvalues which are the algebraically-largest or the algebraically-smallest.

Positive Definite Matrices : An $n \times n$ real *symmetric* matrix A is said to be positive definite if and only if all of its eigenvalues are positive. If all of its eigenvalues are nonnegative then it is said to be positive semidefinite. There are analogous definitions for negative definite and negative semidefinite matrices. Matrices which are not definite or semidefinite are called indefinite.

Nondefective Matrix : An $n \times n$ matrix A is said to be a nondefective matrix if and only if it is diagonalizable. That is there exist a nonsingular matrix X and a diagonal matrix $\Lambda = \text{diag}\{\lambda_1, \lambda_2, \dots, \lambda_n\}$ such that $A \equiv X \Lambda X^{-1}$. If this is the case then clearly $AX = X\Lambda$ and $A^T X^{-T} = X^{-T} \Lambda$. Therefore, the columns of X must be the right eigenvectors of A , the columns of X^{-T} must be left eigenvectors of A , and the λ_i are the eigenvalues of A . Any real symmetric or skew symmetric matrix is nondefective. Furthermore, any $n \times n$ matrix with n distinct eigenvalues is nondefective (diagonalizable).

Band Matrix : A band matrix is a matrix whose nonzero elements are all fairly near the main diagonal.

Trace of a Matrix : A Trace of a Matrix A is the sum of the diagonal elements of a matrix (is also the sum of all eigenvalues if A is diagonal).

Divergence : The Divergence of a vector $\mathbf{A} = \nabla \cdot \mathbf{A}$ is given by

$$\lim_{\Delta V \rightarrow 0} \frac{\oint_S \mathbf{A} \cdot d\mathbf{s}}{\Delta V}$$

The divergence of a vector field is a measure of the net outflow of flux through a closed surface S surrounding a volume ΔV , per unit volume, as the volume shrinks to zero. The positive divergence indicates a source of that vector and a negative divergence indicates a sink.

Curl : The curl of a vector is a measure of the net circulation of the vector field around the boundary of an infinitesimal element of area, that is

$$(\text{curl } \mathbf{A})_n = (\nabla \times \mathbf{A})_n = \lim_{\Delta S \rightarrow 0} \frac{\oint_C \mathbf{A} \cdot d\mathbf{l}}{\Delta S}$$

where $(\nabla \times \mathbf{A})_n$ is the component of the curl of \mathbf{A} in the direction of the normal to the surface ΔS , and C is the boundary of ΔS .

Circulation : They are actually the closed line integrals about each edge. Curl is circulation per unit area. Thus, electromagnetically, the circulation of \mathbf{H} , or $\oint \mathbf{H} \cdot d\mathbf{L}$, is obtained by multiplying the component of \mathbf{H} parallel to the specified closed path at each point along it by the differential path length and summing the results as the differential lengths approach zero and as their number becomes infinite.

Divergence Theorem : The integral of the normal component of any vector field over a closed surface is equal to the integral of the divergence of this vector field throughout the volume enclosed by the closed surface.

Refractive Index : The dimensionless quantity $n \equiv c\sqrt{\mu\epsilon} = ck/\omega$ is the refractive index of the medium. As, $k^2 = \omega^2 \mu \epsilon$, it can be computed that $u \equiv \omega/k = 1/\sqrt{\mu\epsilon}$ is the velocity of an electromagnetic wave in a non-dispersive isotropic medium. When the medium is dispersive, the dispersion relation may be a complicated function between k and ω .

Singular Function : A vector function is said to be singular at those points where it is not well-behaved, that is, where it is discontinuous or has discontinuous derivatives.

APPENDIX A

1. Given two vectors, \mathbf{a} and \mathbf{b} , the scalar (or) dot product is given by

$$\mathbf{a} \cdot \mathbf{b} = |\mathbf{a}||\mathbf{b}| \cos \theta_{ab}$$

Thus, $\mathbf{a} \cdot \mathbf{a} = |\mathbf{a}|^2 \cos \theta_{aa}$. If $\hat{\mathbf{a}}$ and $\hat{\mathbf{b}}$ are unit vectors, then $\hat{\mathbf{a}} \cdot \hat{\mathbf{b}} = \cos \theta_{ab}$. Also, $\hat{\mathbf{a}} \cdot \hat{\mathbf{a}} = \cos 0 = 1$. $\cos \theta_{ab}$ can be negative as it depends on the directions of vectors involved, that is on the projections.

2. Hence,

$$\begin{aligned} \hat{T} \cdot \hat{T}^T &= \begin{bmatrix} \hat{t}_1 \cdot \hat{t}_1 & \hat{t}_1 \cdot \hat{t}_2 & \hat{t}_1 \cdot \hat{t}_3 \\ \hat{t}_2 \cdot \hat{t}_1 & \hat{t}_2 \cdot \hat{t}_2 & \hat{t}_2 \cdot \hat{t}_3 \\ \hat{t}_3 \cdot \hat{t}_1 & \hat{t}_3 \cdot \hat{t}_2 & \hat{t}_3 \cdot \hat{t}_3 \end{bmatrix} \\ &= \begin{bmatrix} 1 & -\cos \theta_3 & -\cos \theta_2 \\ -\cos \theta_3 & 1 & -\cos \theta_1 \\ -\cos \theta_2 & -\cos \theta_1 & 1 \end{bmatrix} \\ &= C \end{aligned}$$

Similarly,

$$\begin{aligned} \hat{N} \cdot \hat{N}^T &= \begin{bmatrix} \hat{n}_1 \cdot \hat{n}_1 & \hat{n}_1 \cdot \hat{n}_2 & \hat{n}_1 \cdot \hat{n}_3 \\ \hat{n}_2 \cdot \hat{n}_1 & \hat{n}_2 \cdot \hat{n}_2 & \hat{n}_2 \cdot \hat{n}_3 \\ \hat{n}_3 \cdot \hat{n}_1 & \hat{n}_3 \cdot \hat{n}_2 & \hat{n}_3 \cdot \hat{n}_3 \end{bmatrix} \\ &= \begin{bmatrix} 1 & \cos(\pi/2 - \theta_3) & \cos(\pi/2 - \theta_2) \\ \cos(\pi/2 - \theta_3) & 1 & \cos(\pi/2 - \theta_1) \\ \cos(\pi/2 - \theta_2) & \cos(\pi/2 - \theta_1) & 1 \end{bmatrix} \\ &= C \end{aligned}$$

This proves (2.18) and (2.19).

3. Also,

$$\hat{N} \cdot \hat{T}^T = \begin{bmatrix} \hat{n}_1 \cdot \hat{t}_1 & \hat{n}_1 \cdot \hat{t}_2 & \hat{n}_1 \cdot \hat{t}_3 \\ \hat{n}_2 \cdot \hat{t}_1 & \hat{n}_2 \cdot \hat{t}_2 & \hat{n}_2 \cdot \hat{t}_3 \\ \hat{n}_3 \cdot \hat{t}_1 & \hat{n}_3 \cdot \hat{t}_2 & \hat{n}_3 \cdot \hat{t}_3 \end{bmatrix}$$

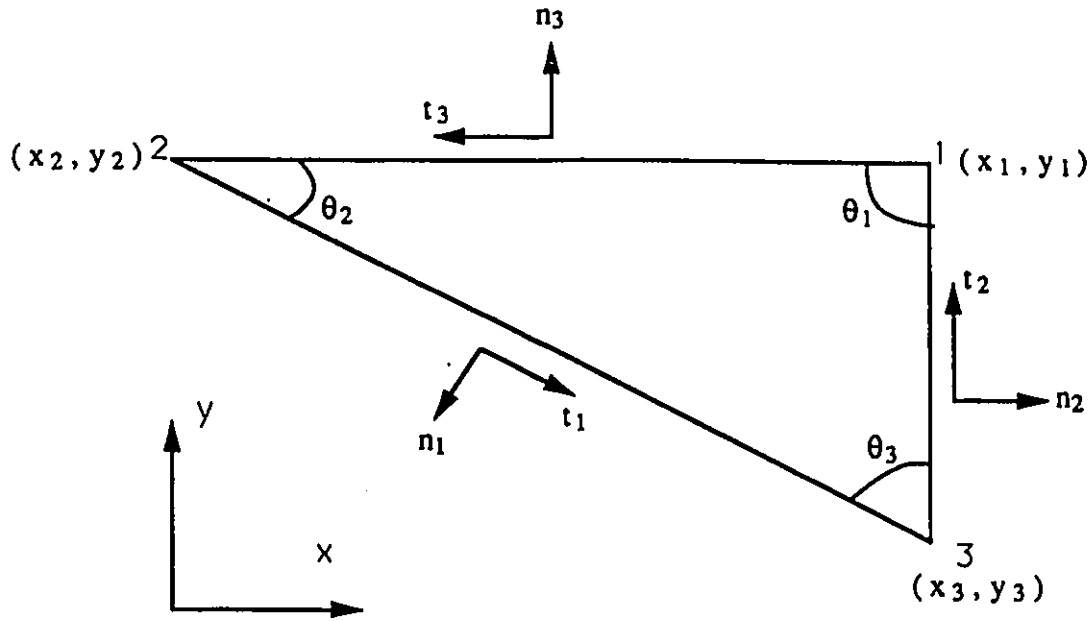


Figure 7.4: To calculate the dot products between unit tangential and normal vectors

$$\begin{aligned}
 &= \begin{bmatrix} \cos \pi/4 & \cos(\pi/4 + \theta_3) & -\cos(\pi/4 + \theta_2) \\ -\cos(\pi/4 + \theta_3) & \cos \pi/4 & \cos(\pi/4 + \theta_1) \\ \cos(\pi/4 + \theta_2) & -\cos(\pi/4 + \theta_1) & \cos \pi/4 \end{bmatrix} \\
 &= \begin{bmatrix} 0 & -\sin \theta_3 & \sin \theta_2 \\ \sin \theta_3 & 0 & -\sin \theta_1 \\ -\sin \theta_2 & \sin \theta_1 & 0 \end{bmatrix} \\
 &= SS \quad .
 \end{aligned}$$

and,

$$\begin{aligned}
 \hat{T} \cdot \hat{N}^T &= \begin{bmatrix} \hat{t}_1 \cdot \hat{n}_1 & \hat{t}_1 \cdot \hat{n}_2 & \hat{t}_1 \cdot \hat{n}_3 \\ \hat{t}_2 \cdot \hat{n}_1 & \hat{t}_2 \cdot \hat{n}_2 & \hat{t}_2 \cdot \hat{n}_3 \\ \hat{t}_3 \cdot \hat{n}_1 & \hat{t}_3 \cdot \hat{n}_2 & \hat{t}_3 \cdot \hat{n}_3 \end{bmatrix} \\
 &= \begin{bmatrix} \cos \pi/4 & -\cos(\pi/4 + \theta_3) & \cos(\pi/4 + \theta_2) \\ \cos(\pi/4 + \theta_3) & \cos \pi/4 & -\cos(\pi/4 + \theta_1) \\ -\cos(\pi/4 + \theta_2) & \cos(\pi/4 + \theta_1) & \cos \pi/4 \end{bmatrix}
 \end{aligned}$$

$$\begin{aligned}
&= \begin{bmatrix} 0 & \sin \theta_3 & -\sin \theta_2 \\ -\sin \theta_3 & 0 & \sin \theta_1 \\ \sin \theta_2 & -\sin \theta_1 & 0 \end{bmatrix} \\
&= -SS = SS^T
\end{aligned}$$

This proves (2.20).

4. Given, from (2.27)

$$\begin{aligned}
V^{(N)} &= -LF^T V^{(X)} \\
&= -\frac{1}{\Delta} \begin{bmatrix} l_1 & 0 & 0 \\ 0 & l_2 & 0 \\ 0 & 0 & l_3 \end{bmatrix} \begin{bmatrix} 1 & x_1 & y_1 \\ 1 & x_2 & y_2 \\ 1 & x_3 & y_3 \end{bmatrix} \begin{bmatrix} q \\ v_x \\ v_y \end{bmatrix} \\
&= -\frac{1}{\Delta} \begin{bmatrix} l_1 & 0 & 0 \\ 0 & l_2 & 0 \\ 0 & 0 & l_3 \end{bmatrix} \begin{bmatrix} q + v_x x_1 + v_y y_1 \\ q + v_x x_2 + v_y y_2 \\ q + v_x x_3 + v_y y_3 \end{bmatrix} \\
&= -\frac{1}{\Delta} \begin{bmatrix} l_1(q + v_x x_1 + v_y y_1) \\ l_2(q + v_x x_2 + v_y y_2) \\ l_3(q + v_x x_3 + v_y y_3) \end{bmatrix}
\end{aligned}$$

Then,

$$\begin{aligned}
\hat{N}^T V^{(N)} &= \hat{N}^T (-LF^T V^{(X)}) \\
&= -\frac{1}{\Delta} [\hat{n}_1 l_1 (q + v_x x_1 + v_y y_1) \\
&\quad + \hat{n}_2 l_2 (q + v_x x_2 + v_y y_2) \\
&\quad + \hat{n}_3 l_3 (q + v_x x_3 + v_y y_3)]
\end{aligned}$$

Therefore,

$$\begin{aligned}
\hat{N}^T V^{(N)} &= \frac{1}{\Delta} [-(b_1 \hat{x} + c_1 \hat{y})(q + v_x x_1 + v_y y_1) \\
&\quad -(b_2 \hat{x} + c_2 \hat{y})(q + v_x x_2 + v_y y_2) \\
&\quad -(b_3 \hat{x} + c_3 \hat{y})(q + v_x x_3 + v_y y_3)] \\
&= \frac{1}{\Delta} [q(b_1 + b_2 + b_3) \hat{x} + (c_1 + c_2 + c_3) \hat{y}]
\end{aligned}$$

$$\begin{aligned}
& + v_x(x_1b_1 + x_2b_2 + x_3b_3)\hat{x} + (y_1b_1 + y_2b_2 + y_3b_3)\hat{y} \\
& + v_y(x_1c_1 + x_2c_2 + x_3c_3)\hat{x} + (y_1c_1 + y_2c_2 + y_3c_3)\hat{y}] \\
& = \frac{1}{\Delta}[q(0\hat{x} + 0\hat{y}) + v_x(\Delta\hat{x} + 0\hat{y}) + v_y(0\hat{x} + \Delta\hat{y})] \\
& = v_x\hat{x} + v_y\hat{y} = \mathbf{v}
\end{aligned}$$

Similarly, $\hat{T}^T V^{(T)} = \hat{T}^T (-LG^T V^{(X)}) = \mathbf{v}$. These prove Eqn. (2.26).

5. It has been inferred from (2.28) that

$$V^{(X)} = -F^{-T}L^{-1}V^{(N)}$$

Equating both sides,

$$\begin{aligned}
\begin{bmatrix} q \\ v_x \\ v_y \end{bmatrix} &= \begin{bmatrix} a_1 & a_2 & a_3 \\ b_1 & b_2 & b_3 \\ c_1 & c_2 & c_3 \end{bmatrix} \begin{bmatrix} \frac{1}{l_1} & 0 & 0 \\ 0 & \frac{1}{l_2} & 0 \\ 0 & 0 & \frac{1}{l_3} \end{bmatrix} V^{(N)} \\
&= - \begin{bmatrix} \frac{a_1}{l_1} & \frac{a_2}{l_2} & \frac{a_3}{l_3} \\ \frac{b_1}{l_1} & \frac{b_2}{l_2} & \frac{b_3}{l_3} \\ \frac{c_1}{l_1} & \frac{c_2}{l_2} & \frac{c_3}{l_3} \end{bmatrix} V^{(N)}
\end{aligned}$$

Thus, taking only the first row,

$$q = - \sum_{i=1}^3 \frac{a_i}{l_i} V_i^{(N)}$$

Similarly,

$$q = \sum_{i=1}^3 \frac{a_i}{l_i} V_i^{(T)}$$

Thus, (2.29) has also been proved.

6. Assuming the (n, τ, λ) coordinates,

$$\begin{aligned}
\oint (\boldsymbol{\xi} \times \mathbf{H}) \cdot dS &= \oint \begin{bmatrix} \hat{n} & \hat{\tau} & \hat{\lambda} \\ \xi_n & \xi_\tau & \xi_\lambda \\ \mathbf{H}_n & \mathbf{H}_\tau & \mathbf{H}_\lambda \end{bmatrix} \cdot dS \\
&= \oint [\hat{n}(\xi_\tau \mathbf{H}_\lambda - \xi_\lambda \mathbf{H}_\tau) + \hat{\tau}(\xi_\lambda \mathbf{H}_n - \xi_n \mathbf{H}_\lambda)]
\end{aligned}$$

$$\begin{aligned}
& + \hat{\lambda}(\xi_n \mathbf{H}_\tau - \xi_\tau \mathbf{H}_n) \cdot d\mathbf{S} \\
& = 0
\end{aligned}$$

by equating each component implies

$$\oint (\xi_\tau \mathbf{H}_\lambda - \xi_\lambda \mathbf{H}_\tau) dS = 0$$

which is (2.81).

Also, as $\nabla \times \mathbf{E} = j\omega\mu\mathbf{H}$,

$$\begin{aligned}
\mathbf{H} &= \frac{1}{j\omega\mu}(\nabla \times \mathbf{E}) \\
&= \frac{1}{j\omega\mu} \begin{bmatrix} \hat{n} & \hat{\tau} & \hat{\lambda} \\ \partial/\partial n & \partial/\partial \tau & \partial/\partial \lambda \\ \mathbf{E}_n & \mathbf{E}_\tau & \mathbf{E}_\lambda \end{bmatrix} \\
&= \frac{1}{j\omega\mu} [\hat{n}(\partial\mathbf{E}_\lambda/\partial\tau - \partial\mathbf{E}_\tau/\partial\lambda) + \hat{\tau}(\partial\mathbf{E}_n/\partial\lambda - \partial\mathbf{E}_\lambda/\partial n) \\
&\quad + \hat{\lambda}(\partial\mathbf{E}_\tau/\partial n - \partial\mathbf{E}_n/\partial\tau)] \\
&= \hat{n}\mathbf{H}_n + \hat{\tau}\mathbf{H}_\tau + \hat{\lambda}\mathbf{H}_\lambda
\end{aligned}$$

the boundary conditions leading to (2.82).

Appendix B

Some calculations pertaining to Chapter 3 are given here:

1. By definition,

$$\begin{aligned}\int_c \int dxdy &= A_c \\ \{U\}_i &= [\tilde{a}_i + \tilde{c}_i y] \\ \{V\}_i &= [\tilde{b}_i - \tilde{c}_i x]\end{aligned}$$

Therefore,

$$\begin{aligned}\{U_y\}_i &= \tilde{c}_i \\ \{V_x\}_i &= -\tilde{c}_i\end{aligned}$$

2.

$$\begin{aligned}\left[\int_c \int \{U_y\} \{U_y\}^T dxdy \right]_{ij} &= \left[\int_c \int \{V_x\} \{V_x\}^T dxdy \right]_{ij} \\ &= - \left[\int_c \int \{U_y\} \{V_x\}^T dxdy \right]_{ij} \\ &= - \left[\int_c \int \{V_x\} \{U_y\}^T dxdy \right]_{ij} \\ &= A_c \tilde{c}_i \tilde{c}_j\end{aligned}$$

3. By simplex coordinates,

$$\begin{aligned}y &= \sum_{i=1}^3 y_i \zeta_i \\ x &= \sum_{i=1}^3 x_i \zeta_i \\ \int_c \int y dxdy &= 2 A_c \int_{\zeta_1} \int_{\zeta_2} y d\zeta_1 d\zeta_2 \\ &= 2 A_c \int_{\zeta_1=0}^1 \int_{\zeta_2=1-\zeta_1}^1 \left(\sum_{i=1}^3 y_i \zeta_i \right) d\zeta_1 d\zeta_2\end{aligned}$$

After doing the normal definite integral derivation,

$$\int_c \int y dx dy = \frac{A_c}{3}(y_1 + y_2 + y_3) = y_c A_c$$

where $y_c = (y_1 + y_2 + y_3)/3$.

Similarly,

$$\int_c \int x dx dy = \frac{A_c}{3}(x_1 + x_2 + x_3) = x_c A_c$$

where $x_c = (x_1 + x_2 + x_3)/3$.

4. In a similar fashion,

$$\begin{aligned} \int_c \int y^2 dx dy &= 2 A_c \int_{\zeta_1} \int_{\zeta_2} y^2 d\zeta_1 d\zeta_2 \\ &= 2 A_c \int_{\zeta_1=0}^1 \int_{\zeta_2=1-\zeta_1}^1 \left(\sum_{i=1}^3 y_i \zeta_i \right)^2 d\zeta_1 d\zeta_2 \end{aligned}$$

After computing the whole integrals,

$$\begin{aligned} \int_c \int y^2 dx dy &= \frac{2 A_c}{12} (y_1^2 + y_2^2 + y_3^2 + y_1 y_2 + y_2 y_3 + y_3 y_1) \\ &= \frac{A_c}{12} (y_1^2 + y_2^2 + y_3^2 + (y_1 + y_2 + y_3)^2) \\ &= \frac{A_c}{12} (y_1^2 + y_2^2 + y_3^2 + 9 y_c^2) \end{aligned}$$

Similarly,

$$\begin{aligned} \int_c \int x^2 dx dy &= 2 A_c \int_{\zeta_1} \int_{\zeta_2} x^2 d\zeta_1 d\zeta_2 \\ &= 2 A_c \int_{\zeta_1=0}^1 \int_{\zeta_2=1-\zeta_1}^1 \left(\sum_{i=1}^3 x_i \zeta_i \right)^2 d\zeta_1 d\zeta_2 \\ &= \frac{A_c}{12} (x_1^2 + x_2^2 + x_3^2 + 9 x_c^2) \end{aligned}$$

5. Therefore, the other integrals necessary to construct the element matrices are :

(a)

$$\begin{aligned} \left[\int_c \int \{U\} \{U\}^T dx dy \right]_{ij} &= \int_c \int [\bar{a}_i + \bar{c}_i][\bar{a}_j + \bar{c}_j]^T \\ &= \int_c \int [\bar{a}_i \bar{a}_j + (\bar{a}_i \bar{c}_j + \bar{a}_j \bar{c}_i)y + \bar{c}_i \bar{c}_j y^2] dx dy \end{aligned}$$

which from the previous derivations would be

$$\begin{aligned} \left[\int_e \int \{U\} \{U\}^T dx dy \right]_{ij} &= A_e \bar{a}_i \bar{a}_j + A_e (\bar{a}_i \bar{c}_j + \bar{a}_j \bar{c}_i) y_c \\ &\quad + \frac{A_e}{12} \bar{c}_i \bar{c}_j (y_1^2 + y_2^2 + y_3^2 + 9 y_c^2) \end{aligned}$$

(b) Likewise,

$$\begin{aligned} \left[\int_e \int \{V\} \{V\}^T dx dy \right]_{ij} &= \int_e \int [\bar{b}_i - \bar{c}_i][\bar{b}_j - \bar{c}_j]^T \\ &= \int_e \int [\bar{b}_i \bar{b}_j - (\bar{b}_i \bar{c}_j + \bar{b}_j \bar{c}_i) y + \bar{c}_i \bar{c}_j y^2] dx dy \end{aligned}$$

which from the previous derivations would be

$$\begin{aligned} \left[\int_e \int \{V\} \{V\}^T dx dy \right]_{ij} &= A_e \bar{b}_i \bar{b}_j - A_e (\bar{b}_i \bar{c}_j + \bar{b}_j \bar{c}_i) x_c \\ &\quad + \frac{A_e}{12} \bar{c}_i \bar{c}_j (x_1^2 + x_2^2 + x_3^2 + 9 x_c^2) \end{aligned}$$

(c)

$$\begin{aligned} \left[\int_e \int \{U\} \{N\}_x^T dx dy \right]_{ij} &= \int_e \int [\bar{a}_i + \bar{c}_i y] \frac{A_e}{2} [b_j]^T dx dy \\ &= \frac{1}{2 A_e} \int_e \int (\bar{a}_i b_j + \bar{c}_i b_j y) dx dy = \frac{1}{2} (\bar{a}_i + \bar{c}_i y_c) b_j \end{aligned}$$

(d)

$$\begin{aligned} \left[\int_e \int \{V\} \{N\}_y^T dx dy \right]_{ij} &= \int_e \int [\bar{b}_i - \bar{c}_i x] \frac{A_e}{2} [c_j]^T dx dy \\ &= \frac{1}{2 A_e} \int_e \int (\bar{b}_i c_j - \bar{c}_i c_j x) dx dy = \frac{1}{2} (\bar{b}_i - \bar{c}_i x_c) c_j \end{aligned}$$

Note that \bar{a} and a are different, the first being the coefficients used in edge elements and the second being in terms of cartesian coordinates.

6. Also, from the direct definition of the local coordinate system,

$$\begin{aligned} \left[\int_e \int xy dx dy \right]_{ij} &= 2 A_e \int_{\zeta_1} \int_{\zeta_2} xy d\zeta_1 d\zeta_2 \\ &= 2 A_e \int_{\zeta_1=0}^1 \int_{\zeta_2=1-\zeta_1}^1 \left(\sum_{i=1}^3 x_i \zeta_i \right) \left(\sum_{i=1}^3 y_i \zeta_i \right) d\zeta_1 d\zeta_2 \\ &= \frac{A_e}{12} (2x_1 y_1 + 2x_2 y_2 + 2x_3 y_3 \\ &\quad + x_1 y_2 + x_2 y_1 + x_3 y_2 + x_2 y_3 + x_1 y_3 + x_3 y_1) \end{aligned}$$

Thus,

$$\begin{aligned}
\left[\int_c \int \{N\} \{N\}^T dx dy \right]_{ij} &= \frac{1}{2A_e} [a_i + b_i x + c_i y] \frac{1}{2A_e} [a_j + b_j x + c_j y]^T \\
&= A_e a_i a_j + \frac{A_e}{12} b_i b_j (x_1^2 + x_2^2 + x_3^2 + 9x_c^2) \\
&\quad + \frac{A_e}{12} c_i c_j (y_1^2 + y_2^2 + y_3^2 + 9y_c^2) + A_e (a_i b_j + a_j b_i) x_c \\
&\quad + A_e (a_i c_j + a_j c_i) y_c + \frac{A_e}{12} (2x_1 y_1 + 2x_2 y_2 + 2x_3 y_3 + x_1 y_2 \\
&\quad + x_2 y_1 + x_3 y_2 + x_2 y_3 + x_1 y_3 + x_3 y_1) (b_i c_j + b_j c_i)
\end{aligned}$$

After thorough expansion,

$$\left[\int_c \int \{N\} \{N\}^T dx dy \right]_{ij} = \begin{cases} \frac{1}{4A_e^2} \frac{2A_e^3}{3} = \frac{2A_e}{12} & \text{if } i = j \\ \frac{1}{4A_e^2} \frac{A_e^3}{3} = \frac{A_e}{12} & \text{if } i \neq j \end{cases}$$

7. Similarly,

(a)

$$\left[\int_c \int \{N_x\} \{N_x\}^T dx dy \right]_{ij} = \frac{1}{2A_e} [b_i x] \frac{1}{2A_e} [b_j x]^T$$

Thus,

$$\left[\int_c \int \{N_x\} \{N_x\}^T dx dy \right]_{ij} = \begin{cases} \frac{1}{4A_e} b_i b_j & \text{if } i = j \\ \frac{1}{4A_e} b_i b_j & \text{if } i \neq j \end{cases}$$

(b)

$$\left[\int_c \int \{N_y\} \{N_y\}^T dx dy \right]_{ij} = \frac{1}{2A_e} [c_i x] \frac{1}{2A_e} [c_j x]^T$$

Thus,

$$\left[\int_c \int \{N_y\} \{N_y\}^T dx dy \right]_{ij} = \begin{cases} \frac{1}{4A_e} c_i c_j & \text{if } i = j \\ \frac{1}{4A_e} c_i c_j & \text{if } i \neq j \end{cases}$$

In all these derivations $[\cdot]_{ij}$, ($ij = 11, 12, 13, \dots, 33$) indicates the (i, j) components of the matrix $[\cdot]$. Also the x_c & y_c are the centroids of the triangle.

APPENDIX C

```
C *****
C *           PROGRAM FREDEEM           *
C *                                           *
C *     FREQUENCY DOMAIN EDGE ELEMENT METHOD PROGRAM     *
C *                                           *
C *     RAJAGOPALAN VENKATACHALAM - M.A.SC. DEGREE     *
C *****
C **           DOUBLE PRECISION           - TWO DIMENSION           **
C
C DESCRIPTION:
C -----
C BASED ON DR. KOSHIBA AND DR. INOUE'S PAPER IN MTT-FEBRUARY 1992.
C This program makes use of a new method of vectorial finite element.
C This can be used in both deterministic and eigen value problems.
C This is more a hybrid method - uses both edges and nodes of a triangle.
C This gives the propagation constant directly and field quantities from that.
C The nodes at the corner of the triangles represent the axial components.
C The edges w.r.t. to the center points represent the transverse components.
C In 3-D, the nodes for the axial direction can be replaced by edges itself.
C Simple triangles are used as basic finite elements.
C The transverse fields are represented by first-order polynomials.
C Also the transverse fields are represented in cartesian coordinates.
C The longitudinal fields are represented by complete first order polynomials.
C Also, the longitudinal fields are represented by simplex(local) coordinates.
C EXAMPLE: ORDINARY MICROSTRIP PROBLEM.
C THIS IS FOR THE HALF SECTION - E-FIELD FORMULATION.
C
C P = TOTAL NUMBER OF TRIANGLES.
C E = TOTAL NUMBER OF EDGES (OR) SIDE POINTS
C DED = TOTAL NUMBER OF DIRICHLET CONDITIONS FOR EDGES
C TE = TOTAL NUMBER OF UNKNOWN EDGES
C NDS = TOTAL NUMBER OF NODES (OR) CORNER POINTS
```

C DND = TOTAL NUMBER OF DIRICHLET CONDITIONS FOR NODES
C TN = TOTAL NUMBER OF UNKNOWN NODES
C
C DIF: DENOTES THE TOTAL NUMBER OF FREQUENCY POINTS.
C YY: DENOTES THE NODES IN THE Y-AXIS.
C XX: DENOTES THE NODES IN THE X-AXIS.
C ND: TOTAL NUMBER OF DIVISIONS ROWWISE IN THE DIELECTRIC
C NT: THIS IS THE TOTAL NUMBER OF DIVISIONS ROWWISE NEAR THE STRIP.
C NA: THIS THE NUMBER OF DIVISIONS ROWWISE IN AIR.
C NS: THIS IS THE NUMBER OF DIVISIONS COLUMNWISE IN THE STRIP.
C NE: THIS THE COLUMNWISE DIVISIONS NEAR EITHER SIDES OF STRIP.
C NRR: THIS IS THE COLUMNWISE DIVISIONS OUTSIDE THE STRIP.
C W: TOTAL WIDTH OF THE MICROSTRIP, IN m.
C SW: CONDUCTOR WIDTH, IN m.
C D: TOTAL HEIGHT OF THE MICROSTRIP, IN m.
C H: HEIGHT OF THE DIELECTRIC LAYER, IN m.
C PRMB: THE PERMEABILITY OF THE MEDIUM (ASSUMED TO BE NON-MAGNETIC).
C TH: THICKNESS OF THE STRIP, IN m. (INITIALLY ASSUMED ZERO).
C AMU: PERMEABILITY OF FREE SPACE, IN H/m.
C EPS: PERMITTIVITY OF FREE SPACE, IN F/m.
C
C AE: AREA OF EACH RIGHT ANGLED FINITE ELEMENT TRIANGLE.
C DE: TOTAL NUMBER OF DIRICHLET EDGES.
C DN: TOTAL NUMBER OF DIRICHLET NODES.
C HE: AN ARRAY WHICH KEEPS TRACK OF DIRICHLET EDGES.
C HE(#,1): 1 IF DIRICHLET ; 0 IF NOT DIRICHLET.
C HE(#,2): GIVES THE TOTAL DIRICHLET ENCOUNTERED TILL THAT EDGE.
C HN: AN ARRAY WHICH KEEPS TRACK OF DIRICHLET NODES.
C HN(#,1): 1 IF DIRICHLET ; 0 IF NOT DIRICHLET.
C HN(#,2): GIVES THE TOTAL DIRICHLET ENCOUNTERED TILL THAT NODE.
C
C FREQ(#): THE FREQUENCY OF ANALYSIS.
C KO: THE FREE SPACE WAVELENGTH.
C PHASE: THE FINAL BETA'S NEEDED FOR DISPERSION DIAGRAM.

C

IMPLICIT NONE

PARAMETER P = 364, E = 573, DED = 44, TE = 529

PARAMETER NDS = 210, DND = 46, TN = 164, DIF = 12

C

INTEGER COL, DE, DF, DN, EDG, HE, HN, I, I1, I2, I3, IER, G1, G2, G3, G4

INTEGER IPV, ITR, IV, J, K, M, NC, NC1, NODES, NOPTL

INTEGER NOTR, NR, NR1, ROW, SIDES, TNO, TOT, NA, ND, NT, NE

C

REAL * 8 AE, AK, AL, AM, AMU, BB, BBK, BBL, AKTZ, AKZT

REAL * 8 BBM, BK, BL, BM, CCK, CCL, CCM, CK, CL, CM, D, DELTA, DET

REAL * 8 EPS, ERX, ERY, FI, FR, FREQ

REAL * 8 GKTT, GK TZ, GKZT, GKZZ, GMTT, KO, KTT, KTZ

REAL * 8 KZZ, MBAR, MIK, MTT, NN, NX, NY, OMEGA, PHASE, PI, PRMB

REAL * 8 RHS, TEKP3, TELP3, TEMP3, TMP, U, UN, UV, V, VN

REAL * 8 W, W1, WR, X, XC, XKP3, XLP3, XMP3, Y, YC, YKP3, YLP3, YMP3

C

INTEGER IS1, IS2, NEIG, IV1, JJ, NRR, NS

REAL * 8 FM1, FV1, FV2, FV3, OUT, YY, XX, FRQ, SW, H, TH

C

LOGICAL SLCT

C

DIMENSION SLCT(TE), FM1(TE, TE+2), FV1(TE), FV2(TE), FV3(TE), IV1(TE)

DIMENSION BB(TN, TN), EDG(P, 3), ERX(P), ERY(P), FI(TE), FR(TE)

DIMENSION FREQ(DIF), GKTT(TE, TE), GK TZ(TE, TN), GKZT(TN, TE)

DIMENSION GKZZ(TN, TN), GMTT(TE, TE), HE(E, 2), HN(NDS, 2)

DIMENSION IV(P, 3), KTT(3, 3), KTZ(3, 3), KZZ(3, 3), MBAR(TE, TE)

DIMENSION MIK(TE, TE), MTT(3, 3), NN(3, 3), NX(3, 3), NY(3, 3)

DIMENSION OUT(TE, TE), PHASE(TE), RHS(TE, TE), TMP(TE, TN)

DIMENSION U(3, 3), UN(3, 3), UV(3, 3), V(3, 3), VN(3, 3), WI(TE)

DIMENSION WR(TE), X(NDS), XX(15), Y(NDS), YY(14)

C

C NOW DIVIDE THE STRUCTURE INTO NODES FOR THE TRIANGLES.

C MAKE MORE FINER MESH NEAR THE SINGULARITIES.

```

C
DATA YY/12.7,11.248571,9.797143,8.345714,6.894286,5.442857,
*      3.991428,2.54,1.7145,1.397,1.27,1.143,0.8255,0.0/
DATA XX/0.0,0.3,0.508,0.635,0.762,0.97,1.27,1.905,2.54,
*      3.175,3.81,4.445,5.08,5.715,6.35/
C
OPEN (UNIT =2, FILE = 'OUTPUT.OP',STATUS = 'UNKNOWN')
C *****
C I. INPUT ALL PARAMETERS ( this could be done from input file too)::
C -----
C INPUT THE DIVISIONS:
C DIVIDE CRISS-CROSS INTO RECTANGLES .
C
ND = 2
NT = 1
NA = 9
NS = 2
NE = 2
NRR = 10
C
C THE MAGNETIC SYMMETRY IS ASSUMED AND ONLY HALF SECTION IS ANALYZED.
WRITE (2,10)
10 FORMAT('SUBDIVIDE ONE HALF OF MICROSTRIP CROSS-SECTION INTO EDGES'/)
C *****
C SET THE STRUCTURE DIMENSIONS(WIDTH,HEIGHT,ETC):
FRQ = 1.0
W = 12.7E-3
SW = 1.27E-3
TH = 0.0E0
D = 12.7E-3
H = 1.27E-3
PRMB = 1.0
C
WRITE (2,20) PRMB,TH

```

```

20 FORMAT('PERMEABILITY(R) =',F8.4,/, 'STRIP THICKNESS =',E13.6/)
C
    WRITE (2,30) W,SW
30 FORMAT('TOTAL WIDTH : ',E13.6,/, 'STRIP WIDTH : ',E13.6/)
C
    WRITE(2,40) D,H
40 FORMAT('TOTAL HEIGHT AND DIELECTRIC HEIGHT : ',2(E13.6,3X)/)
C
    WRITE (2,50) NA,NT,ND, NS,NE,NRR
50 FORMAT ( 'COLUMN MESH DIVISION - AIR AND DIELEC =',3(I3,4X),/,
*          'ROW MESH DIVISION - WHOLE AND STRIP = ',3(I3,4X)/)
C
    WRITE(*,60)
60 FORMAT('DIELECTRIC REGION HEIGHT IS ONE-TENTH OF THE TOTAL HEIGHT'/)
    WRITE(*,70)
70 FORMAT('ALL LENGTHS ARE GIVEN IN m AND FREQUENCIES IN HZ'/)
C
    PI = ACOS(-1.0)
    PI = DBLE(PI)
    AMU = 4.0*PI*1E-7
    EPS = 8.854*1E-12
C
C NOW SET THE FREQUENCIES(GHZ) AT WHICH THE STRUCTURE IS TO BE ANALYZED.
C
    DF = 12
C DF: DENOTES THE TOTAL NUMBER OF FREQUENCY POINTS.
C
    DO 80 I = 1,DF
        FREQ(I) = FRQ*1.0E9
        FRQ=FRQ+3.0
80 CONTINUE
C *****
C THE GIVEN STRUCTURE IS DIVIDED INTO NR BY NC RECTANGLES
C EACH RECTANGLE IS DIVIDED INTO TWO TRIANGLES.

```

```

C EACH TRIANGLES ARE ASSUMED TO BE ISOSLES RIGHT ANGLED.
NR = NS+NE+NRR
NC = ND+2*NT+NA
C NR1 AND NC1 GIVE THE TOTAL NODES POSSIBLE IN X AND Y DIRECTIONS.
NR1 = NR+1
NC1 = NC+1
C
C NR1*NC1 GIVES THE TOTAL NUMBER OF THE NODES IN THE STRUCTURE.
NODES = NR1*NC1
WRITE (2,90) NODES
90 FORMAT('THE TOTAL NUMBER OF NODES IS =',I4/)
C
C NOTR IS THE TOTAL NUMBER OF TRIANGLES POSSIBLE IN THE STRUCTURE.
NOTR = 2*NR*NC
WRITE (2,100) NOTR
100 FORMAT('THE TOTAL NUMBER OF TRIANGLES IS =',I4/)
C
C NOW LET US FIND THE TOTAL NUMBER OF EDGES IN THE GIVEN STRUCTURE.
SIDES = NR+NC*(3*NR+1)
WRITE (2,110) SIDES
110 FORMAT('THE TOTAL NUMBER OF EDGES IS =',I4/)
C
C THE G'S GIVEN BELOW ARE JUST VARIABLES FOR FORCING B.C.S.
G1 = 2*NR*(NA+NT-1)
G2 = 2*(NR*(NA+NT-1)+NS+NE/2)
G3 = 2*NR*(NA+NT)
G4 = 2*(NR*(NA+NT)+NS+NE/2)
C *****
C II. COORDINATE GENERATOR ::
C -----
C NOW SET THE X AND Y COORDINATES OF ALL NODES:
DO 130 J = 1,NC1
DO 120 I = 1,NR1
K = (J-1)*NR1+I

```

```

X(K) = XX(I)/1000.0
Y(K) = YY(J)/1000.0
WRITE(2,140) K,X(K),Y(K)
120 CONTINUE
130 CONTINUE
140 FORMAT( 1X,'NODE NUMBER=',I4,3X,'X CO-ORDINATE=',
*          F12.8,3X,'Y CO-ORDINATE =',F12.8/)
C
C CHECK:
IF (K .NE. (NR1*NC1)) THEN
WRITE(*,150)
150 FORMAT (1X,'THERE IS AN ERROR IN NUMBERING OF NODES-PLEASE CHECK')
STOP
ENDIF
C *****
C III. NODE & EDGE GENERATOR::
C -----
C THE AUTOMATIC MESH GENERATION PART :
C IV ARE THE GLOBAL NODE NUMBERS OF THE TRIANGLES.
ITR = 0
C NOW THE NUMBER OF TRIANGLES AND NODES THAT MAKE THEM UP ARE GIVEN.
C
DO 170 J=1,NC
DO 160 I = 1,NR
ITR = 2*(J-1)*NR + (2*I-1)
IV(ITR,1) = J*NR1+I+1
IV(ITR,2) = J*NR1+I
IV(ITR,3) = (J-1)*NR1+I
EDG(ITR,1) = J*(3*NR+1)+I
EDG(ITR,2) = (J-1)*(2*NR+1)+J*NR+(2*I-1)
EDG(ITR,3) = (J-1)*(2*NR+1)+J*NR+2*I
C
WRITE(2,180) ITR,IV(ITR,1),IV(ITR,2),IV(ITR,3),
*          EDG(ITR,1),EDG(ITR,2),EDG(ITR,3),

```

```

*           X(IV(ITR,1)),X(IV(ITR,2)),X(IV(ITR,3)),
*           Y(IV(ITR,1)),Y(IV(ITR,2)),Y(IV(ITR,3))
C
  ITR = ITR+1
  IV(ITR,1) = (J-1)*NR1+I+1
  IV(ITR,2) = (J-1) *NR1+I
  IV(ITR,3) = (J*NR1)+I+1
  EDG(ITR,1) = (J-1)*(3*NR+1)+I
  EDG(ITR,2) = (J-1)*(2*NR+1)+J*NR+2*I
  EDG(ITR,3) = (J-1)*(2*NR+1)+J*NR+(2*I+1)
C
  WRITE(2,180) ITR,IV(ITR,1),IV(ITR,2),IV(ITR,3),
*           EDG(ITR,1),EDG(ITR,2),EDG(ITR,3),
*           X(IV(ITR,1)),X(IV(ITR,2)),X(IV(ITR,3)),
*           Y(IV(ITR,1)),Y(IV(ITR,2)),Y(IV(ITR,3))
160 CONTINUE
170 CONTINUE
C
180 FORMAT (1X,'THE TRIANGLE NUMBER IS ='I3/,' THE NODES THAT COMPRISE
*           THAT TRIANGLE LOCALLY BEING =' , 3(I3,2X)/,' THE EDGES THAT
*           COMPRISE THAT TRIANGLE LOCALLY ARE =' , 3(I3,2X)/,
*           'THE X AND Y COORDINATES OF THE NODES =' ,2(3(F12.8,4X))//)
C  OBVIOUSLY, NOW THE X AND Y COORDINATES OF EACH NODE THAT MAKE
C  THE TRIANGLE ARE KNOWN
C
C  CHECK:( RULE OF THUMB)
  IF ((2*SIDES-2*(NR+NC)) .NE. 3*ITR) THEN
    WRITE (*,190)
190 FORMAT('THERE IS SOME MISMATCH IN 2E-B=3F FORMULA. CHECK IT OUT!')
    STOP
  ENDIF
  WRITE (*,200)
200 FORMAT('THE RELATIONSHIP 2E-B=3F HOLDS GOOD. HAPPILY PROCEED NOW')
  IF(ITR .NE. NOTR) THEN

```

```

WRITE (*,210)
210 FORMAT(1X,'THERE IS AN ERROR IN NUMBERING OF THE TRIANGLES-CHECK'//)
STOP
ENDIF

C *****
C IV. BOUNDARY CONDITIONS SET-UP::
C -----
C NEUMANN BOUNDARY CONDITIONS ARE NATURAL IN THE FORMULATION.
C NOW SET THE DIRICHLET BOUNDARY CONDITIONS :
C
C INITIALIZE:
DO 240 M = 1, ITR
DO 220 I = 1, 3
HE(EDG(M,I),1) = 0
HN(EDG(M,I),1) = 0
220 CONTINUE
C
C NOW ON RIGHT SIDES, SET DIRICHLET.
IF((X(IV(M,3)).EQ.W/2.0).AND.
* (X(IV(M,1)).EQ.W/2.0)) THEN
HE(EDG(M,3),1) = 1
ENDIF
C LEFT SIDE IS A MAGNETIC WALL OF SYMMETRY AND NO CONDITIONS ON E FIELD.
C
C NOW, ON TOP AND BOTTOM, SET DIRICHLET
IF((Y(IV(M,1)) .EQ. 0.0) .AND.
* (Y(IV(M,2)) .EQ. 0.0)) THEN
HE(EDG(M,1),1) = 1
ENDIF
IF((Y(IV(M,1)) .EQ. D) .AND.
* (Y(IV(M,2)) .EQ. D)) THEN
HE(EDG(M,1),1) = 1
ENDIF
C

```

```

C NOW ON THE STRIP, SET DIRICHLET
  IF((M.GT.G1) .AND. (M .LE. G2) .AND.
*   ((Y(IV(M,1))-H) .LE. 1.0E-8) .AND. ((Y(IV(M,2))-H)
*   .LE. 1.0E-8)) THEN
HE(EDG(M,1),1) = 1
  ENDIF
  IF((M.GT.G3) .AND. (M .LE. G4) .AND.
*   ((Y(IV(M,1))-H) .LE. 1.0E-8) .AND. ((Y(IV(M,2))-H)
*   .LE. 1.0E-8)) THEN
HE(EDG(M,1),1) = 1
  ENDIF
C
C NOW SET D.B.C. FOR THE NODES ON ALL CONDUCTORS.
DO 230 I = 1,3
  IF(Y(IV(M,I)) .EQ. D) HN(IV(M,I),1) = 1
  IF(X(IV(M,I)) .EQ.W/2.0) HN(IV(M,I),1) = 1
  IF(Y(IV(M,I)) .EQ. 0.0) HN(IV(M,I),1) = 1
  IF((X(IV(M,1)) .LE. SW/2.0) .AND. (Y(IV(M,1)).EQ.H))
*   HN(IV(M,1),1) = 1
  IF((X(IV(M,2)) .LT. SW/2.0) .AND. (Y(IV(M,2)).EQ.H))
*   HN(IV(M,2),1) = 1
230 CONTINUE
240 CONTINUE
C
  DE =0
  DN =0
C
C THE VALUE OF DIRICHLET EDGES MUST BE KNOWN.
C BUT, VALUE OF DIRICHLET NODES NEED NOT BE KNOWN.
C ONLY IF THE NODE IS DIRICHLET OR NOT NEED TO BE KNOWN.
C PRINT THE DIRICHLET NODES AND EDGES INFORMATIONS:
C
DO 250 M = 1,SIDES
HE(M,2) = DE

```

```

DE = DE+HE(M,1)
WRITE (2,260) M,HE(M,1),HE(M,2),DE
250 CONTINUE
260 FORMAT('SIDE = ',I4,' HE(M,1) = ',I3,' HE(M,2) = ',I3,' DE = ',I3/)
C
DO 270 M = 1,NODES
HN(M,2) = DN
DN = DN+HN(M,1)
WRITE (2,280) M,HN(M,1),HN(M,2),DN
270 CONTINUE
280 FORMAT('NODE = ',I4,' HN(M,1) = ',I3,' HN(M,2) = ',I3,' DN = ',I3/)
C *****
C V. NUMERICAL FORMULATION::
C -----
C START THE FORMULATION :
TOT = SIDES-DE
TNO = NODES-DN
WRITE(2,290) TOT,TNO
290 FORMAT ('THE ORDERS OF FINAL MATRIX = ', 2(I4,3X)/)
C
C TOT: TOTAL NUMBER OF UNKNOWN EDGES - FINAL ORDER OF E.V.P.
C TNO: TOTAL NUMBER OF UNKNOWN NODES.
C
C NOW DO THE WHOLE PROCEDURE FOR EACH AND EVERY FREQUENCY.
OMEGA = 0.0
C THE FREQUENCY IS TAKEN TO BE FROM 1.0GHZ.
DO 710 K = 1,DF
IF(FREQ(K) .GT.0.0E0) THEN
WRITE (2,300) FREQ(K)
300 FORMAT( '**THE FREQUENCY IN HZ** = ', E13.6/)
ELSE
WRITE(*,*) '**CHECK FREQUENCY NOW!**'
STOP
ENDIF

```

```

C
C NOW DO THE INITIALIZATION OF ALL GLOBAL MATRICES.
C
DO 320 I = 1,TOT
DO 310 J = 1,TOT
GKTT(I,J) = 0.0
GMTT(I,J) = 0.0
MIK(I,J) = 0.0
RHS(I,J) = 0.0
OUT(J,I) = 0.0
IF(HE(I,1) .EQ. 1) OUT(J,I) = 1.0
310 CONTINUE
FR(I) = 0.0
FI(I) = 0.0
320 CONTINUE
DO 340 I = 1,TNO
DO 330 J = 1,TNO
GKZZ(I,J) = 0.0
BB(I,J) = 0.0
330 CONTINUE
340 CONTINUE
DO 360 I = 1,TOT
DO 350 J = 1,TNO
GKTZ(I,J) = 0.0
GKZT(J,I) = 0.0
TMP(I,J) = 0.0
350 CONTINUE
360 CONTINUE
C
OMEGA = 2.0*PI*FREQ(K)
KO = AMU*EPS*OMEGA**2
C
C NOW START AND DO FOR ALL TRIANGLES.
C

```

```

DO 500 ITR = 1,NOTR
C  SET THE PERMITTIVITY ALONG EVERY DIRECTION FOR EACH LOCAL TRIANGLE.
C  HERE AN ISOTROPIC CASE IS ASSUMED WITH DIELECTRIC PERMITTIVITY = 8.875.
C
IF (ITR .LE. (2*NR*(NA+NT))) THEN
ERX(ITR) =1.0
ERY(ITR) =1.0
ELSE
ERX(ITR) = 8.875
ERY(ITR) = 8.875
ENDIF
C
C  INITIALIZE ALL LOCAL MATRICES.
DO 380 I = 1,3
DO 370 J = 1,3
KTT(I,J) = 0.0
KTZ(I,J) = 0.0
KZZ(I,J) = 0.0
MTT(I,J) = 0.0
370 CONTINUE
380 CONTINUE
C
C  READ THE NODAL INFORMATION OF EACH TRIANGLE ONCE AGAIN.
C
I1 = IV(ITR,1)
I2 = IV(ITR,2)
I3 = IV(ITR,3)
C  PRINT ONLY FOR ONE FREQUENCY,AS IT REMAINS THE SAME FOR ALL FREQS.
C
IF (K.EQ.1) THEN
WRITE(2,390) ITR,I1,I2,I3,ERX(ITR),ERY(ITR)
390 FORMAT(5X,'TRIANGLE =', I3, 5X, 'NODES =', 3(I3,3X),
*          'PERMITTIVITY ON X AND Y ARE : ', 2(E15.7,3X)/)
ENDIF

```

```

C
C  CALCULATE THE MID POINTS COORDINATES.
XKP3 = (X(I1)+X(I2))/2.0
YKP3 = (Y(I1)+Y(I2))/2.0
XLP3 = (X(I2)+X(I3))/2.0
YLP3 = (Y(I2)+Y(I3))/2.0
XMP3 = (X(I3)+X(I1))/2.0
YMP3 = (Y(I3)+Y(I1))/2.0

C
C  NOW CALCULATE THE BS AND CS OF THE LOCAL COORDINATE SYSTEM
BBK = Y(I2)-Y(I3)
BBL = Y(I3)-Y(I1)
BBM = Y(I1)- Y(I2)
CCK = X(I3)-X(I2)
CCL = X(I1)-X(I3)
CCM = X(I2)-X(I1)

C
C  CALCULATE THE THETA ANGLES.
IF(X(I1) .EQ.X(I2)) THEN
TEKP3 = PI/2.0
ELSE
TEKP3 = DATAN2((Y(I1)-Y(I2)),(X(I1)-X(I2)))
IF (TEKP3 .LT. 0.0) TEKP3 = TEKP3+PI
IF ((Y(I1).EQ.Y(I2)).AND.(X(I1).LT.X(I2))) TEKP3 = 0.0
ENDIF
IF(X(I2) .EQ.X(I3)) THEN
TELP3 = PI/2.0
ELSE
TELP3 = DATAN2((Y(I2)-Y(I3)),(X(I2)-X(I3)))
IF (TELP3 .LT. 0.0) TELP3 = TELP3+PI
IF ((Y(I2).EQ.Y(I3)).AND.(X(I2).LT.X(I3))) TELP3 = 0.0
ENDIF
IF(X(I3) .EQ.X(I1)) THEN
TEMP3 = PI/2.0

```

```

ELSE
TEMP3 = DATAN2((Y(I3)-Y(I1)),(X(I3)-X(I1)))
IF (TEMP3 .LT. 0.0) TEMP3 = TEMP3+PI
IF ((Y(I3).EQ.Y(I1)).AND.(X(I3).LT.X(I1))) TEMP3 = 0.0
ENDIF

C
C PRINT ONLY FOR ONE FREQUENCY,AS IT REMAINS THE SAME FOR ALL FREQS.
C PRINT ANGLES IN DEGREES.
IF (K.EQ.1) THEN
WRITE (2,400) ITR,TEKP3*180.0/PI,TELP3*180.0/PI,TEMP3*180.0/PI
400 FORMAT('TRI = ', I3, ' THE ANGLES ARE = ',3(F10.5,3X)/)
ENDIF

C
C CALCULATE ALL COEFFICIENTS USED IN FORMULATION.
C
C CALCULATE THE DELTA - THE COMMON DENOMINATOR.
DELTA = (YKP3*DCOS(TEKP3)-XKP3*DSIN(TEKP3))*(DCOS(TELP3)*
* DSIN(TEMP3)-DCOS(TEMP3)*DSIN(TELP3))+
* (YLP3*DCOS(TELP3)-XLP3*DSIN(TELP3))*(DCOS(TEMP3)*DSIN(TEKP3)-
* DCOS(TEKP3)*DSIN(TEMP3))+
* (YMP3*DCOS(TEMP3)-XMP3*DSIN(TEMP3))*(DCOS(TEKP3)*DSIN(TELP3)-
* DCOS(TELP3)*DSIN(TEKP3))
C
C CALCULATE THE AK,AL,AM
AK = ((YMP3*DCOS(TEMP3)-XMP3*DSIN(TEMP3))*DSIN(TELP3)-
* (YLP3*DCOS(TELP3)-XLP3*DSIN(TELP3))*DSIN(TEMP3))/DELTA
AL = ((YKP3*DCOS(TEKP3)-XKP3*DSIN(TEKP3))*DSIN(TEMP3)-
* (YMP3*DCOS(TEMP3)-XMP3*DSIN(TEMP3))*DSIN(TEKP3))/DELTA
AM = ((YLP3*DCOS(TELP3)-XLP3*DSIN(TELP3))*DSIN(TEKP3)-
* (YKP3*DCOS(TEKP3)-XKP3*DSIN(TEKP3))*DSIN(TELP3))/DELTA
C
C NOW CALCULATE BK,BL,BM
BK = ((YLP3*DCOS(TELP3)-XLP3*DSIN(TELP3))*DCOS(TEMP3)-
* (YMP3*DCOS(TEMP3)-XMP3*DSIN(TEMP3))*DCOS(TELP3))/DELTA

```

```

BL = ((YMP3*DCOS(TEMP3)-XMP3*DSIN(TEMP3))*DCOS(TEKP3)-
*      (YKP3*DCOS(TEKP3)-XKP3*DSIN(TEKP3))*DCOS(TEMP3))/DELTA
BM = ((YKP3*DCOS(TEKP3)-XKP3*DSIN(TEKP3))*DCOS(TELP3)-
*      (YLP3*DCOS(TELP3)-XLP3*DSIN(TELP3))*DCOS(TEKP3))/DELTA
C
C NOW CALCULATE CK,CM.,CL
CK = (DCOS(TELP3)*DSIN(TEMP3)-DCOS(TEMP3)*DSIN(TELP3))/DELTA
CL = (DCOS(TEMP3)*DSIN(TEKP3)-DCOS(TEKP3)*DSIN(TEMP3))/DELTA
CM = (DCOS(TEKP3)*DSIN(TELP3)-DCOS(TELP3)*DSIN(TEKP3))/DELTA
C
C CALCULATE THE AREA OF EACH TRIANGLE.
DET = X(I2)*Y(I3)-X(I3)*Y(I2)+X(I1)*Y(I2)-X(I2)*Y(I1)+
*      X(I3)*Y(I1)-X(I1)*Y(I3)
AE = DABS(DET/2.0)
C
C PRINT ONLY FOR ONE FREQUENCY,AS IT REMAINS THE SAME FOR ALL FREQS.
IF (K.EQ.1) THEN
WRITE (2,410) ITR,AE
410 FORMAT('TRIANGLE =', I5,' AREA=', E17.7/)
ENDIF
C
C CALCULATE THE CENTROID XC AND YC OF THE TRIANGLE:
XC = (X(I1)+X(I2)+X(I3))/3.0
YC = (Y(I1)+Y(I2)+Y(I3))/3.0
C
C CALCULATE THE INTEGRAL OF U*U^T - PURELY EDGE & SYMMETRIC.
U(1,1)=AE*(AK*AK+YC*(AK*CK+CK*AK)+CK*CK/12.0*(Y(I1)**2+
*      Y(I2)**2+Y(I3)**2+9.0*YC**2))
U(1,2)=AE*(AK*AL+YC*(AK*CL+CK*AL)+CK*CL/12.0*(Y(I1)**2+
*      Y(I2)**2+Y(I3)**2+9.0*YC**2))
U(1,3)=AE*(AK*AM+YC*(AK*CM+CK*AM)+CK*CM/12.0*(Y(I1)**2+
*      Y(I2)**2+Y(I3)**2+9.0*YC**2))
U(2,2)=AE*(AL*AL+YC*(AL*CL+CL*AL)+CL*CL/12.0*(Y(I1)**2+
*      Y(I2)**2+Y(I3)**2+9.0*YC**2))

```

```

U(2,3)=AE*(AL*AM+YC*(AL*CM+CL*AM)+CL*CM/12.0*(Y(I1)**2+
*      Y(I2)**2+Y(I3)**2+9.0*YC**2))
U(3,3)=AE*(AM*AM+YC*(AM*CM+CM*AM)+CM*CM/12.0*(Y(I1)**2+
*      Y(I2)**2+Y(I3)**2+9.0*YC**2))
U(2,1) = U(1,2)
U(3,2) = U(2,3)
U(3,1) = U(1,3)

C
C NOW CALCULATE V*V^T - PURELY EDGE AND SYMMETRIC.
C
V(1,1)=AE*(BK*BK-XC*(BK*CK+CK*BK)+CK*CK/12.0*(X(I1)**2+
*      X(I2)**2+X(I3)**2+9.0*XC**2))
V(1,2)=AE*(BK*BL-XC*(BK*CL+CK*BL)+CK*CL/12.0*(X(I1)**2+
*      X(I2)**2+X(I3)**2+9.0*XC**2))
V(1,3)=AE*(BK*BM-XC*(BK*CM+CK*BM)+CK*CM/12.0*(X(I1)**2+
*      X(I2)**2+X(I3)**2+9.0*XC**2))
V(2,2)=AE*(BL*BL-XC*(BL*CL+CL*BL)+CL*CL/12.0*(X(I1)**2+
*      X(I2)**2+X(I3)**2+9.0*XC**2))
V(2,3)=AE*(BL*BM-XC*(BL*CM+CL*BM)+CL*CM/12.0*(X(I1)**2+
*      X(I2)**2+X(I3)**2+9.0*XC**2))
V(3,3)=AE*(BM*BM-XC*(BM*CM+CM*BM)+CM*CM/12.0*(X(I1)**2+
*      X(I2)**2+X(I3)**2+9.0*XC**2))
V(2,1) = V(1,2)
V(3,2) = V(2,3)
V(3,1) = V(1,3)

C
C UX IS THE DERIVATIVE OF U WITH RESPECT TO X AND SO ON.
C CALCULATE UY*UY^T=VX*VX^T=-UY*VX^T=-VX*UY^T .
C ALL THESE ARE PURELY EDGE AND SYMMETRIC.
C
UV(1,1) = AE*CK*CK
UV(1,2) = AE*CK*CL
UV(1,3) = AE*CK*CM
UV(2,2) = AE*CL*CL

```

```

UV(2,3) = AE*CL*CM
UV(3,3) = AE*CM*CM
UV(2,1) = UV(1,2)
UV(3,2) = UV(2,3)
UV(3,1) = UV(1,3)
C   CALCULATE U*NX^T
C   THIS IS BOTH EDGE AND NODE AND HENCE UNSYMMETRIC.
C
UN(1,1) = (AK+CK*YC)*BBK/2.0
UN(1,2) = (AK+CK*YC)*BBL/2.0
UN(1,3) = (AK+CK*YC)*BBM/2.0
UN(2,1) = (AL+CL*YC)*BBK/2.0
UN(2,2) = (AL+CL*YC)*BBL/2.0
UN(2,3) = (AL+CL*YC)*BBM/2.0
UN(3,1) = (AM+CM*YC)*BBK/2.0
UN(3,2) = (AM+CM*YC)*BBL/2.0
UN(3,3) = (AM+CM*YC)*BBM/2.0 .
C   CALCULATE V*NY^T
C   THIS IS BOTH EDGE AND NODE AND HENCE UNSYMMETRIC.
C
VN(1,1) = (BK-CK*XC)*CCK/2.0
VN(1,2) = (BK-CK*XC)*CCL/2.0
VN(1,3) = (BK-CK*XC)*CCM/2.0
VN(2,1) = (BL-CL*XC)*CCK/2.0
VN(2,2) = (BL-CL*XC)*CCL/2.0
VN(2,3) = (BL-CL*XC)*CCM/2.0
VN(3,1) = (BM-CM*XC)*CCK/2.0
VN(3,2) = (BM-CM*XC)*CCL/2.0
VN(3,3) = (BM-CM*XC)*CCM/2.0
C   CALCULATE N*N^T
C   THIS IS PURELY NODAL & SYMMETRIC.
C
NN(1,1) = AE/6.0
NN(1,2) = AE/12.0

```

```

NN(1,3) = AE/12.0
NN(2,2) = AE/6.0
NN(2,3) = AE/12.0
NN(3,3) = AE/6.0
NN(2,1) = NN(1,2)
NN(3,2) = NN(2,3)
NN(3,1) = NN(1,3)
C  CALCULATE NX*NX^T
C  NX IS THE DERIVATE OF N W.R.T. X.
C  THIS IS PURELY NODAL & SYMMETRIC.
C
NX(1,1) = BBK*BBK/(4.0*AE)
NX(1,2) = BBK*BBL/(4.0*AE)
NX(1,3) = BBK*BBM/(4.0*AE)
NX(2,2) = BBL*BBL/(4.0*AE)
NX(2,3) = BBL*BBM/(4.0*AE)
NX(3,3) = BBM*BBM/(4.0*AE)
NX(2,1) = NX(1,2)
NX(3,2) = NX(2,3)
NX(3,1) = NX(1,3)
C  CALCULATE NY*NY^T
C  NY IS THE DERIVATE OF N W.R.T. Y.
C  THIS IS PURELY NODAL & SYMMETRIC.
C
NY(1,1) = CCK*CCK/(4.0*AE)
NY(1,2) = CCK*CCL/(4.0*AE)
NY(1,3) = CCK*CCM/(4.0*AE)
NY(2,2) = CCL*CCL/(4.0*AE)
NY(2,3) = CCL*CCM/(4.0*AE)
NY(3,3) = CCM*CCM/(4.0*AE)
NY(2,1) = NY(1,2)
NY(3,2) = NY(2,3)
NY(3,1) = NY(1,3)
C

```

```

C   ERZ IS THE SAME AS ERX = SO DEFINE IT TO BE THE SAME. SAVE STORAGE.
C   AS NOTICABLE, ONLY KTZ HAS BOTH EDGE AND NODE CONTRIBUTION.
C   KTT AND MTT HAVE ONLY EDGE CONTRIBUTIONS.
C   KZZ HAS ONLY NODE CONTRIBUTION.
C   WHILE ASSEMBLING GLOBALLY, ELIMINATE THE DIRICHLET B.C.S
C   FIRST ASSEMBLE EACH TERMS LOCALLY:
C
      DO 430 I = 1,3
      DO 420 J = 1,3
C   ONLY SIDES:
      KTT(I,J) = ERX(ITR)*KO*U(I,J)+ERY(ITR)*KO*V(I,J)-4.0*UV(I,J)
      MTT(I,J) = V(I,J)+U(I,J)
C   ONLY NODES:
      KZZ(I,J) = ERX(ITR)*KO*NN(I,J)-NY(I,J)-NX(I,J)
C   SIDES AND NODES:
      KTZ(I,J) = VN(I,J)+UN(I,J)
420 CONTINUE
430 CONTINUE
C   ELIMINATE THE DIRICHLET BOUNDARY CONDITIONS NOW:
C   ONLY EDGE:
C
      DO 450 I = 1,3
      IF(HE(EDG(ITR,I),1) .NE. 1) THEN
C   NOT DIRICHLET EDGE- SO ASSEMBLE IT IN SUITABLE ROW..
      ROW = EDG(ITR,I)-HE(EDG(ITR,I),2)
      DO 440 J = 1,3
      IF(HE(EDG(ITR,J),1) .NE. 1) THEN
C   NOT DIRICHLET EDGE- SO ASSEMBLE IT IN SUITABLE COLUMN..
      COL = EDG(ITR,J)-HE(EDG(ITR,J),2)
C
      GKTT(ROW,COL) = GKTT(ROW,COL)+KTT(I,J)
      GMTT(ROW,COL) = GMTT(ROW,COL)+MTT(I,J)
      ENDIF
440 CONTINUE

```

```

        ENDIF
450 CONTINUE
C   BOTH [GKTT] AND [GMTT] ARE SYMMETRIC AND SPARSE.
C   ONLY NODE:
C
      DO 470 I = 1,3
        IF(HN(IV(ITR,I),1) .NE. 1) THEN
C   NOT DIRICHLET NODE- SO ASSEMBLE IT IN SUITABLE ROW..
          ROW = IV(ITR,I)-HN(IV(ITR,I),2)
          DO 460 J = 1,3
            IF(HN(IV(ITR,J),1) .NE. 1) THEN
C   NOT DIRICHLET NODE- SO ASSEMBLE IT IN SUITABLE COLUMN..
              COL =IV(ITR,J)-HN(IV(ITR,J),2)
C
              GKZZ(ROW,COL) = GKZZ(ROW,COL)+KZZ(I,J)
            ENDIF
          ENDIF
        ENDIF
460 CONTINUE
      ENDIF
470 CONTINUE
C   [GKZZ] IS SYMMETRIC AND SPARSE.
C   EDGES AND NODES:
C
      DO 490 I = 1,3
        IF(HE(EDG(ITR,I),1) .NE. 1) THEN
C   NOT DIRICHLET EDGE- SO ASSEMBLE IT IN SUITABLE ROW..
          ROW = EDG(ITR,I)-HE(EDG(ITR,I),2)
          DO 480 J = 1,3
            IF(HN(IV(ITR,J),1) .NE. 1) THEN
C   NOT DIRICHLET NODE- SO ASSEMBLE IT IN SUITABLE COLUMN..
              COL =IV(ITR,J)-HN(IV(ITR,J),2)
C
              GKTZ(ROW,COL) = GKTZ(ROW,COL)+KTZ(I,J)
            ENDIF
          ENDIF
        ENDIF
480 CONTINUE

```

```

        ENDIF
490 CONTINUE
C   REPEAT FOR NEXT TRIANGLE.
500 CONTINUE
C *****
C   NOW TAKE THE TRANSPOSE OF [GKTZ] TO OBTAIN [GKZT].
      CALL TRPOSE(GKTZ,GKZT,TOT,TNO)
C   BOTH [GKTZ] AND [GKZT] ARE NON-SYMMETRIC AND SPARSE.
C   GKTT,GKTZ,GKZZ,GMTT ARE ALL GLOBAL, REAL, SPARSE MATRICES.
C
C   GKZZ IS SPARSE TILL NOW AND REAL, SYMMETRIC
      CALL GAUSSJ(GKZZ,TNO,TNO,BB,TNO,TNO)
C   ON INVERSE, GKZZ LOOSES SPARSITY AND BECOMES DENSE.
C   YET GKZZ IS STILL REAL AND SYMMETRIC.
C
C   NOW CALL A ROUTINE FOR MULTIPLYING THE THREE MATRICES,
C   NAMELY GKTZ*INV(GKZZ)*GKZT.
      CALL MATMPY(TOT,TNO,TNO,GKTZ,GKZZ,TMP)
      CALL MATMPY(TOT,TNO,TOT,TMP,GKZT,RHS)
C
C   NOW ADD GMTT AND RHS TO GET GMTTBAR
      CALL MTXADD(TOT,GMTT,RHS,MBAR)
C   GMTTBAR AND RHS ARE DENSE, NON-SPARSE, REAL (LUCKILY) SYMMETRIC.
C   GENERALLY, THEY HAVE TO BE NON-SYMMETRIC.
C *****
C   NOW GET THE EIGEN VECTOR ROUTINE TO SOLVE THE GENERALIZED EVP.
C   BE CAREFUL: THE PROBLEM CONSISTS OF INDEFINITE MATRICES.
C   TO SOLVE  $[K]*X = \text{BETASQ}*[M]*X$ 
C   NOTICE, THIS FINAL EQUATION HAS ONLY EDGE VARIABLES OF TRANSVERSAL PLANE.
C   CHANGE THE GENERALIZED EVP TO STANDARD EVP.
C   THIS IS POSSIBLE AS LONG AS  $[M]^{-1}$  IS NON-SINGULAR.
C
C   FOR CONVENIENCE AND EFFICIENCY, USE THE SAME DUMMY ARRAYS.
      DO 520 I = 1,TOT

```

```

DO 510 J = 1,TOT
RHS(I,J) = 0.0
510 CONTINUE
520 CONTINUE
    CALL GAUSSJ(MBAR,TOT,TOT,RHS,TOT,TOT)
C   GKTT IS STILL SYMMETRIC, SPARSE AND REAL.
    CALL MATMPY(TOT,TOT,TOT,MBAR,GKTT,MIK)
C   [MIK] IS REAL, INDEFINITE BUT NON-SYMMETRIC AND DENSE.
C   NOW, TO SOLVE {[MIK]-BETASQ} = 0
C *****
C VI. SOLVER FOR EVP AND RESULTS::
C -----
C   IT IS IMPOSSIBLE TO DESIGN SATISFACTORY ALGORITHMS FOR
C   NONSYMMETRIC MATRIX.  HERE, THE EIGENVALUES CAN BE VERY
C   SENSITIVE TO SMALL CHANGES IN THE MATRIX ELEMENTS.  THE
C   MATRIX ITSELF CAN BE DEFECTIVE, SO THAT THERE IS NO COMPLETE
C   SET OF EIGENVALUES.  THESE DIFFICULTIES ARE INTRINSIC
C   PROPERTIES OF CERTAIN NONSYMMETRIC MATRICES, AND
C   "NO" NUMERICAL PROCEDURE CAN "CURE" THEM.
C
C   IT IS ALWAYS RECOMMENDED THAT ONE 'BALANCE'
C   NON-SYMMETRIC MATRICES.IT SUBSTANTIALLY IMPROVES ACCURACY.
C   A SYMMETRIC IS ALWAYS BALANCED AND HENCE UNAFFECTED.
    CALL BALANC(TOT,TOT,MIK,IS1,IS2,FV1)
C
C   NOW CALL THE SET OF EISPACK ROUTINES - QR ALGORITHM.
C   SOLVE FOR EIGEN VECTORS USING INVERSE INTERATION.
C   ALSO, CHECK FOR CONVERGENCE OF EIGENVECTORS.
    CALL ELMHES(TOT,TOT,IS1,IS2,MIK,IV1)
DO 540 I = 1,TOT
DO 530 J = 1,TOT
    FM1(I,J) = MIK(I,J)
530 CONTINUE
540 CONTINUE

```

```

    CALL HQR(TOT,TOT,IS1,IS2,FM1,FR,FI,IER)
    IF(IER .NE. 0) GO TO 640
    DO 550 I = 1,TOT
    WRITE(*,*) FR(I),FI(I)
550 CONTINUE
    DO 560 I = 1,TOT
    SLCT(I) =(( FR(I) .GT.0.OEO) .AND. (FI(I) .EQ. 0.OEO))
560 CONTINUE
    CALL INVIT(TOT,TOT,MIK,FR,FI,SLCT,TOT,NEIG,OUT,IER,FM1,FV2,FV3)
    IF(IER .NE. 0) GO TO 640
    IF(NEIG. EQ. 0) GO TO 680
    WRITE(*,*) NEIG
    CALL ELMLBAK(TOT,IS1,IS2,MIK,IV1,NEIG,OUT)
    CALL BALBAK(TOT,TOT,IS1,IS2,FV1,NEIG,OUT)
    WRITE(2,570) NEIG
570 FORMAT('THE NUMBER OF EIGENVALUES SELECTED IS ', I4)
C   NOW GET THE REQUIRED RESULTS:
C   ONLY PROPAGATING MODES ARE OF INTEREST.
C   ELIMINATE COMPLEX BETAS WITH NON ZERO IMAGINARY PARTS.
C   ALSO NEGATIVE BETAS CAN BE ELIMINATED.
C
C   FR : STORES REAL PART OF BETA-SQUARED.
C   FI : STORES THE IMAGINARY PART OF BETA-SQUARED.
    JJ = 0
    DO 590 I = 1,TOT
    IF((FR(I).GE.0.OEO).AND.(FI(I).EQ.0.OEO)) THEN
    JJ = JJ+1
    WRITE(2,580) I,JJ,FR(I),FI(I)
    ENDIF
580 FORMAT (3X,2I4,' EIGENVALUE = ',1X, 2(E15.7)/)
590 CONTINUE
    IF(JJ .EQ. NEIG) WRITE(*,*) 'O.K.'
C
C   NOW SQUARE ROOT AND GET POSITIVE ROOT OF BETA-SQUARED.

```

```

C   DIVIDE BY 1000 TO GET IN RAD/MM.
    JJ = 0
    DO 600 I = 1,TOT
      IF((FR(I).GE.0.0EO).AND.(FI(I).EQ.0.0EO)) THEN
        JJ = JJ+1
        PHASE(JJ) = DSQRT(FR(I))/1000
      ENDIF
600 CONTINUE
C
C   SORT THE EIGEN VALUES IN DESCENDING ORDER.
    CALL EIGSORT(PHASE,JJ,JJ)
    DO 610 I = 1,JJ
      WRITE(2,620) PHASE(I)
      WRITE(4,630) FREQ(K),PHASE(I)
610 CONTINUE
620 FORMAT(/,3X,'BETA IN RAD/MM = ', E15.6/)
630 FORMAT(E15.6,7X,E15.6/)
C
C   SPURIOUS MODES ARE TO BE ELIMINATED BY EIGENVECTOR ANALYSIS.
    GO TO 700
640 IF(IER .GT. 0) GO TO 660
    IER = -IER
    WRITE(2,650) IER
650 FORMAT('AT LEAST ONE EIGENVECTOR FAILED TO
*           CONVERGE,NAMELY', I5)
    GO TO 700
660 WRITE(2,670) NEIG
670 FORMAT(/'NOT ENOUGH SPACE ALLOCATED FOR THE ',I4,
*           'EIGENVALUES')
    GO TO 700
680 WRITE(2,690) NEIG
690 FORMAT('NO EIGENVALUES FOUND ON SELECTION ')
C
700 WRITE(2,*) 'MIN.EV. = ',DSQRT(K0)

```

C REPEAT FOR NEXT FREQUENCY.

710 CONTINUE

END

C.....

BIBLIOGRAPHY

- [1]. Jin-fa Lee, " *Finite Element Methods for Modelling Passive Microwave Devices* ", Ph. D. Dissertation, Dept. of Electrical Engineering, Carnegie Mellon University, May 1989.
- [2]. M.Koshiba, K.Hayata and M.Suzuki, " Vectorial finite-element formulation without spurious modes for dielectric waveguides ", *Trans. Inst. Electron. Commnc. Engg. Japan*, Vol E67, No.4, April 1989, pp 191-196.
- [3]. B.M.Azizur Rahman and J.B.Davies, " Penalty Function Improvement of Waveguide Solution by Finite Elements ", *IEEE Transactions on Microwave Theory and Techniques*, Vol. 32, No.8, August 1984, pp 922-928.
- [4]. Masanori Koshiba, Kazuya Hayata and Michio Suzuki, " Improved Finite-Element Formulation in Terms of the Magnetic Field Vector for Dielectric Waveguides ", *IEEE Transactions on Microwave Theory and Techniques*, Vol. 33, No. 3, March 1985, pp 227-233.
- [5]. M.Koshiba, K.Hayata and M.Suzuki, " Finite-Element Formulation in Terms of the Electric-Field Vector for electromagnetic waveguide problems ", *IEEE Transactions on Microwave Theory and Techniques*, Vol. 33, No.10, October 1985, pp 900-906.
- [6]. K.Hayata, M. Eguchi, M.Koshiba and M.Suzuki, " Vectorial wave analysis of side tunnelled type polarization-mounting optical fibers by variational finite elements ", *Jour. Lightwave Technology*, Vol. LT4, August 1986.
- [7]. J.C.Nédelec, " Mixed Finite elements in R^3 ", *Numerical Mathematics*, No. 3, 1981.
- [8]. A. Bossavit and J.C.Verité, " The " TRIFOU " code: Solving the 3-D Eddy-Currents Problem by using H as State Variable ", *IEEE Transactions on Magnetics*, Vol. 19, No.6, November 1983, pp 2465-2470.
- [9]. Gerrit Mur and Adrianus T. de Hoop, " A Finite-Element Method for Computing Three-Dimensional Electromagnetic Fields in Inhomogeneous Media ", *IEEE Transactions on Magnetics*, Vol. 21, No. 6, November 1985, pp 2188-2191.
- [10]. Mitsuo Hano, " Finite-Element Analysis of Dielectric-Loaded Waveguides ", *IEEE Transactions on Microwave Theory and Techniques*, Vol. 32, No.10, October 1984, pp 1275-1279.

- [11]. Mitsuo Hano, " Vector Finite-Element Solution of Anisotropic Waveguides Using Novel Triangular Elements ", *Electronics and Communications in Japan*, Part 2, Vol.71, No.8 , 1988, pp 71-80.
- [12]. M.L.Barton and Z.J.Cendes, " New vector finite elements for three-dimensional magnetic field computations ", *Journal of Applied Physics* , Vol.61, No. 8, April 1987, pp 3919-3921.
- [13]. R.Albanese and Prof. G.Rubinacci, " Integral formulation for 3-D eddy-current computation using edge elements ", *IEE Proceedings*, Vol. 135, Pt. A., No. 7, September 1988, pp 457-462.
- [14]. J.P.Webb and B.Forghani, " A Single Scalar Potential Method for 3D Magnetostatics using Edge Elements ", *IEEE Transactions on Magnetics*, Vol. 25, No. 5, September 1989, pp 4126-4128.
- [15]. Alain Bossavit, " Whitney Forms: a class of finite elements for three-dimensional computations in electromagnetism ", *IEE Proceedings*, Vol. 135, Pt. A., No. 8., November 1988, pp 493-500.
- [16]. Alain Bossavit, " Simplicial Finite Elements for Scattering Problems in Electromagnetism ", *Computer Methods in Applied Mechanics and Engineering*, 76, (1989), pp 299-316.
- [17]. T.Nakata, N.Takahashi, K.Fujiwara and Y.Shiraki, " Comparison of Different Finite Elements for 3D Eddy Current Analysis ", *IEEE Transactions on Magnetics*, Vol. 26, No. 2, March 1990, pp 434-437.
- [18]. Akihisa Kameari, " Calculation of Transient 3D Eddy Current using Edge Elements ", *IEEE Transactions on Magnetics*, Vol. 26, No. 2, March 1990, pp 466-469.
- [19]. M.Tanaka, H.Tsuboi, F.Kobayashi and T.Misaki, " An Edge Element for Boundary Element Method using Vector Variables ", *IEEE Transactions on Magnetics*, Vol. 28, No. 2, March 1992, pp 1623-1626.
- [20]. Jin-Fa Lee, " Analysis of Passive Microwave Devices by Using Three-Dimensional Tangential Vector Finite Elements ", *International Journal of Numerical Modelling: Electronic Networks, Devices and Fields*, Vol.3, December 1990, pp 235-246.
- [21]. Jin-Fa Lee, Din-Kow Sun and Zoltan J.Cendes, " Full-Wave Analysis of Dielec-

- tric Waveguides using Tangential Vector Finite Elements ", *IEEE Transactions on Microwave Theory and Techniques*, Vol. 39, No. 8, August 1991, pp 1262-1271.
- [22]. Zoltan J.Cendes , " Vector Finite Elements for Electromagnetic Field Computation ", *IEEE Transactions on Magnetics*, Vol. 27, No. 5, September 1991, pp 3958-3966.
- [23]. Tuptim Angkaew, Masanori Matsuhara and Nobuaki Kumagai, " Finite-Element Analysis of Waveguide modes : A Novel Approach that Eliminates Spurious Modes ", *IEEE Transactions on Microwave Theory and Techniques*, Vol. 35, No. 2, February 1987, pp 117-123.
- [24]. Kazuya Hayata, Kazunori Miura and Masanori Koshiba, " Finite-Element Formulation for Lossy Waveguides ", *IEEE Transactions on Microwave Theory and Techniques*, Vol. 36, No.2, February 1988, pp 268-276.
- [25]. Jan A.M.Svedin , " A Numerically Efficient Finite-Element Formulation for the General Waveguide Problem without Spurious Modes ", *IEEE Transactions on Microwave Theory and Techniques*, Vol. 37, No. 11, November 1989, pp 1708-1715.
- [26]. W.C.Chew and M.A.Nasir, " A Variational analysis of anisotropic inhomogeneous dielectric waveguides ", *IEEE Transactions on Microwave Theory and Techniques*, Vol. 37, No. 4, April 1989, pp 661-668.
- [27]. F.A.Fernandez and Y.Lu , " Variational finite element analysis of dielectric waveguides with no spurious solution ", *Electronic Letters*, Vol. 26, December 1990, pp 2125-2126.
- [28]. Masanori Koshiba and Kazuhiro Inoue, " Simple and Efficient Finite-element Analysis of Microwave and Optical Waveguides ", *IEEE Transactions on Microwave Theory and Techniques*, Vol. 40, No.2 , February 1992, pp 371-377.
- [29]. Todd H.Hubing, " A Survey of Numerical Electromagnetic Modeling Techniques ", *ITEM Update 1991*, pp 17-30,60-62.
- [30]. E. Thomas Moyer Jr. and Erwin A.Schroeder, " Finite Element Formulations of Maxwells Equations - Advantages and Comparisons between Available Approaches ", *IEEE Transactions on Magnetics*, Vol. 27, No.5, September 1991, pp 4217-4220.
- [31]. C.J.Carpenter , " Comparison of alternative formulations of 3-dimensional magnetic-field and eddy-current problems at power frequencies ", *IEE Proceedings*, Vol. 124, (11),

1977, pp 1026-1034.

[32]. R.L.Ferrari, " Complementary variational formulation for eddy-current problems using the field variables E and H directly ", *IEE Proceedings*, Vol. 132, Pt. A (4), 1985, pp 157-164.

[33]. Whitney H. , *Geometric Integration Theory* , Princeton University Press, 1957.

[34]. P.P.Silvester and R.L.Ferrari, *Finite Elements for Electrical Engineers* , 2nd Ed., Cambridge University Press, New York, 1990.

[35]. A.Bossavit, " Solving Maxwell Equations in a Closed Cavity, and the Question of ' Spurious Modes ' ", *IEEE Transactions on Magnetics*, Vol. 26, No.2, March 1990, pp 702-705.

[36]. B.T.Smith et al. , *Matrix Eigensystem Routines - EISPACK Guide*, Vol. 6 of Lecture Notes in Computer Science, Springer-Verlag , New York 1974.

[37]. J.H.Wilkinson and C.Reinsch , *Handbook for Automatic Computation*, Vol II - Linear Algebra, Springer-Verlag, New York, 1971.

[38]. William H.Press, Brian P.Flannery , Saul A.Teukolsky and William T.Vetterling, *Numerical Recipes : the art of Scientific Computing*, Cambridge University Press, Cambridge 1986.

[39]. Liang Chi Shen and Jin Au Kong, *Applied Electromagnetism*, Brooks/Cole Engineering Division, California, 1983, pp 88-93.

[40]. E.E.Kriezis et al., " Eddy Currents: Theory and Applications " , *Proceedings of the IEEE*, Vol.80, No.10, October 1992, pp 1556-1589.

[41]. Jinxing Shen and Arnulf Kost, " BEM with Mixed Special Shape functions for 2D Eddy Current problems " , *IEEE Transactions on Magnetics*, Vol. , Vol.28, No.2, March 1992, pp 1220-1223.

[42]. E.A.J.Marcatalli, " Dielectric rectangular waveguide and Directional coupler for Integrated Optics " , *Bell Systems Technical Journal*, Vo.48, September 1969, pp 2079-2102.

[43]. K.C.Gupta, Ramesh Garg and I.J.Bahl, *Microstrip Lines and Slotlines*, Artech House Inc., Massachusetts, 1979.

[44]. Raj Mittra and Tatsuo Itoh, " A New Technique for the Analysis of the Disper-

- sion Characteristics of Microstrip Lines ", *IEEE Transactions on Microwave Theory and Techniques*, Vol. 19, No.1, January 1971, pp 47-56.
- [45]. Jon P.Webb ,“ Finite element analysis of Dispersion in Waveguides with Sharp Metal Edges ”, *IEEE Transactions on Microwave Theory and Techniques*, Vol. 36, No.12, December 1988, pp 1819-1824.
- [46]. D.Mirshekar-Syahkal and J.Brian Davies ,“ Accurate Solution of Microstrip and Coplanar Structures for Dispersion and for the Dielectric and Conductor Losses ”, *IEEE Transactions on Microwave Theory and Techniques*, Vol. 27, No. 7, July 1979, pp 694-699.
- [47]. Ruth Miniowitz and J.P.Webb,“ Covariant-Projection Quadrilateral Elements for the Analysis of Waveguides with Sharp Edges ”, *IEEE Transactions on Microwave Theory and Techniques*, Vol. 39, No.3, March 1991, pp 501-505.
- [48]. G.H.Golub and C.F.Van Loan, *Matrix Computations*, Baltimore: The John Hopkins University Press, 1985, pp 202-204.
- [49]. Adalbert Konrad, *Triangular Finite Elements for vector fields in electromagnetics*, Ph. D. Thesis, Dept. of Electrical Engineering, McGill University, Montreal, September 1974.
- [50]. Darcy N.Ladd, *Three Dimensional Finite Element Method applied to study the Penetration of Electromagnetic Fields in cavities*, M. A. Sc. Thesis, Dept. of Electrical Engineering, University of Ottawa, Ottawa, February 1990.
- [51]. Hiroyo Ogawa, Takao Hasegawa, Seiichi Banba and Hiroyuki Nakamoto,“ MMIC Transmission Lines for multilayered MMICs ”, *1991 IEEE-MTT Symposium Digest*, pp 1067-1070.
- [52]. T.Hasegawa, S.Banba, H.Ogawa and H.Nakamoto,“ Characteristics of Valley Microstrip lines for Use in multilayer MMIC's ”, *Microwave and Guided Wave Letters*, Vol.1, No.10, October 1991, pp 275-277.
- [53]. A.David Olver, *Microwave and Optical Transmission*, John Wiley and Sons, England, 1992.